Geol. Mag. **155** (*2*), *2018, pp. 377–421. © Cambridge University Press 2018*
doi:10.1017/S0016756817000942

From obduction to continental collision: new data from Central Greece

GIUSEPPE NIRTA*†, GIOVANNA MORATTI‡, LUIGI PICCARDI‡, DOMENICO MONTANARI‡, NICOLAOS CARRAS§, RITA CATANZARITI¶, MARCO CHIARI‡ & MARTA MARCUCCI*

*Dipartimento di Scienze della Terra, Università di Firenze, Via La Pira 4, 50121, Firenze, Italy
‡C.N.R., Istituto di Geoscienze e Georisorse, U.O di Firenze, Via La Pira 4, 50121, Firenze, Italy
§Institute of Geology and Mineral Exploration (IGME), Spirou Loui 1, 13677 Acharnes, Greece
¶C.N.R., Istituto di Geoscienze e Georisorse, Via Moruzzi 1, 56124 Pisa, Italy

(*Received* 10 October 2016; *accepted* 12 October 2017)

Abstract – The aim of this paper is to contribute to deciphering the evolutionary history of the Hellenides by the study of a large sector of the chain located between the front of the ophiolitic units and the external zones classically attributed to the continental margin of Adria. In particular, the tectonic units located in Boeotia – a key area located in Central Greece at the boundary between the Internal and External Hellenides – were studied from structural, stratigraphic and biostratigraphic points of view. Addressing the main debated aspects concerning the origin of the ophiolite nappe(s), the tectonic evolution of the Hellenic orogen was revised with a particular emphasis on the period between obduction and continental collision. New findings were compared with consolidated data concerning the main metamorphic events recorded in the more Internal Hellenides, geochemistry and age of the ophiolites and main stratigraphic constraints obtained in other sectors of the belt. Finally, a new reconstruction of the tectonic evolution of this area was introduced and, in the context of the dispute concerning the origin of the 'ophiolitic belts' as a possible record of multiple oceanic basins, we put forward for consideration a 'single ocean' tectonic model spanning from Triassic up to Tertiary times, and valid for the whole Hellenic–Albanian sector.

Keywords: Hellenic–Dinaric orogen, structural geology, stratigraphy, biostratigraphy, ophiolite, Boeotia, Greece

1. Introduction

The Triassic–Jurassic ophiolites scattered throughout the Hellenic–Dinaric orogen testify to events of obduction and subduction. However, since the early studies, the interpretation of these ophiolites has been characterized by the contrast between researchers who see the existence of a single ocean basin interposed between Africa–Adria and Eurasia and others who propose the existence of multiple oceans separated by microcontinents.

In the last decades, increasingly detailed data on the geochemistry of the ophiolites, their age and metamorphism, including the continental units involved in the orogenic process, has strengthened the first-order geological constraints allowing more reliable geodynamic reconstructions. The reconstruction of the deformation history often focuses in areas where large ophiolitic masses are in contact with the continental units, or in the inner sectors of the chain characterized by orogenic-related metamorphism.

Convergence between Africa and Eurasia – that led to intraoceanic subduction in Early–Middle Jurassic times – is still active. This has resulted in a complex structure of the chain, where the stages of compressive strain, linked to subduction–obduction and continental collision processes, are added to those related to the Aegean extension.

The study of a large sector of the chain located between the front of the ophiolitic units and the external sectors of the continental margin of Adria was used to shed light on the evolutionary history of the Hellenides.

In particular, we studied, from structural, stratigraphic and biostratigraphic points of view, the units located in Boeotia, a key area between the Pelagonian and the Parnassus units (considered alternatively as microcontinents or part of Adria). The fact that such a broad disagreement exists in the palaeogeographic interpretation of these geotectonic zones exposed in Boeotia reflects the great complexity of the area and its importance in interpreting the geodynamic evolution of the entire chain.

2. Overview of the geology and geodynamics of the Hellenic Chain

The Hellenic orogen evolved through (i) a Permo-Triassic intracontinental rifting stage related to Pangaea break-up (Ferrière, 1982; Capedri *et al.*

†Author for correspondence: giuseppe.nirta@gmail.com

https://doi.org/10.1017/S0016756817000942 Published online by Cambridge University Press

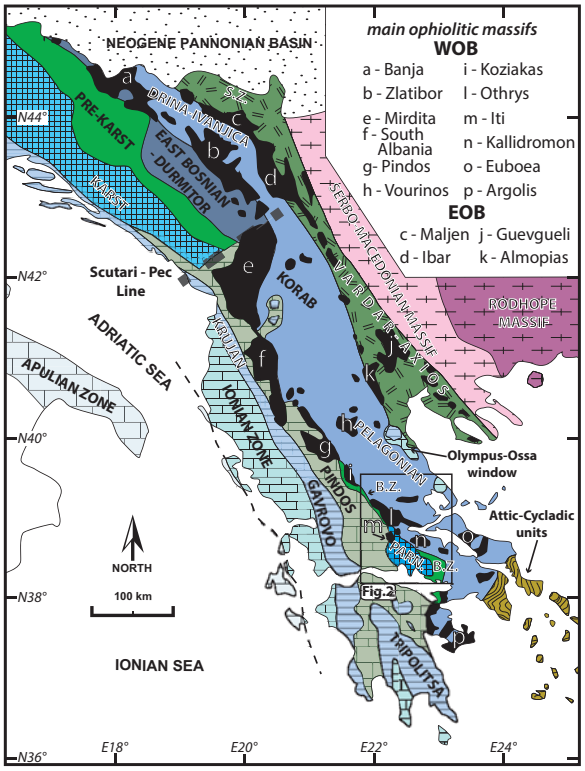


Figure 1. (Colour online) Tectonic sketch map of the Dinaric–Hellenic Orogenic Belt showing the main geotectonic zones and distribution of ophiolitic massifs (in solid black). WOB – western ophiolite belt; EOB – eastern ophiolite belt; B.Z. – Boeotian Zone; S.Z. – Sava Zone; PARN. – Parnassus Zone (modified after Bortolotti *et al.* 2013).

1997; Pe-Piper, 1998; Bortolotti & Principi, 2005; Robertson, 2012 and many others); (ii) oceanic spreading from Middle Triassic time with mid-ocean ridge (MOR) lithosphere production (Bortolotti *et al.* 2005, 2013; Dilek, Shallo & Furnes, 2005 and many others); (iii) intraoceanic subduction in Early–Middle Jurassic times along with island arc and back-arc basin formation (Mercier, 1968; Bébien, Platvoet & Mercier, 1994; Shallo, 1994; Beccaluva *et al.* 1994; Bortolotti *et al.* 1996; Robertson & Shallo, 2000; Rassios & Smith, 2000 and many others); (iv) intraoceanic thrusting associated with high temperature – low pressure (HT–LP) metamorphism since Middle Jurassic time (Spray & Roddick, 1980; Dimo-Lahitte, Monié & Vergély, 2001) followed by obduction since Late Jurassic time (Ferrière, 1975; Baumgartner, 1985; Çollaku *et al.* 1992; A. De Bono, unpub. Ph.D. thesis, Univ. Lausanne, 1998 among many others); (v) continental collision in Cretaceous time and ongoing shortening until middle Eocene time; and finally (vi) late orogenic extension of the nappe stack, starting in late Eocene time (Lips, White & Wijbrans, 2000; Jolivet *et al.* 2003 and many others). In mainland Greece the orogenic wedge is represented by thrust sheets stacked with a NNW trend and generally with a top-to-the-W vergence (Figs 1–3).

Aubouin (1959, 1965), applying the geosyncline theory, proposed the first comprehensive description of the geological evolution of the Hellenic belt: the orogen was divided according to the Mesozoic stratigraphy of the involved terrains into 'isopic zones'; then the orogenic process allowed the differentiation of the External Hellenides, as the zones affected by deformation during Tertiary time and occupying the western part of the chain, and the Internal Hellenides to the east, which recorded older orogenic deformations since Middle Jurassic time (Brunn, 1960).

Nowadays the nomenclature of Aubouin and coworkers is still used even if the term 'isopic zone' has been transfigured into 'geotectonic zones', partly corresponding to the 'terranes' concept.

Basement and supracrustal rocks cropping out in the Internal Hellenides are grouped mainly within the Pelagonian geotectonic zone (or Pelagonia) whereas the External Hellenides are mostly represented by supracrustal thrust sheets consisting, from east to west, of the Boeotian Zone, Parnassus Zone, Pindos Zone, Gavrovo–Tripolitsa Zone and Ionian Zone (Figs 1, 2).

The Pindos and Ionian zones are characterized by pelagic sedimentation beginning in Late Triassic and late Early Jurassic times, respectively. Moreover, the Pindos deep-sea sedimentation is alternatively interpreted as pertaining to a thinned continental crust characterized by mafic intrusion of Middle–Late Triassic age (Fleury, 1980), as an oceanic domain (Aubouin, 1959; Thiébault, 1982; Robertson *et al.* 1991) or a combination of thinned continental crust passing through a transitional zone in the oceanic domain (Degnan & Robertson, 1998, 2006).

The Pelagonian, Boeotian, Parnassus and Gavrovo–Tripolitsa zones share a similar Triassic–Middle Jurassic stratigraphy represented by shallow-water carbonates. The shallow-water sedimentation on the Pelagonian and Boeotian platforms ceased in Late Jurassic time as a direct consequence of the obduction processes (Baumgartner, 1985; Celet, Clément & Ferrière, 1988; A. De Bono, unpub. Ph.D. thesis, Univ. Lausanne, 1998) whereas general shallow-water conditions persisted in the Parnassus and Gavrovo–Tripolitsa zones throughout Mesozoic and Eocene times, respectively (Fig. 4).

This differentiation in the stratigraphy of the External Hellenides and Pelagonia is attributed to the control exerted by tectonic structures inherited from the Permo-Triassic rifting stage, or by the influence of the compressional tectonic regime starting from Middle–Late Jurassic times, or as a combination of both.

The Pelagonian Zone consists of Palaeozoic continental basement and its mostly carbonate Mesozoic cover that are bounded to the east by the ophiolite-bearing units of the Vardar–Axios Zone (East Vardar ophiolites of Schmid *et al.* 2008, here referred to as the Eastern Ophiolite Belt, EOB) and to the west by several ophiolitic massifs, including the Vourinos, Pindos, Koziakas, Othrys, Iti, Kallidromon and Argolis ophiolite complexes, arranged along an external ophiolite

https://doi.org/10.1017/S0016756817000942 Published online by Cambridge University Press

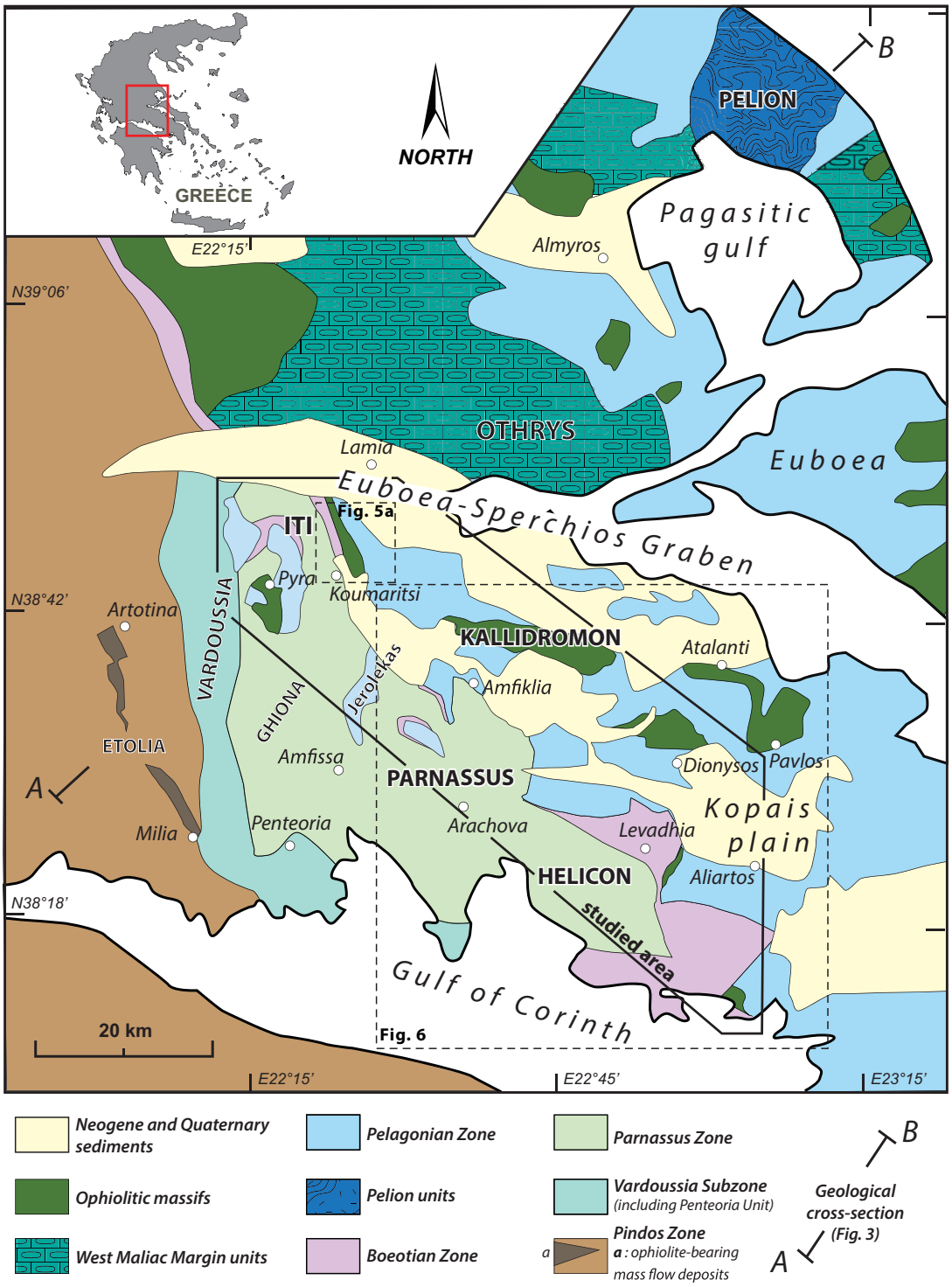


Figure 2. (Colour online) Simplified geological map of Central Greece, with main tectonic units. Location of the studied area is indicated. Modified after Celet, Ferrière & Wigniolle (1977), Ferrière (1982) and geological maps of the IGME (Greek Institute of Geology and Mineral Exploration).

https://doi.org/10.1017/S0016756817000942 Published online by Cambridge University Press

belt (West Vardar ophiolites of Schmid *et al.* 2008, here referred to as the Western Ophiolite Belt, WOB). Both ophiolite belts can be traced northwards into the Balkans: the WOB continues into the Mirdita Zone of Albania, curves along the Scutari–Pec line and then continues in the Dinaride Ophiolite Belt whereas the EOB continues straight into the Sava Zone up to the Pannonian Basin (Fig. 1).

The ophiolites of the EOB thrust onto the eastern margin of the Pelagonian Zone whereas the WOB units are emplaced both on the western margin of Pelagonia and over the Pindos Zone (namely over the Tertiary Pindos Flysch) of the External Hellenides. Whereas a general consensus exists about the location of the root zone of the EOB in the Vardar–Axios Zone (or Sava Zone, Schmid *et al.* 2008), the origin of the WOB represents a long-lasting point of dispute among authors. Depending on where the root zones of the two ophiolitic belts are located, two main palaeogeographic interpretations were proposed for the Pelagonian Zone. In the hypothesis that both the EOB and WOB shared a unique root zone in the Vardar–Axios Zone (Bernoulli & Laubscher, 1972; Dercourt, 1972; Zimmerman, 1972; Zimmerman & Ross, 1976; Jacobshagen *et al.* 1978; Ferrière, 1982; Bortolotti *et al.* 1996, 2005, 2013; Schmid *et al.* 2008; Kilias *et al*. 2010), a unique ocean basin is postulated (Maliac–Vardar Ocean) while Pelagonia represents the easternmost rim of the Adria continental margin facing the oceanic domain to the east. On the other hand, the assumption of the root zone of the WOB in a different location, classically located in the Pindos Zone (Hynes *et al.* 1972; Mercier, Vergély & Bébien, 1975; Nance, 1981; Jones & Robertson, 1991; Shallo, Kodra & Gjata, 1992; Smith, 1993; Beccaluva *et al*. 1994; Robertson *et al.* 1996; Clift & Dixon, 1998; Rassios & Dilek, 2009; Ghikas, Dilek & Rassios, 2010; Robertson, 2012), necessarily implies the presence of a microcontinent, namely Pelagonia. According to more complex reconstructions, especially around the Parnassus Zone, the main Pindos 'Ocean' would be structured into several oceanic branches isolating continental slivers or microplates (Robertson & Degnan, 1993; Skourlis & Doutsos, 2003; Papanikolaou, 2009; Kaplanis *et al.* 2013).

This study investigates from the lithostratigraphic, biostratigraphic and structural points of view the complex tectonic stack exposed in Boeotia in Central Greece (Fig. 2). This area is located at the boundary between the Internal Hellenides (Pelagonian thrust sheets) and the External Hellenides (Boeotian Unit and Parnassus Unit). Ophiolite-bearing units top the tectonic pile, resulting from Mesozoic obduction and collisional events. The tectonic stack is further complicated by the Cenozoic compressional and extensional phases.

Addressing the main debated aspects concerning the origin of the WOB, the ages of deformation and their effects on the stratigraphic evolution of the involved rocks, we aim to propose a reconstruction of the Hellenic orogen with a particular emphasis on the period between obduction and continental collision. This intent was pursued by comparing the obtained data with consolidated data concerning the main metamorphic events recorded in the more Internal Hellenides, the geochemistry and age of the ophiolites and the main stratigraphic constraints obtained in other sectors of the belt.

3. Geology and lithostratigraphy of the Boeotian tectonic units

The study area belongs to the Boeotia region in Central Greece. It is located between the North Euboea–Sperchios graben to the north, the Corinth Gulf to the south, the Parnassus massif to the west and the Kopais plain to the east (Fig. 2).

The tectonic stack includes at its top the oceanic units that crop out as a large thrust nappe in the Kallidromon and Iti massifs or as small tectonic slices between the Pelagonian Unit, on top, and the Boeotian or Parnassus units, below (Fig. 3). The Ophiolite Unit is almost totally represented by an ophiolitic mélange embedding mostly ultramafic rocks in a shaly-sandy matrix. These ophiolites, along with the nearby Othrys ophiolites, are attributed to the WOB (Fig. 1). In this work we favour a working hypothesis in which ophiolites of both the EOB and WOB originated from a unique oceanic basin (i.e. the Maliac–Vardar Ocean, see Ferrière, Chanier & Ditbanjong, 2012 and Bortolotti *et al.* 2013 for discussion).

From Late Jurassic times onwards the ocean-derived units overthrust the carbonate sequences of the Pelagonian Unit, here regarded as the inner deformed rim of the Adria continental margin, and during Early–Late Cretaceous times both the ocean-derived and Pelagonian units overthrust the Boeotian Unit. Aptian to Upper Cretaceous deposits unconformably cover this tectonic stack, which in turn is superimposed westwards above the Parnassus carbonate platform. This tectonic pile was further cut by out-of-sequence thrusts and extensional events of Tertiary age that further complicated the Late Cretaceous superposition geometry (Fig. 3).

In Boeotia, the Pelagonian, Boeotian and Parnassus units represent the continental-derived units. The exposed portions of these units evidence a similar stratigraphy for the Late Triassic – Middle Jurassic age range, characterized by shallow-water carbonate. Crystalline Variscan basement followed by a syn-rift sequence of Late Permian – Early Triassic age (De Bono *et al.* 2001) underlie the Pelagonian Platform, whereas the basement of the Boeotian and Parnassus carbonates is not exposed. Since Middle–Late Jurassic times transition pelagic sedimentation took place in the Boeotian Zone (Celet, Clément & Ferrière, 1976, 1988; Danelian & Robertson, 1998). In the same period the Parnassus Zone and external Pelagonian Zone experienced an emersion episode marked by bauxite deposits (b1 horizon, Papastamatiou, 1960;

https://doi.org/10.1017/S0016756817000942 Published online by Cambridge University Press

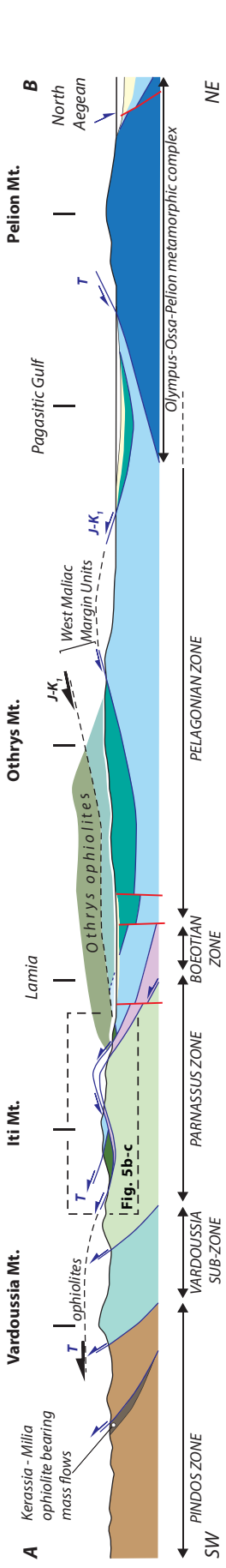


Figure 3. (Colour online) Schematic geological cross-section showing relationships between the main tectonic units in Central Greece (see Fig. 2 for location and legend). J-K_1 – Late Jurassic – Early Cretaceous deformations; T – Tertiary deformations.

Papastamatiou *et al.* 1962*a*,*b*). Following gradual Late Jurassic westward obduction, the sedimentation in the Pelagonian Platform ended after a phase of pelagic sedimentation (Celet, Ferrière & Wigniolle, 1977; Ferrière, 1982; Baumgartner, 1985) while the Parnassus Zone experienced neritic sedimentation punctuated by subaerial exposure events until Late Cretaceous time (Papastamatiou, 1960; Celet, 1962, 1979; Carras & Tselepidis, 2001).

Some authors have interpreted the Pelagonian Platform as a microcontinent drifted away from the Adria margin during Early Triassic times and separated by the Pindos 'Ocean' (Robertson *et al.* 1991; Smith, 1993; Jones & Robertson, 1994; Degnan & Robertson, 1998; Robertson & Shallo, 2000; Stampfli & Borel, 2004). Similarly, the Parnassus Platform was also regarded as a continental block detached from Adria and separated by a secondary oceanic strand (Kerassia-Milia Ocean; Robertson & Degnan, 1993; Pe-Piper & Piper, 2002). Conversely, in the working hypothesis adopted here, we consider the Pelagonian, Boeotian and Parnassus units as units detached from the Adria continental margin and successively overthrust westwards during the Mesozoic to Tertiary compressional phases (Bernoulli & Laubscher, 1972; Ferrière, 1982, 1985; Baumgartner, 1985; Bortolotti *et al.* 2004*b*, 2013; Schmid *et al.* 2008; Ferrière, Chanier & Ditbanjong, 2012).

The stratigraphy of the various units described below and the main tectono-metamorphic events are summarized in Figure 4.

3.a. Adria-derived units

3.a.1. Pelagonian Unit

Palaeozoic crystalline basement of the Pelagonian Unit is sporadically exposed in Boeotia and Euboea Island; it is locally intruded by granites (A. De Bono, unpub. Ph.D. thesis, Univ. Lausanne, 1998) and represents the lowermost part of the Pelagonian Unit in the study area (B. Clément, unpub. Ph.D. thesis, Univ. Lille, 1983). Above this basement lies a clastic series ('Verrucano-like') of Late Permian age (Clément, 1976; De Bono *et al.* 2001) that, in turn, grades into a Middle Triassic carbonate platform and volcano-sedimentary deposits of Middle–Late Triassic age (B. Clément, unpub. Ph.D. thesis, Univ. Lille, 1983; Pe-Piper, Matarangas & Jacobshagen, 1996; Pe-Piper, 1998). These sequences are commonly correlated with a syn- to post-rifting phase linked with the Pangaea break-up and formation of the Maliac–Vardar oceanic basin (De Bono *et al.* 2001). Upwards follows an Upper Triassic to Middle–Upper Jurassic shallow-water limestone sequence grading to deep-water facies in the Middle–Upper Jurassic and that is locally topped by Oxfordian–Tithonian radiolarites and clastic ophiolite-bearing mélange (Celet & Ferrière, 1978; Baumgartner *et al.* 1993) (Fig. 4).

The transitional facies widely exposed in the Othrys Massif (West Maliac Margin Units; Ferrière, 1982,

https://doi.org/10.1017/S0016756817000942 Published online by Cambridge University Press

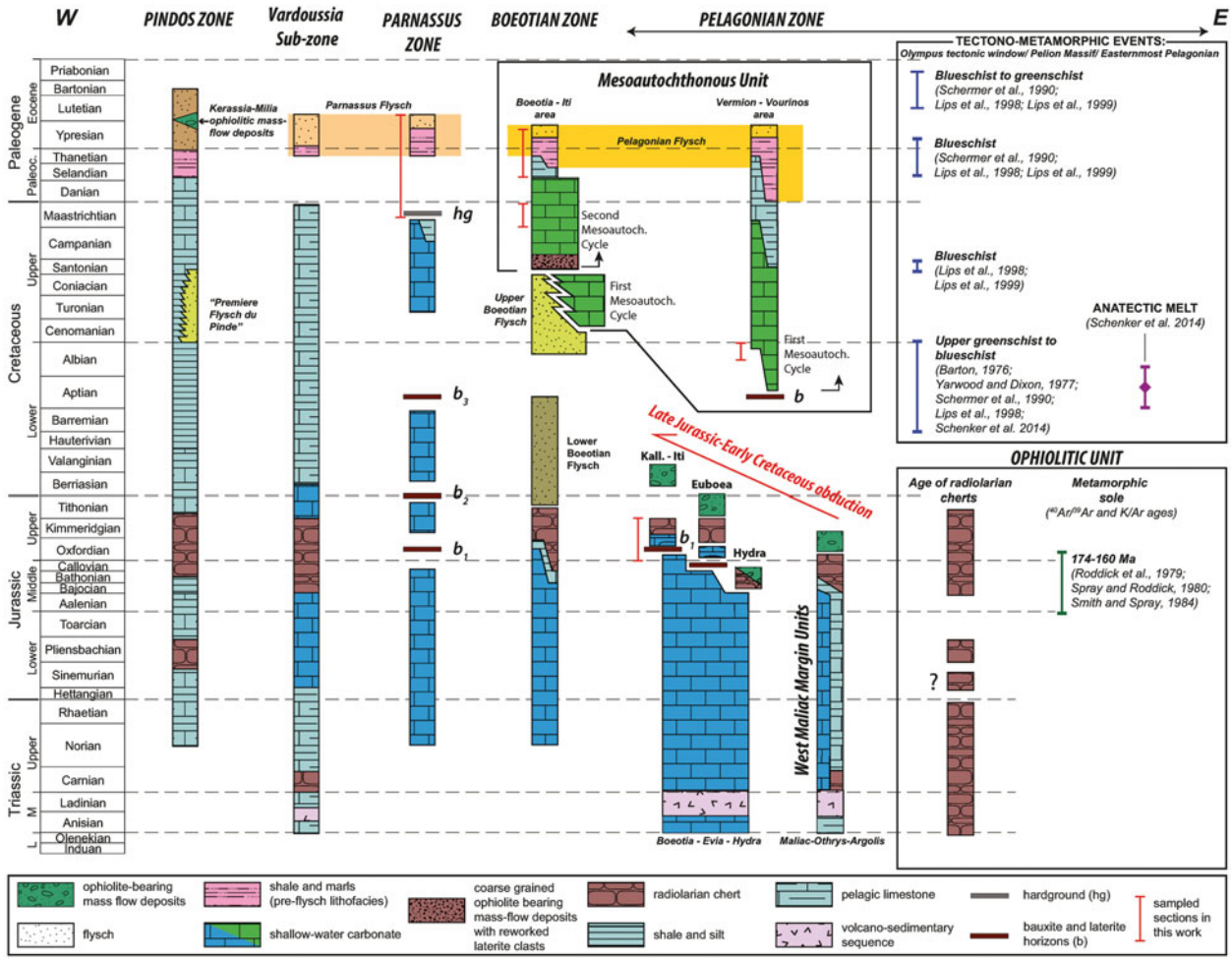


Figure 4. (Colour online) Synoptic table representing schematic lithostratigraphic columns of various units pertaining to the different geotectonic zones and tectono-metamorphic events in the ophiolite nappe and Pelagonian Unit. New data presented in this work integrate the following literature: Pindos zone: C. Beck, unpub. Ph.D. thesis, Univ. Science and Technology, Lille (1975); Fleury (1980); Ananiadis *et al.* (2004); Neumann & Zacher (2004). Vardoussia Sub-zone: R. Ardaens, unpub. Ph.D. thesis, Univ. Lille (1978); Celet (1979). Parnassus Zone: Celet (1962); Richter *et al.* (1995); Carras & Tselepidis (2001). Boeotian Zone: B. Clément, unpub. Ph.D. thesis, Univ. Lille (1983); Steuber (1993); Steuber *et al.* (1993); Danelian & Robertson (1998); Nirta *et al.* (2015). West Maliac Margin Units: Ferrière (1982); Baumgartner (1985); Baumgartner *et al.* (1993); Ferrière *et al.* (2016). Mesoautochthonous Unit: Wigniolle (1977); B. Clément, unpub. Ph.D. thesis, Univ. Lille (1983); Steuber *et al.* (1993); Steuber, Raeder & Walter (1994); Richter, Müller & Mihm (1996); Richter, Müller & Risch (1996); Fazzuoli & Carras (2007); Photiades *et al.* (2007). Pelagonian Zone: Baumgartner & Bernoulli (1976); Celet & Ferrière (1978); B. Clément, unpub. Ph.D. thesis, Univ. Lille (1983); Baumgartner (1985); Baumgartner *et al.* (1993, 1995*a*); Danelian (1994); Richter, Müller & Risch (1996); A. De Bono, unpub. Ph.D. thesis, Univ. Lausanne (1998). Ophiolitic Unit: Baumgartner (1984, 1985, 1995); Jones, De Wever & Robertson (1992); De Wever (1995); Danelian, Robertson & Dimitriadis (1996); Danelian & Robertson (2001); Chiari *et al.* (2003, 2012, 2013); Bortolotti *et al.* (2003, 2008, 2009); Nirta *et al.* (2010); Kukoč *et al.* (2012); Ozsvart *et al.* (2012).

1985; Thiébault *et al.* 1994; Ferrière, Baumgartner & Chanier, 2016) are regarded as a distal part of the Pelagonian passive margin passing eastwards to the Maliac–Vardar Ocean (see discussion in Ferrière, Baumgartner & Chanier, 2016).

A progressive transition from platform to deep-water sedimentation of Middle–Late Jurassic age reached its climax with the deposition of clastic deposits characterized by ophiolite-derived elements and tectono-sedimentary mélange. These deposits represent forerunners of the emplacement of the obducting ophiolite nappe (Baumgartner & Bernoulli, 1976; Baumgartner, 1985). In the Argolis Peninsula the oldest ages of ophiolite detritus above the Pelagonian Margin, dated through radiolarian assemblages (Baumgartner, 1985, 1995), show rejuvenation from the transitional facies (i.e. West Maliac Margin Units; middle Callovian – lower Oxfordian) towards the more internal Pelagonian units (i.e. Dhidhimi–Trapezona Composite Unit; middle–upper Oxfordian) and external Pelagonian units (i.e. Adhami Composite Unit; upper Oxfordian – lower Kimmeridgian). Furthermore, the youngest age of the basal ophiolite-bearing sediments above the Pelagonian Platform is late Kimmeridgian – early Tithonian (A. De Bono, unpub. Ph.D. thesis, Univ. Lausanne, 1998) from Central Euboea. This age distribution, in relation to palaeogeographic interpretations of the sedimentary facies

https://doi.org/10.1017/S0016756817000942 Published online by Cambridge University Press

within the Pelagonian Margin (Ferrière, Baumgartner & Chanier, 2016), points to a westward younging of the first ophiolite detritus above the continental margin and seems to reflect the westward advancement of the ophiolite nappe from the Maliac–Vardar Ocean towards the Pelagonian Platform (Baumgartner, 1985; Baumgartner *et al.* 1993).

However, the oldest ophiolitic detritus studied so far in Greece is late Bajocian to late Bathonian – early Callovian in age (Baumgartner *et al.* 1993) and is located within the siliceous mudstones lying above the Pelagonian Platform in Hydra Island (south of the Argolis Peninsula; Baumgartner *et al.* 1993; Baumgartner & Bernoulli, 2015).

In Boeotia and on Euboea Island the shallow-water limestone sedimentation of the Pelagonian Platform is also marked by the occurrence of an emersion episode recorded by laterization and the formation of bauxite horizons of Middle–Late Jurassic age, thus coeval with the first bauxite horizon of the Parnassus Platform (b1; Papastamatiou, 1960; Maratos, Rigopoulos & Athanassiou, 1965, 1967; Katsikatsos, 1979; B. Clément, unpub. Ph.D. thesis, Univ. Lille, 1983; Carras, 1995; Scherreiks *et al.* 2014) and with the oldest ophiolite-bearing detritus on Hydra Island (Baumgartner & Bernoulli, 2015) (Fig. 4).

3.a.2. Boeotian Unit

The Boeotian Unit is represented by a thick Triassic–Jurassic carbonate series topped by a Cretaceous flysch. This geotectonic zone, characterized by pelagic sedimentation since late Middle Jurassic time (Celet & Clément, 1971; Celet, Clément & Ferrière, 1976; B. Clément, unpub. Ph.D. thesis, Univ. Lille, 1983; Robertson *et al.* 1991; Thiébault *et al.* 1994; Danelian & Robertson, 1998; Nirta *et al.* 2015), is classically located between the Pelagonian Platform, to the east, and the Parnassus Platform, to the west.

The stratigraphy of the Boeotian Unit is substantially comparable to that of the external Pelagonian Platform until the Middle Jurassic. A differentiation occurred during Middle Jurassic times when the Boeotian platform started drowning (B. Clément, unpub. Ph.D. thesis, Univ. Lille, 1983; Celet, Clément & Ferrière, 1988). Drowning in the Boeotian Zone was synchronous with broad doming of the Parnassus and westernmost Pelagonian platforms that suffered emersion and laterization (b1 laterite horizon; Papastamatiou *et al.* 1962*b*, 1971; Maratos, Rigopoulos & Athanassiou, 1967). After the emersion event shallow-water sedimentation resumed in the Parnassus Zone while the western borders of the Pelagonian Platform were characterized by progressive deep-water conditions, thus representing a transitional zone to the evolving Boeotian Basin to the west (Fig. 4).

Similarly, the limestone sequence cropping out in the Koziakas area (Central Greece; Fig. 1) is regarded as a transition from the Pelagonian Platform towards the Boeotian and Pindos pelagic basins to the west (R. Ardaens, unpub. Ph.D. thesis, Univ. Lille, 1978; Jaeger, 1980; Ferrière, Chanier & Ditbanjong, 2012).

Pelagic sedimentation in the Boeotian Zone started with radiolarite and siliceous shale, locally pre-dated by cherty limestone, and finally followed by the turbidite deposits of the 'Boeotian Flysch' (Celet & Clément, 1971). The primary contact between the Boeotian Flysch and the underlying radiolarite and limestone basement is rarely preserved because this horizon represented a preferential site of décollement during the Cretaceous and Tertiary deformation phases. However, Danelian & Robertson (1998) reported a primary contact near Makariotissa monastery, where the Triassic to Lower Jurassic shallow-water limestone of the Boeotian Zone is covered by a pelagic sequence composed of limestone and marls of Oxfordian–Kimmeridgian age, which in turn pass upwards to a shale and radiolarite sequence dated to the middle Oxfordian – lower Tithonian and finally to the uppermost Jurassic–Cretaceous Boeotian Flysch (Clément, 1971, 1972; B. Clément, unpub. Ph.D. thesis, Univ. Lille, 1983; Terry & Mercier, 1971; Richter, Müller & Mihm, 1996; Nirta *et al.* 2015).

The Boeotian Flysch was subdivided according to its stratigraphic features, age and composition into two distinct turbiditic systems: the Lower Boeotian Flysch (LBF) of Tithonian–Aptian age and the Upper Boeotian Flysch (UBF) of Cenomanian–Coniacian age (Nirta *et al.* 2015). The LBF was further subdivided into three lithostratigraphic units depicting, as a whole, a thickening– coarsening-upward trend. A composite provenance from oceanic-derived units with minor coarse- and fine-grained inputs from dismantling carbonate platforms is clearly recognizable (Nirta *et al.* 2015). Ophiolite detritus was derived from the ophiolitic nappe obducted onto the Pelagonian Zone (Celet, Clément & Ferrière, 1976; Richter, Müller & Mihm, 1996; Nirta *et al.* 2015), whereas carbonate inputs derived from the neighbouring Parnassus Platform and from ephemeral carbonate platforms set onto the advancing ophiolite nappe (Nirta *et al.* 2015).

The LBF and UBF are separated by a sedimentary hiatus of middle Aptian – late Albian age (Nirta *et al.* 2015). Near Koumaritsi village (Mount Iti, Figs 2, 5) the lowermost UBF sediments seal, through an unconformity surface, deformations of the underlying LBF turbiditic system (Nirta *et al*. 2015).

The UBF in the studied area is represented by two lithostratigraphic units depicting a fining- and thinning-upwards sequence of Cenomanian–Coniacian age (Richter, Müller & Mihm, 1996; Nirta *et al.* 2015). From the Santonian the UBF sequence shows in turn increasing breccia layers composed of neritic limestone, laterite and ophiolitic material that are then unconformably capped by post-nappe sequences consisting of Upper Cretaceous shallow carbonate (Second Mesoautochthonous Cycle; Wigniolle, 1977; Jacobshagen, 1986; Nirta *et al.* 2015).

https://doi.org/10.1017/S0016756817000942 Published online by Cambridge University Press

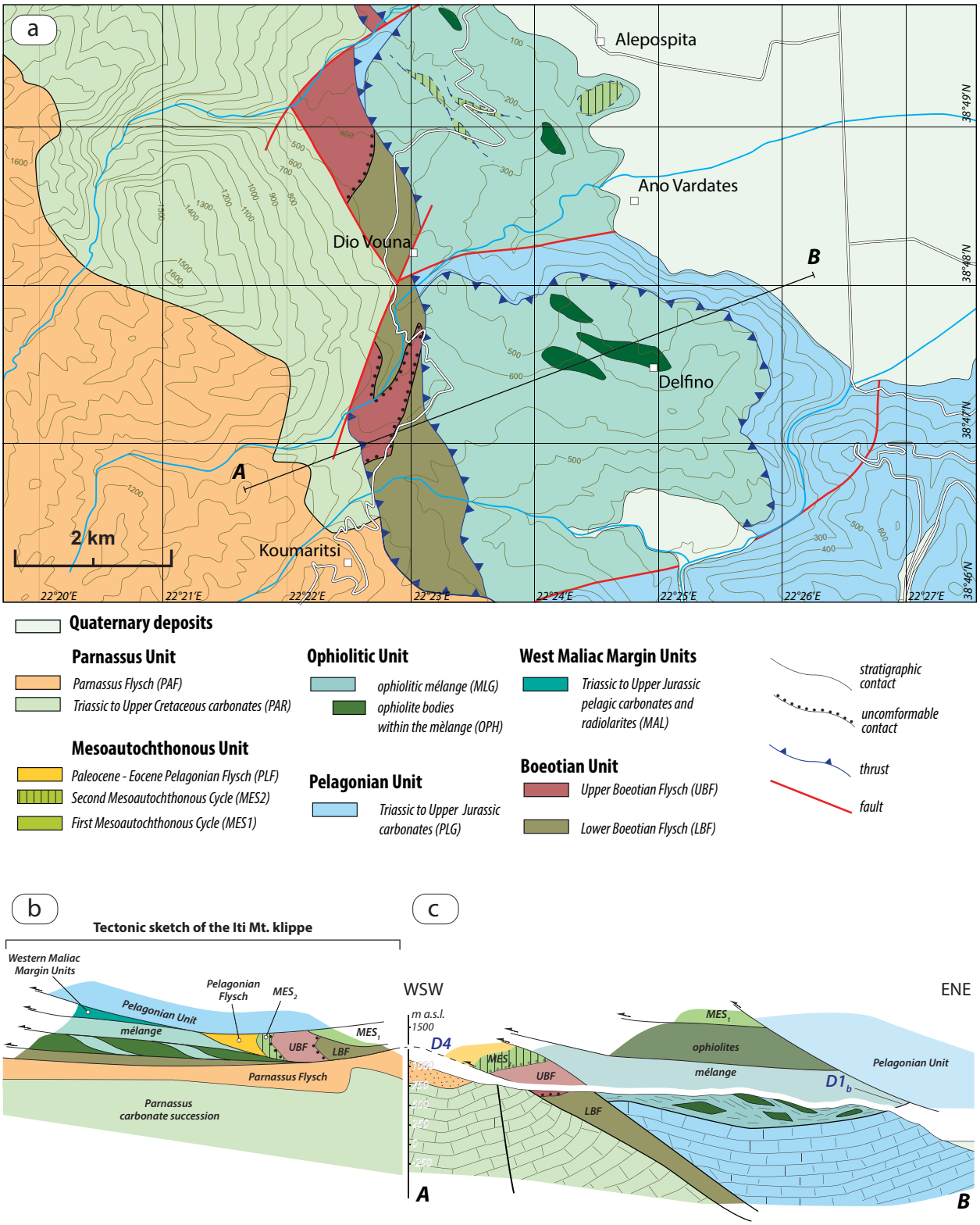


Figure 5. (Colour online) (a) Geological map of the Koumaritsi area (modified after Marinos *et al.* 1967 and Richter Müller & Mihm, 1996), see Figure 2 for location. (b) Sketch structural cross-section of the Mount Iti area (modified after Wigniolle, 1977). (c) Cross-section across the Koumaritsi area.

Steuber *et al.* (1993), although not differentiating the UBF succession from the Mesoautochthonous Complex, recognized a gradual transition from the deep-water clastic successions (namely the UBF) and the shallow-water carbonate succession of the Aptian–Coniacian portion of the Mesoautochthonous Complex (First Mesoautochthonous Cycle, see Section 3.c; Fig. 4).

Although deciphering palaeocurrents is complicated by superimposed tectonic events it is possible to assume a provenance from northern sectors for UBF turbidite currents.

https://doi.org/10.1017/S0016756817000942 Published online by Cambridge University Press

3.a.3. Parnassus Unit

The Parnassus Unit consists of a shallow-water carbonate platform of Late Triassic – Late Cretaceous age that lies between the Pindos and Pelagonian units. It is limited to the north by the Sperchios fault system and to the south by the Corinth Gulf fault system (Fig. 2). These still active tectonic structures (Kilias *et al.* 2008; Jolivet *et al.* 2010; Taylor *et al.* 2011) are thought to have been inherited from lithospheric structures active in the Middle Triassic – Middle Jurassic period (Brunn, 1956; Fleury, 1980; Ferrière, 1982; Ferrière, Baumgartner & Chanier, 2016), thus driving the development of the Parnassus Platform as a distinct isopic zone within the eastern Adria continental margin.

The Parnassus Unit is composed of a 1800 m thick carbonate sequence resulting from continuous carbonate platform sedimentation from Triassic to Late Cretaceous times in a shallow-water marine environment (Renz, 1955; Papastamatiou, 1960; Celet, 1962; Carras, 1995).

Three main emersion episodes punctuated the shallow-water deposition resulting in karstification. These correspond to three major stratigraphic discontinuous horizons marked by bauxitic material, named b1 (upper Bathonian/lower Callovian – upper Oxfordian), b2 (upper Tithonian) and b3 (Aptian–lower Turonian) (Carras & Tselepidis, 2001 and references therein). Mineralogical, geochemical and sedimentological studies indicate that bauxitic material derived from erosion, transport and reworking of lateritic bauxites developed at the expense of mafic and ultramafic rocks that suffered alteration in a warm climate (Aronis, 1955; Combes, 1977, 1979, 1984; B. Clément, unpub. Ph.D. thesis, Univ. Lille, 1983; Valeton *et al.* 1987).

Pelagic sedimentation took place during latest Cretaceous time (Campanian–Maastrichtian) with deposition of platy limestone with chert. Condensed sedimentation followed during the Cretaceous–Tertiary (K–T) boundary with the formation of iron-phosphate-rich hardgrounds (Papastamatiou, 1960; Celet, 1962; Richter & Mariolakos, 1974*a*,*b*, 1975; Kalpakis, 1979; Solakius, Pomoni-Papaioannou & Marangoudakis, 1989; Pomoni-Papaioannou & Solakius, 1991; Carras & Tselepidis, 2001). Sedimentation resumed in Paleocene time in a pelagic environment with deposition of thin-bedded limestone (Gregou, Solakius & Pomoni-Papaioannou, 1994) followed by a thick succession of red marls ('Pre-Flysch'; Gregou, 1996; Gregou & Solakius, 1997), and finally topped by siliciclastic flysch of late Paleocene–Eocene age. The diachronous establishment of pelagic sedimentation in the Parnassus Zone was a consequence of tectonics at the K–T transition that produced pronounced relief with horst and graben geometry (Richter & Mariolakos, 1975; Gregou, Solakius & Pomoni-Papaioannou, 1994; Richter *et al.* 1995). The seafloor was then levelled in early Eocene time just before flysch sedimentation (Gregou, 1996).

The western transition of the Parnassus Zone towards the Pindos pelagic basin occurs with the interposition of the Vardoussia and Penteoria units, characterized by deeper slope and sea-mount facies, respectively (Papastamatiou, 1960; Papastamatiou *et al.* 1962*a*; Celet, 1962, 1979; R. Ardaens, unpub. Ph.D. thesis, Univ. Lille, 1978; Fleury, 1980). The Vardoussia Unit comprises a Middle Triassic volcanic event related to continental extension (Lefèvre *et al.* 1993; Pe-Piper, 1998) followed by pelagic carbonate and siliceous deposits of Jurassic–Cretaceous age, and finally topped by Eocene siliciclastic flysch. Neritic sedimentation was limited temporally (Triassic, under the Penteoria condensed series). Coarse breccia deposits containing shallow-water limestone clasts were recognized at different stratigraphic levels within the pelagic deposition, testifying to the vicinity of the dismantling carbonate platform (i.e. the Parnassus Platform; R. Ardaens, unpub. Ph.D. thesis, Univ. Lille, 1978; Fig. 4).

West of the Parnassus/Vardoussia units the Pindos Unit consists of Triassic to Upper Cretaceous pelagic carbonate, radiolarite and shale, overlain by Paleocene–Eocene syn-orogenic flysch (Pindos Flysch; Richter, Mariolakos & Risch, 1978). In the Etolia region, west of the frontal thrust of the Vardoussia Unit above the Pindos Unit, the Pindos Flysch encloses a continuous level of slide blocks and debris flow deposits bearing ophiolitic material (Celet, 1962, 1979; C. Beck, unpub. Ph.D. thesis, Univ. Science and Technology, Lille, 1975; Fig. 4). Where preserved by Tertiary tectonic movements, the relationships of ophiolitic mass flow deposits with the Pindos Flysch are clearly stratigraphic. Even if the larger ophiolitic blocks show unclear relationships with the flysch, the presence of ophiolite-bearing debris flow deposits closely associated with the huge blocks permits considering the latter also as slide blocks (Beck, 1980). Alternatively, this ophiolite-bearing material is regarded as a remnant of the closure, during the Tertiary compressive phases, of a small strand of the Pindos 'Ocean' (Kerassia-Milia 'Ocean'; Robertson *et al.* 1991; Robertson & Degnan, 1993; Pe-Piper & Hatzipanagiotou, 1993) that bordered to the west the Parnassus Platform, which is thus isolated as a microcontinent, the main branch of the Pindos 'Ocean' being located to the east of it (Robertson & Degnan, 1993).

Further moving towards the west, thus towards the undeformed Adria margin, the Pindos Unit structurally overlies the Gavrovo–Tripolitza Unit in the west that, in turn, overthrusts the Ionian Unit, and this latter thrusts onto the Apulian Unit.

3.b. Ocean-derived units

Obduction is the most widely accepted emplacement mechanism for the ophiolitic bodies widespread throughout the Dinaric–Hellenic orogen. A major constraint for this kind of process is the presence at

https://doi.org/10.1017/S0016756817000942 Published online by Cambridge University Press

the base of the ultramafic mantle section of slices of HT–LP metamorphic rocks (amphibolite sole). Metamorphism is assumed to have been acquired by underplated units soon after the inception of intraoceanic thrusting of a young and exceptionally hot ophiolite nappe originated near the spreading axis (Spray *et al.* 1984; Carosi *et al.* 1996; Searle & Cox, 1999; Dimo-Lahitte, Monié & Vergély, 2001; Myhill, 2011).

Continuing thrusting of the ophiolite nappe was also linked with the production of a 'tectono-sedimentary mélange' supplied by both the ophiolite thrust sheets and from off-scraping of pelagic shaly-siliceous sediments from the overthrust ocean bottom. Major slide block and tectonic slivers originated from the ophiolite thrust sheets and scraped-off sediments from the underplating of both oceanic and continental margin units were also embedded in the mélange matrix. Today, ophiolites and obduction-related mélange are arranged along two main belts separated by the Pelagonian continental units and its continuation to the north (i.e. the Korab Unit in Albania and Drina–Ivanjica Unit in Serbia; Fig. 1). However, this distinction is not evident in Bosnia where the Drina–Ivanjica and Durmitor units are overthrust by a unique and continuous ophiolite nappe (Schmid *et al.* 2008).

In the studied area the Ophiolitic Unit is mostly represented by sheared shaly-sandy matrix chaotically enveloping rock fragments of both oceanic and continental origin (Ophiolitic Mélange) and dismembered portions of the ophiolite nappe mainly represented by serpentinized harzburgite and lherzolite. The main ophiolite occurrences are located in Mount Iti, the Kallidromon Mountains and near Aliki Village on the Corinth Gulf (Figs 2, 6). Large slivers of amphibolite sole were observed within the ophiolitic mélange in a small abandoned quarry near Agios Georgios village and in small blocks east of Agia Triada village (Fig. 6). Amphibolite sole underlies the ophiolite nappe of Mount Iti (northwest of Pyra village) and in the Gerania Mountains (Kaplanis *et al.* 2013).

3.c. Upper Cretaceous sedimentation (Mesoautochthonous Complex)

A thick sequence of Aptian to Upper Cretaceous shallow-water carbonates sealed older deformations recorded in the tectonic stack composed by the ophiolitic, Pelagonian and Boeotian units. These sediments, known as the Mesoautochthonous Complex (Jacobshagen, 1986) or sediments of the 'Cretaceous transgression' (Photiades *et al.* 2007; Fazzuoli *et al.* 2008), are widespread in all of the Hellenic–Dinaric Belt with a similar tectonic position and sedimentation age. The Mesoautochthonous Complex also unconformably covers tectonized remnants of an older carbonate platform possibly sedimented above the ophiolite nappe during obduction and seals the syn-obduction deformations they recorded (Bortolotti *et al.* 2004*a*; Fazzuoli & Carras, 2007). The existence of syn-obduction Late Jurassic to Valanginian carbonate platforms is testified to throughout the Dinaric–Hellenic orogen by tectonized remnants above ophiolites (Bortolotti *et al.* 2004*a*; Schlagintweit *et al.* 2006; Photiades *et al.* 2007) and, in most of the cases, by clasts and slide blocks resedimented, after total dismantling episodes, within the ophiolitic mélange, or within Late Jurassic – Early Cretaceous foreland basins (e.g. the Pogari Formation in Serbia, Firza Flysch in Albania, Lower Boeotian Flysch in Greece; Blanchet *et al.* 1970; Schlagintweit *et al.* 2008; Nirta *et al.* 2015).

Based on their age, substratum and main sequence boundaries, we propose a subdivision of the Mesoautochthonous Complex into two main sedimentary cycles. Sedimentation above the ophiolite nappe and the Pelagonian Unit generally starts in Aptian/Albian–Cenomanian times above a level of karstic or redeposited laterites lasting, without regional unconformities, until Coniacian–Santonian times (First Mesoautochthonous cycle, MES_1; B. Clément, unpub. Ph.D. thesis, Univ. Lille, 1983; Photiades *et al.* 2007; Fazzuoli & Carras, 2007). A younger sedimentation cycle of late Santonian – Maastrichtian age, also underlined by an unconformity, is present above the ophiolites and the UBF (Second Mesoautochthonous cycle, MES_2; E. Wigniolle, unpub. Ph.D. thesis, Univ. Lille, 1975; Steuber *et al.* 1993).

In Boeotia and Attica, stratigraphic contacts of the MES_1 were described in the Avlona area (northern Attic region), above ophiolites (B. Clément, unpub. Ph.D. thesis, Univ. Lille, 1983), and in the Aliartos (Fig. 2) and Mandra-Megara areas (Elefsina Gulf, Attica region) above the Pelagonian carbonates (B. Clément, unpub. Ph.D. thesis, Univ. Lille, 1983; Steuber *et al.* 1993). The MES_1 is coeval and partially heteropic with the UBF (Steuber *et al.* 1993) that in turn unconformably seals the deformed Tithonian–Aptian LBF (Nirta *et al.* 2015) (Fig. 4).

Primary contacts of the MES_2 above the UBF were preserved in Mount Iti (E. Wigniolle, unpub. Ph.D. thesis, Univ. Lille, 1975) (Fig. 5) and above ophiolites located northeast of Levadhia (Dionysos–Pavlos area; Steuber *et al.* 1993; Fig. 2). In the Levadhia and Jerolekas (northern Parnassus; Fig. 2) areas the basal primary contact of the MES_2 is underlined by ophiolite-bearing conglomerate deposits with abundant laterite clasts and a rudist fauna of Santonian–Campanian age (Steuber, Raeder & Walter, 1994; Steuber, 1999; Morycowa & Marcopoulou-Diacantoni, 2002). Conglomerates unconformably cover the lower Cenomanian MES_1 limestone after an episode of emersion and laterization (Steuber, Raeder & Walter, 1994).

Similarly to the Parnassus Unit, reddish marls and shale of middle–late Paleocene age underlie the siliciclastic turbiditic sedimentation of late Paleocene–Eocene age (Pelagonian Flysch) above the Campanian–Maastrichtian limestone of the MES_2 (Wigniolle, 1977; Richter, Müller & Risch, 1996).

https://doi.org/10.1017/S0016756817000942 Published online by Cambridge University Press



Figure 6. (Colour online) Tectonic–geological map of Boeotia (location in Fig. 2). New data and observations integrate and modify former mapping by Papastamatiou *et al.* (1962*b*, 1971), Maratos, Rigopoulos & Athanassiou (1965, 1967) and B. Clément, unpub. Ph.D. thesis, Univ. Lille (1983). DSTF – Distomon Fault; ATRF – Agia Triada Fault; ALKF – Aliki Fault.

4. Biostratigraphic data

With the aim of refining the age of key stratigraphic events, sampling was performed in the Pelagonian, Boeotian and Parnassus units. Radiolarian, nannofossil and foraminiferal associations were analysed after sampling the following stratigraphic units in the Iti, Kallidromon, Parnassus and Boeotia areas (Figs 2, 4): (i) mass flow deposits on top of the Jurassic carbonates of the Pelagonian Unit; (ii) Lower Boeotian Flysch (LBF, Boeotian Unit); (iii) Mesoautochthonous sequences; (iv) Parnassus Flysch (Parnassus Unit), Pelagonian Flysch (Pelagonian Unit).

The biozonations adopted for dating the calcareous nannofossil assemblages use the CNP and CNE zones proposed by Agnini *et al.* (2014) with the corresponding standard NP zones of Martini (1971) for the Paleocene and Eocene, and the CC zones of Sissingh (1977) for the Early Cretaceous period. Tables 1–6 report the calcareous nannofossil taxa recognized according to the taxonomy proposed by Perch-Nielsen (1985*a*,*b*) and Bown (1998). Total abundance in every sample was categorized as follows: common – C $\geq$ 10 specimens per FOV (field of view); frequent/few – F $\geq$ 1 specimens per FOV; rare/very rare – R/VR $\leq$ 1 specimens per FOV. Quantitative analyses were

https://doi.org/10.1017/S0016756817000942 Published online by Cambridge University Press

Table 1. Nannofossil associations in the LBFa Unit

			LBFa									
Sample	Number of specimens observed	Preservation	*Conusphaera mexicana*	*Watznaueria* spp.	*Nannoconus* spp.	*Polycostella beckmannii*	*Cyclagelosphaera margerelii*	*Diazomatolithus lehmanii*	*Hexalithus noeliae*	*Zeugrhabdotus embergeri*	*Cruciellipsis cuvillieri*	Age
GR70	300	P	1.0	50.0	43.3	0.6	4.0	0.3	0.0	0.6	cf.	late Tithonian – early Berriasian
GR69	300	P	37.6	47.0	6.0	7.3	1.0	1.0	0.3	0.0	0.0	middle – late Tithonian

performed only in samples GR69–70 where at least 300 specimens were counted. Preservation was evaluated as between poor (P) and bad (B), on account of both heavy etching and dissolution.

4.a. Siliceous deposits and mass flow deposits on top of the Jurassic carbonates of the Pelagonian Unit (Iti and Kallidromon areas)

In the Iti area, E. Bléhaut (unpub. Ph.D. thesis, Univ. Lille, 1975) and E. Wigniolle (unpub. Ph.D. thesis, Univ. Lille, 1975) described several sections of detritic material stratigraphically topping the Pelagonian limestone. On the whole, the sequence consists of Upper Jurassic neritic limestone passing upwards to siliceous limestone, radiolarite and shale (*c.* 10 m thick), thin-bedded turbidites (*c.* 20 m thick) and finally decametric levels of ophiolite-bearing cohesive debris flow deposits.

Three samples rich in radiolarian fauna (samples G03, G04, G05; Fig. 7) were collected on the northern flank of Tsikeri Mountain (about 2 km east of Pyra village; 38° 44′ 57.1″ N, 22° 17′ 54.2″ E; Fig. 2), in an overturned sequence characterized by a thin-bedded turbidite stratigraphically overlain by metre-thick cohesive debris flow deposits containing ophiolite material. The turbidite strata are geometrically overlain, through a tectonic contact, by siliceous limestone and bedded limestone of the Pelagonian Platform. In turn the mass flow sequence tectonically overlies the Parnassus Flysch with interposing slices of Boeotian Flysch (Fig. 5b). Unfortunately, the samples are always characterized by poor preservation of the radiolarian forms hampering dating. Nevertheless, the common presence in these samples of the nannofossil *Watznaueria barnesiae* and the lithostratigraphic similarities with other well-dated sections (see Baumgartner & Bernoulli, 1976) allow us to tentatively attribute a Late Jurassic – Early Cretaceous age to these deposits.

In the Kallidromon Mountains foothills, 1.4 km west of Xyliki village, siliceous limestone and shaly-radiolarite strata top a well-bedded Pelagonian limestone succession. This is interrupted by the thrust of the above ophiolitic mélange and ophiolite nappe (Fig. 6 and cross-section A–A′ in Fig. 8). Samples were collected in the siliceous limestone (GR63, GR64, GR66) and in the shaly-radiolarite section (GR65, GR67, GR68) (Fig. 7).

The following radiolarian assemblage was obtained from sample GR66: *Archaeodictyomitra apiarium* (Rüst), *Archaeodictyomitra* aff. *apiarium* (Rüst), *Archaeodictyomitra* cf. *apiarium* (Rüst), *Archaeodictyomitra* sp., *Campanomitra* cf. *tuscanica* (Chiari, Cortese & Marcucci), *Cinguloturris* (?) sp., *Crococapsa* sp., *Loopus* cf. *blabla* (Schaaf) *sensu* Dumitrica, Immenhauser & Dumitrica-Jud (1997), *Protunuma* sp., *Thanarla patricki* gr. (Kocher), *Transhsuum* sp., *Xitus* cf. *normalis* (Wu & Li), *Xitus* (?) sp., *Zhamoidellum ovum* Dumitrica, *Zhamoidellum*

https://doi.org/10.1017/S0016756817000942 Published online by Cambridge University Press

Table 2. Nannofossil associations in the LBFb Unit

			LBFb	
Sample	Abundance	Preservation	Calcareous Nannofossil Assemblage	Age
GR09	F	B	*Assipetra infracretacea, Calcicalathina oblongata, Cyclagelosphaera margerelii, Cruciellipsis cuvillieri, Diazomatolithus lehmanii, Lithraphidites carniolensis, Micrantholithus hoschulzii, Micrantholithus obtusus, Nannoconus* sp., *Nannoconus steinmannii, Retecapsa angustiforata, Watznaueria* spp., *Zeugrhabdotus embergeri*	late Valanginian – early Hauterivian CC3-CC4 p.p.
GR22	F	B	*Assipetra infracretacea, Calcicalathina oblongata, Cyclagelosphaera margerelii, Cruciellipsis cuvillieri, Diazomatolithus lehmanii, Helenea chiastia, Nannoconus* sp., *Nannoconus steinmannii, Retecapsa crenulata, Watznaueria* spp., *Zeugrhabdotus embergeri*	late Valanginian – early Hauterivian CC3-CC4 p.p.
GR23	F	B	*Assipetra infracretacea, Cretarhabdus* sp., *Cyclagelosphaera margerelii, Diazomatolithus lehmanii, Micrantholithus hoschulzii, Helenea chiastia, Nannoconus* sp., *Watznaueria* spp., *Zeugrhabdotus embergeri*	Early Cretaceous
GR25	F	B	*Assipetra infracretacea, Calcicalathina oblongata, Cyclagelosphaera margerelii, Cretarhabdus* sp., *Cruciellipsis* cf. *cuvillieri*, *Diazomatolithus lehmanii, Helenea chiastia, Rucinolithus wisei, Watznaueria* spp., *Zeugrhabdotus embergeri*	late Valanginian CC3 p.p.
GR38	VR	B	*Assipetra* sp., *Braarudosphaera* sp., *Micrantholithus* sp., *Micrantholithus obtusus*, *Nannoconus* sp., *Watznaueria* sp.	Early Cretaceous
GR39	F	B	*Assipetra infracretacea, Calcicalathina oblongata, Diazomatolithus lehmanii, Micrantholithus hoschulzii, Nannoconus* spp., *Watznaueria* spp., *Zeugrhabdotus embergeri*	late Hauterivian CC5
GR54	C	P	*Assipetra infracretacea, Calcicalathina oblongata, Cyclagelosphaera margerelii, Lithraphidites bollii, Helenea chiastia, Micrantholithus* sp., *Micrantholithus hoschulzii, Nannoconus* sp., *Nannoconus circularis, Nannoconus inornatus, Watznaueria* spp., *Zeugrhabdotus embergeri*	late Hauterivian – early Barremian CC4 p.p.-CC5 p.p.

cf. *ovum* Dumitrica, *Zhamoidellum* cf. *ventricosum* Dumitrica. This assemblage allow the attribution of a middle Callovian – early Oxfordian to late Kimmeridgian – early Tithonian age (UAZ. 8–11; UA zones after Baumgartner *et al.* 1995*a*) based on the occurrence of *Archaeodictyomitra apiarium* (Rüst) with *Zhamoidellum ovum* Dumitrica (ranges after Baumgartner *et al.* 1995*b*; Smuc & Goričan, 2005) (Fig. 9).

4.b. Lower Boeotian Flysch

Biostratigraphic investigations in the Levadhia area allow the refinement of the ages of the lithostratigraphic Units A and B of the Lower Boeotian Flysch (LBFa and LBFb; see Nirta *et al.* 2015 for details). The lowermost portion of unit LBFa, detached from its substratum, was sampled 4.5 km west of Levadhia (Fig. 10). According to Bornemann, Aschwer & Mutterlose (2003), the nannofossil assemblages in samples GR69–70 (Fig. 7) allow the attribution of a middle–late Tithonian to early Berriasian age to the older sediments of the LBF on account of the dramatic increase of nannoconids (from 6 % to above 40 %) and the contemporary decrease of *Conusphaera mexicana* (from above 30 % to 1 %) and *Polycostella beckmannii* (from above 7 % to below 1 %) (see Table 1). The samples collected in unit LBFb in different outcrops located along the Levadhia–Arachova road (samples GR09, GR22–23, GR25, GR38–39, GR54; Fig. 7) allow us to constrain an age spanning from late Valanginian to the Hauterivian–Barremian boundary, based on the presence of *Rucinolithus wisei*, *Calcicalathina oblongata*, *Cruciellipsis cuvillieri*, common nannoconids and *Lithraphidites bollii* (zones CC3–CC5 p.p.; see Table 2).

4.c. The Mesoautochthonous Complex

This unit was sampled northwest of Levadhia, in overturned sections linked with imbricate thrusts exposed from the Distomon Fault to Cheronia village (Figs 10, 11).

In the Cheronia area the stratigraphically lowermost levels of the Mesoautochthonous Complex are represented by platform material resedimented in a slope environment with a reddish bauxitic matrix (sample GR04; Fig. 7). The fossil assemblage consisting of *Orbitolina* cf. *conica* (D'Archiac), *Ticinella* cf. *roberti* Gandolfi and abundant Radiolitidae, Caprinidae, bryozoa and echinoderm fragments allows the attribution

https://doi.org/10.1017/S0016756817000942 Published online by Cambridge University Press

Table 3. Nannofossil associations in the pre-flysch facies of the Parnassus Flysch

			Pre-flysch – Parnassus	
Sample	Abundance	Preservation	Calcareous Nannofossil Assemblage	Age
G25a	F	P	*Coccolithus pelagicus, Discoaster multiradiatus, Sphenolithus moriformis, Toweius callosus, Toweius pertusus, Toweius rotundus, Toweius selandianus, Zygrhablithus bijugatus*	Ypresian CNE2/NP10
G26a	F	P	*Coccolithus pelagicus, Discoaster* cf. *delicatus, Discoaster multiradiatus, Ericsonia subpertusa, Prinsius* sp., *Prinsius martinii, Sphenolithus moriformis, Toweius rotundus, Toweius pertusus*	Ypresian CNE2/NP10
G27a	F	P	*Coccolithus pelagicus, Discoaster multiradiatus, Fasciculithus* sp., *Fasciculithus tympaniformis, Sphenolithus moriformis, Toweius pertusus*	Thanetian CNP11/NP9
GR33	C	P	*Coccolithus pelagicus, Discoaster* sp., *Fasciculithus alanii, Fasciculithus lillianae, Fasciculithus schaubii, Fasciculithus tympaniformis, Fasciculithus thomasii, Prinsius* sp., *Sphenolithus moriformis, Toweius eminens, Toweius pertusus, Zygrhablithus bijugatus*	Thanetian CNP11/NP9
GR35	R	P	*Cyclicargolithus floridanus, Dictyococcites* sp., *Sphenolithus radians, Sphenolithus moriformis, Reticulofenestra dictyoda*	Impoverished assemblage compatible with Ypresian CNE5/NP13

Table 4. Nannofossil associations in the Parnassus Flysch

			Parnassus Flysch	
Sample	Abundance	Preservation	Calcareous Nannofossil Assemblage	Age
GR31	C	P	*Cyclicargolithus floridanus, Chiasmolithus solitus, Chiasmolithus nitidus, Dictyococcites* sp., *Discoaster kuepperi, Girgisia gammation, Ericsonia formosa, Sphenolithus radians, Sphenolithus spiniger, Reticulofenestra dictyoda, Reticulofenestra hillae*	Ypresian CNE5/NP13
GR32	C	P	*Cyclicargolithus floridanus, Dictyococcites* sp., *Discoaster kuepperi, Discoaster lodoensis, Girgisia gammation, Ericsonia formosa, Sphenolithus radians, Coccolithus crassus* (=*Toweius crassus*), *Zygrhablithus bijugatus*	Ypresian CNE5/NP13
G19	C	B	*Coccolithus pelagicus, Chiasmolithus* sp., *Discoaster lodoensis, Discoaster* sp., *Ericsonia subpertusa, Sphenolithus moriformis, Sphenolithus radians, Pontosphaera* sp., *Toweius pertusus, Zygrhablithus bijugatus*	Ypresian CNE4?/NP12?

of a late Albian age to the penecontemporaneous bioclasts. This datum is in good accordance with the contemporaneous subaerial exposure and laterization of the Parnassus Platform and of wide areas of the more external Pelagonian Platform. The sampled section possibly represents the base of the First Mesoautochthonous sedimentary cycle (MES_1).

The carbonate levels sampled in another overturned section exposed further west, near the Distomon Fault (DSTF in Fig. 6) and just above the tectonic contact with the underlying Pelagonian Flysch (Fig. 12), are attributed a late Campanian – Maastrichtian age on the basis of the following microfauna assemblage: *Siderolites calcitrapoides* Lamarck, *Cuneolina pavonia* D'Orbigny (fragment), *Lepidorbitoides* sp., *Orbitoides* sp., *Rugoglobigerina* sp., *Griphoporella*? sp., fragments of Corallinaceae, Radiolitidae, stromatoporoids and echinoderms (sample GR46; Fig. 7). Upwards, the sedimentation shifts towards pelagic conditions with deposition of marls and marly limestones. A single sample (GR45) collected in the marly sequence gave the following nannofossil assemblage: *Coccolithus pelagicus*, *Chiasmolithus* sp., *Chiasmolitus danicus*, *Bomolithus* sp., *Ericsonia subpertusa*, *Ericsonia robusta*, *Fasciculithus* sp., *Fasciculithus billii*, *Fasciculithus janii*, *Fasciculithus pileatus*, *Fasciculithus tympaniformis*, *Fasciculithus ulii*, *Heliolithus* sp., *Prinsius bisulcus*, *Sphenolithus* sp., *Sphenolithus anarrhopus*, *Sphenolithus moriformis*, *Thoracosphaera* sp., *Toweius pertusus*, *Toweius rotundus*. This association allows the attribution of a late Paleocene age to this pelagic transition (Selandian–Thanetian Zone CNP8, corresponding to zones NP5 p.p.–NP6). As a whole, this sequence is possibly attributable to the upper part of the Second Mesoautochthonous sedimentary cycle (MES_2).

4.d. Parnassus Flysch

Samples were collected in the lower part of the pre-flysch facies near the contact with the carbonate substratum at several sites on Mount Parnassus and in

https://doi.org/10.1017/S0016756817000942 Published online by Cambridge University Press

Table 5. Nannofossil associations in the pre-flysch facies of the Pelagonian Flysch

			Pre-Flysch – Pelagonian	
Sample	Abundance	Preservation	Calcareous Nannofossil Assemblage	Age
GR50	F	P	*Coccolithus pelagicus, Discoaster* sp., *Ellipsolithus macellus, Ericsonia subpertusa, Prinsius bisulcus, Prinsius* cf. *martinii, Toweius rotundus, Toweius pertusus, Toweius callosus, Sphenolithus moriformis*	early Eocene
GR51a	R	B	*Coccolithus pelagicus, Discoaster* sp., *Prinsius* sp., *Toweius rotundus, Toweius pertusus, Toweius callosus, Sphenolithus moriformis, Zygrhablithus bijugatus*	early Eocene
GR51b	C	P	*Coccolithus pelagicus, Chiasmolithus bidens, Discoaster* sp., *Discoaster mohleri, Discoaster* cf. *diastypus, Girgisia gammation* (=*Toweius gammation*), *Ericsonia* cf. *formosa, Sphenolithus radians, Sphenolithus editus, Toweius callosus, Toweius pertusus, Toweius rotundus, Zygrhablithus bijugatus, Zygrhablithus bijugatus nolfi*	Ypresian CNE3/NP11
GR48	R	B	*Coccolithus pelagicus*, cf. *Discoaster* sp., *Ericsonia subpertusa, Fasciculithus* sp., *Sphenolithus* sp., *Sphenolithus moriformis, Toweius callosus, Toweius rotundus, Toweius pertusus, Toweius* sp., *Zygrhablithus bijugatus*	late Paleocene – early Eocene
GR42	R	B	*Coccolithus pelagicus, Ellipsolithus macellus, Fasciculithus* sp., *Sphenolithus* sp., *Sphenolithus anarrhopus*	late Paleocene
GR43	F	B	*Coccolithus pelagicus, Chiasmolithus* sp., *Discoaster* sp., *Ericsonia subpertusa, Fasciculithus* sp., *Fasciculithus schaubii, Fasciculithus tympaniformis, Heliolithus* sp., *Prinsius bisulcus, Sphenolithus* sp., *Toweius* sp.	Thanetian CNP11/NP9
GR44	F	B	*Coccolithus pelagicus, Chiasmolithus* sp., *Discoaster* sp., *Ericsonia subpertusa, Fasciculithus* sp., *Fasciculithus lillianae, Fasciculithus tympaniformis, Prinsius bisulcus, Sphenolithus* sp., *Sphenolithus anarrhopus, Sphenolithus moriformis, Toweius pertusus, Toweius rotundus*	Thanetian CNP11/NP9
GR06	C	P	*Coccolithus pelagicus, Chiasmolithus danicus, Discoaster* sp., *Discoaster* cf. *mohleri*, *Fasciculithus magnicordis, Fasciculithus tympaniformis, Fasciculithus ulii, Prinsius bisulcus, Sphenolithus moriformis, Sphenolithus anarrhopus, Toweius eminens, Toweius pertusus*	Thanetian CNP9/NP7 p.p.
GR07	C	P	*Coccolithus pelagicus, Chiasmolithus danicus, Discoaster* sp., *Discoaster* cf. *mohleri, Fasciculithus magnicordis, Fasciculithus tympaniformis, Fasciculithus ulii, Prinsius bisulcus, Sphenolithus moriformis, Sphenolithus anarrhopus, Toweius eminens, Toweius pertusus*	Thanetian CNP9/NP7 p.p.
GR52	F	B	*Coccolithus pelagicus, Chiasmolithus bidens, Ericsonia* cf. *robusta, Fasciculithus clinatus, Fasciculithus tympaniformis, Fasciculithus* sp., *Heliolithus* sp., *Heliolithus kleinpellii, Prinsius bisulcus, Toweius pertusus, Toweius magnicrassus, Toweius* sp., *Sphenolithus anarrhopus*	Selandian–Thanetian CNP8/NP5 p.p.–NP6

Table 6. Nannofossil associations in the Pelagonian Flysch

			Pelagonian Flysch	
Sample	Abundance	Preservation	Calcareous Nannofossil Assemblage	Age
GR08	R	P	*Cyclicargolithus floridanus, Coccolithus pelagicus, Dictyococcites* sp., *Sphenolithus* spp.	Impoverished assemblage compatible with Ypresian CNE5/NP13
GR47	R	B	*Coccolithus pelagicus*, cf. *Discoaster* sp., *Ericsonia subpertusa, Prinsius bisulcus, Sphenolithus* sp., *Sphenolithus moriformis, Toweius callosus, Toweius magnicrassus*, cf. *Zygrhablithus bijugatus*	early Eocene
GR49	C	P	*Coccolithus pelagicus, Discoaster kuepperi, Discoaster lodoensis, Girgisia gammation, Ericsonia subpertusa, Sphenolithus radians, Coccolithus crassus, Toweius magnicrassus, Tribrachiatus orthostylus*	Ypresian CNE4/NP12

https://doi.org/10.1017/S0016756817000942 Published online by Cambridge University Press

https://doi.org/10.1017/S0016756817000942 Published online by Cambridge University Press

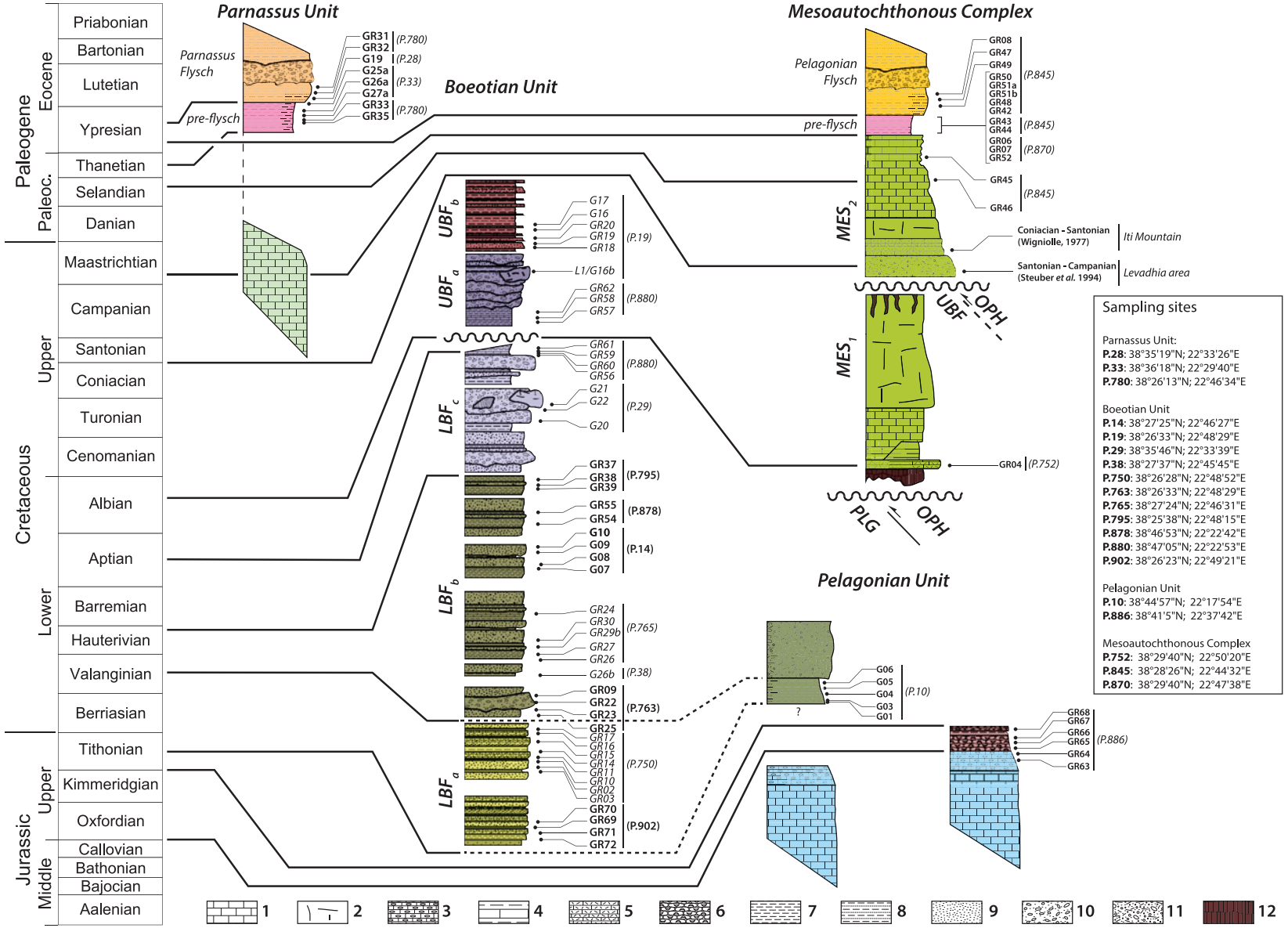


Figure 7. (Colour online) Schematic lithostratigraphic columns of the sampled units. Samples in bold are analysed in this work; samples in italic were analysed in Nirta *et al.* (2015). 1 – bedded limestone; 2 – massive limestone; 3 – cherty limestone; 4 – shale and fine-grained limestone; 5 – calcarenites; 6 – radiolarite and shale; 7 – shale; 8 – fine-grained sandstone and shale; 9 – coarse-grained sandstone; 10 – cohesive and granular debris flow deposit; 11 – ophiolite-bearing mass flow deposits and slide blocks; 12 – laterite. Dating of radiolarian chert from the Pelagonian Unit is expressed as the minimum age range.

https://doi.org/10.1017/S0016756817000942 Published online by Cambridge University Press

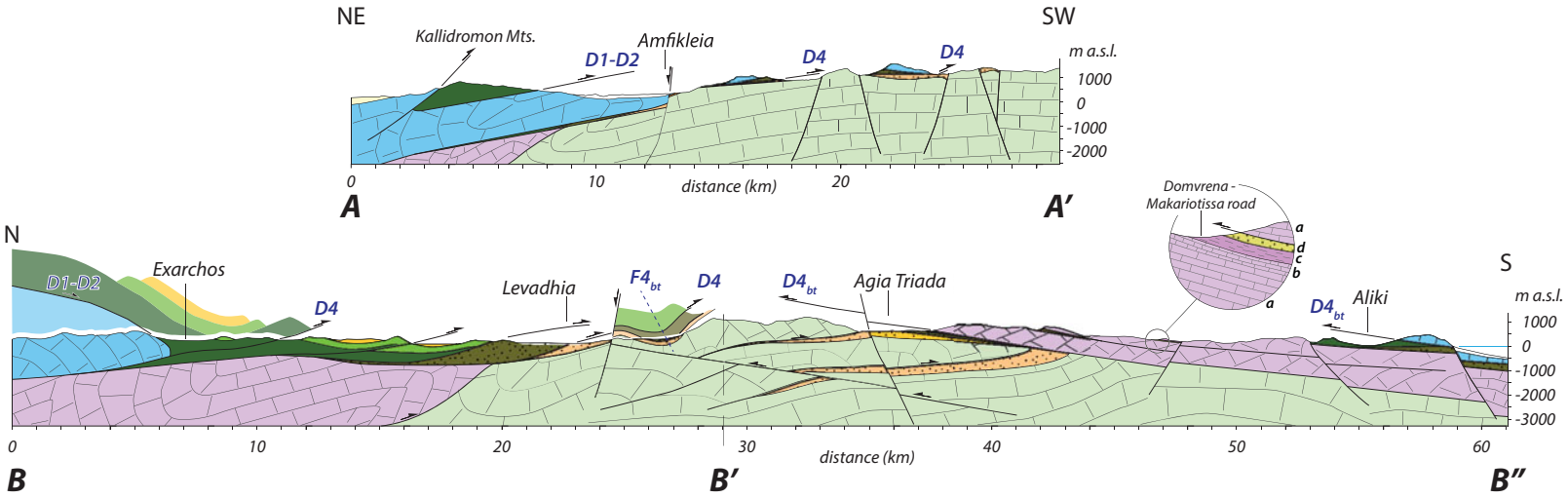


Figure 8. (Colour online) Regional geological cross-sections across the Boeotia region (see Fig. 6 for location and legend). The basal portion of the Lower Boeotian Flysch cropping out in the Domvrena–Makariotissa area is described in the circle: a – Triassic – Lower Jurassic neritic limestone; b – Middle–Upper Jurassic pelagic limestone and siliceous limestone; c – Upper Jurassic radiolarian cherts and shale; d – Upper Jurassic ophiolite-bearing mass flows, shales and marlstones (Lower Boeotian Flysch) (modified after B. Clément, unpub. Ph.D. thesis, Univ. Lille, 1983). D1, D2, D4, $D4_{bt}$ – tectonic contacts with deformation phase attribution (see Section 5.c for details); $F4_{bt}$ – $D4_{bt}$ deformation phase megafold.

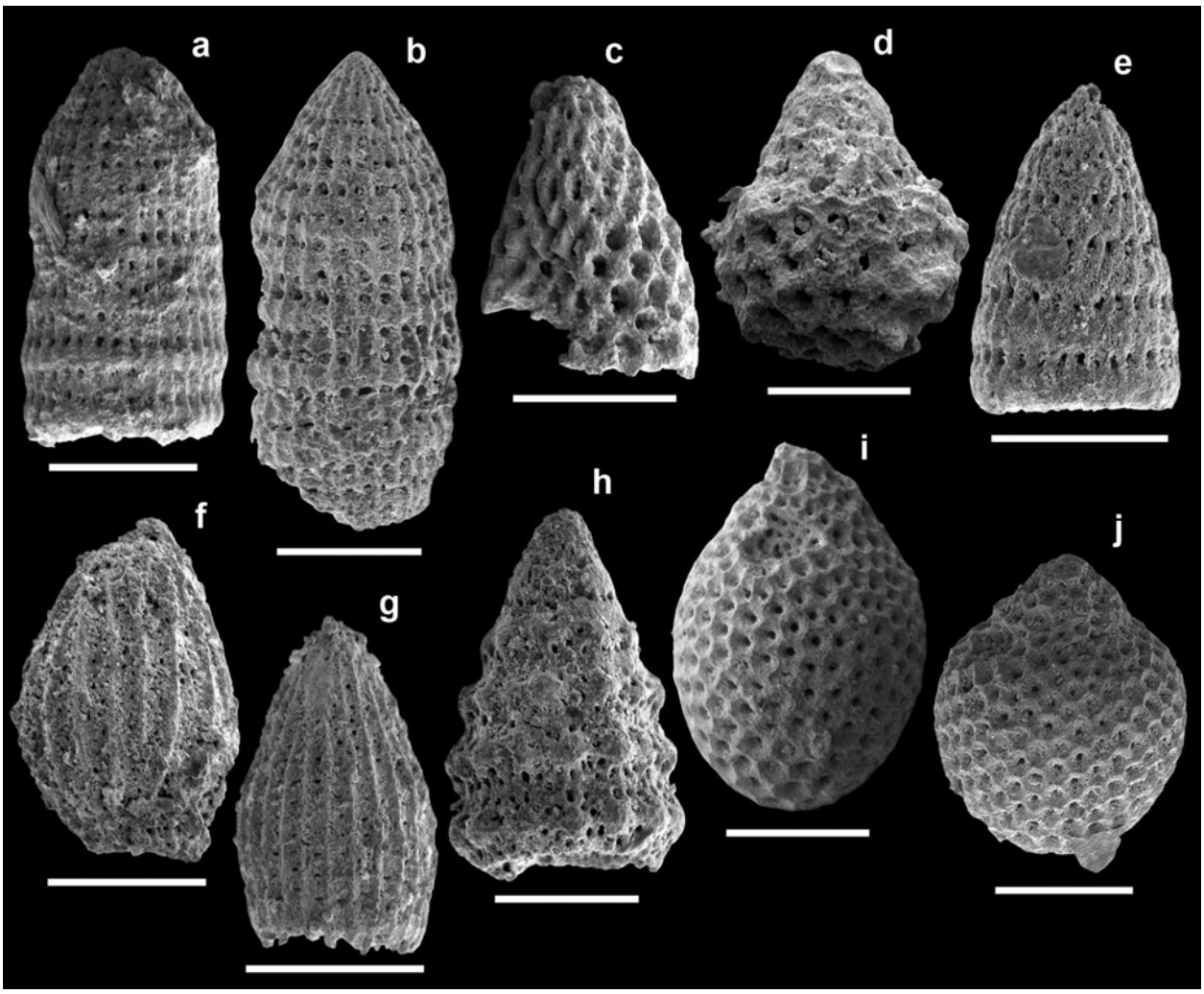


Figure 9. Scanning electron micrographs of radiolarians from sample GR66 (scale bar = 50 μm). (a) *Archaeodictyomitra apiarium* (Rüst); (b) *Archaeodictyomitra* aff. *apiarium* (Rüst); (c) *Campanomitra* cf. *tuscanica* (Chiari, Cortese & Marcucci); (d) *Crococapsa* sp., (e) *Loopus* cf. *blabla* (Schaaf) *sensu* Dumitrica, Immenhauser & Dumitrica-Jud (1997); (f) *Protunuma* sp.; (g) *Thanarla patricki* gr. (Kocher); (h) *Xitus* cf. *normalis* (Wu & Li); (i) *Zhamoidellum ovum* Dumitrica; (j) *Zhamoidellum* cf. *ventricosum* Dumitrica.

the northern Helicon range (GR25a–27a, GR31–33, GR35) (Figs 4, 6, 7). Nannofossil assemblages in the pre-flysch facies are attributable to the latest Paleocene – earliest Eocene. On Mount Parnassus, late Thanetian – early Ypresian zones CNP11 and CNE2, corresponding to zones NP9–NP10, were documented by the occurrence and absence of *Fasciculithus* spp., respectively (see Table 3). The early Eocene was recorded in the Helicon range, where late Ypresian Zone CNE5, corresponding to Zone NP13, was documented by the common occurrence of the first specimens belonging to Noelaerhabdaceae (*Cyclicargolithus floridanus*, *Dictyococcites* sp. and *Reticulofenestra dictyoda*; see Table 3). The transition to frank flysch sedimentation occurred during middle–late Ypresian zones CNE4 and CNE5 (corresponding to zones NP12 and NP13) characterized by the presence of common specimens referable to *Toweius* and Noelaerhabdaceae (see Table 4).

The obtained results are in agreement with the diachronous establishment of pelagic conditions in the Parnassus Zone after the Late Cretaceous tectonic events that levelled the seafloor bathymetry before flysch deposition (Gregou, 1996).

4.e. Pelagonian Flysch

The Pelagonian Flysch was sampled in several sites in the hills located between Levadhia and Cheronia villages and nearby Davlia village (Fig. 6). In this area the Pelagonian Flysch is both exposed in its primary position at the top of the limestone of the Mesoautochthonous Complex or tectonically below it. In general, the Mesoautochthonous Complex and Pelagonian Flysch are overthrust southwards, through out-of-sequence thrusts, above the Boeotian and Parnassus units.

Nannofossil assemblages from the reddish marls at the base of the flysch sequence (pre-flysch facies; samples GR06–07, GR42–44, GR48, GR50–51a/b; Fig. 7) indicate a late Paleocene – early Eocene age (see Table 5). The Selandian/Thanetian Zone CNP8 (corresponding to zones NP5 p.p.–NP6) was documented by the occurrence of *Heliolithus kleinpellii*. The Thanetian Zone CNP9 (corresponding to Zone

https://doi.org/10.1017/S0016756817000942 Published online by Cambridge University Press

https://doi.org/10.1017/S0016756817000942 Published online by Cambridge University Press

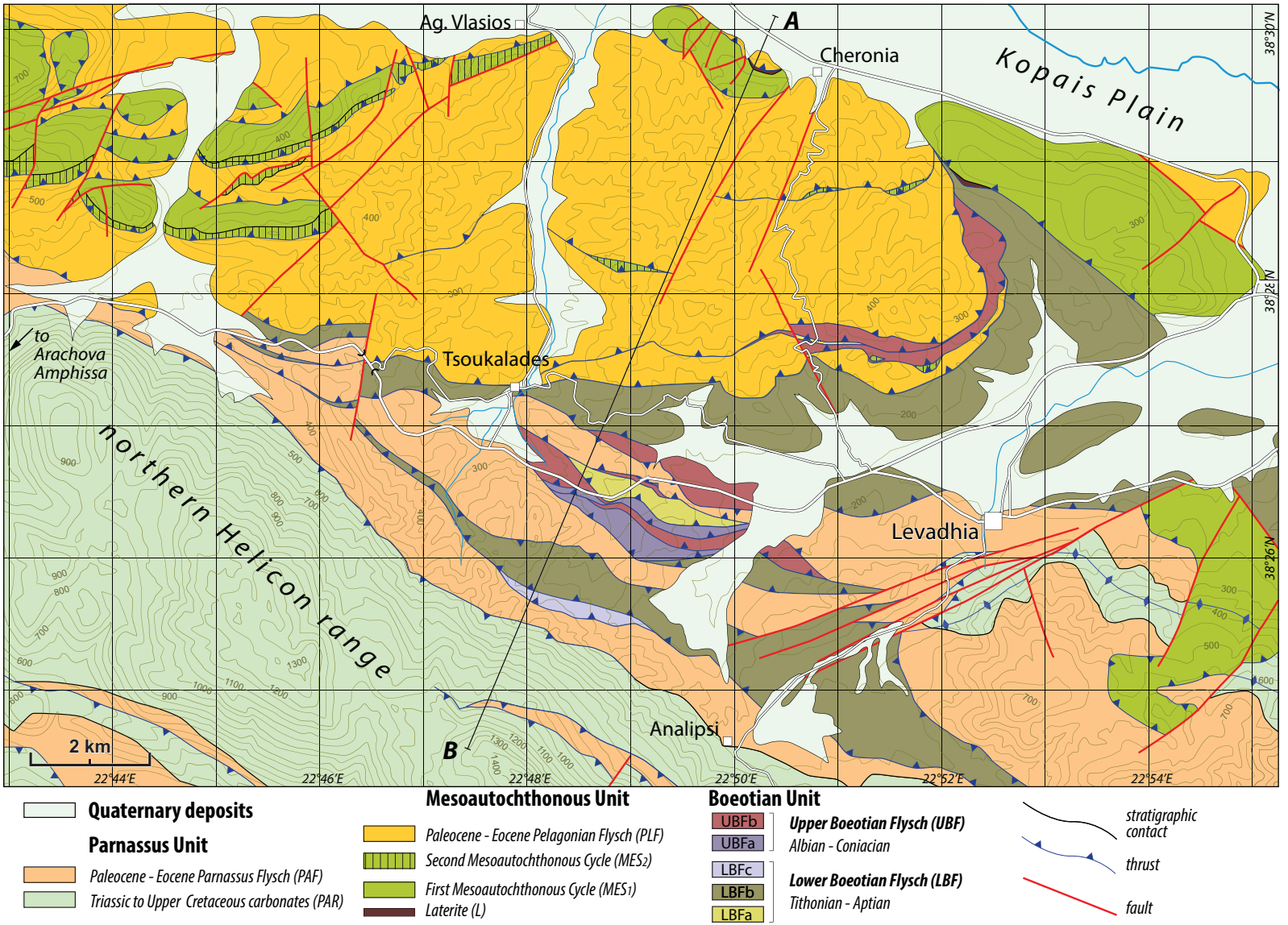


Figure 10. (Colour online) Geological map of the Levadhia area (location in Fig. 6).

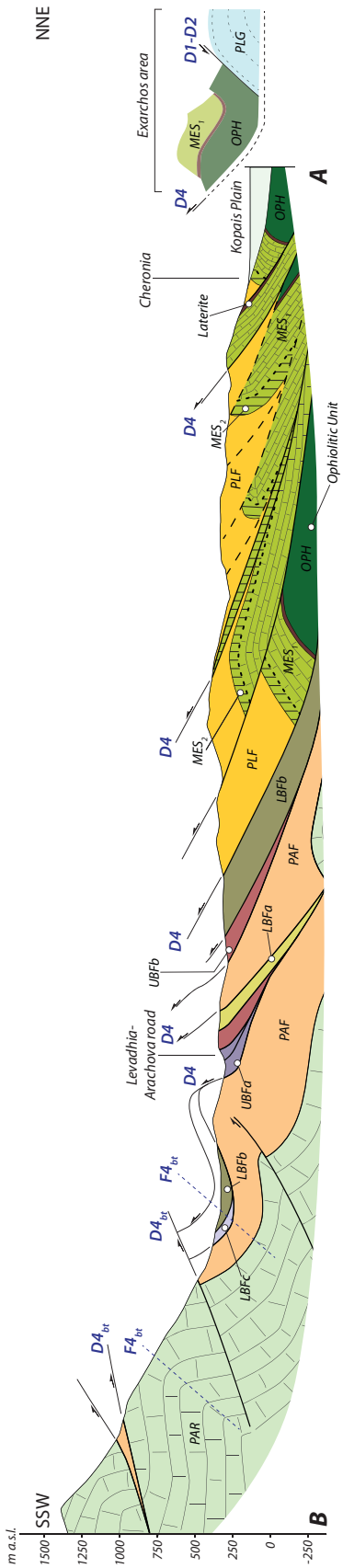


Figure 11. (Colour online) Geological cross-section along the Helicon range – Kopais plain transect (Levadhia area). On the right is reported the schematic structural profile of the Exarchos area. See Figure 10 for location and legend.

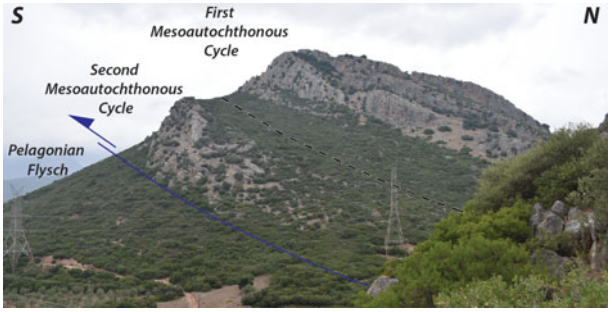


Figure 12. (Colour online) Overturned section of the Mesoautochthonous Complex (Levadhia area; 38° 28′ 33″ N; 22° 44′ 10″ E).

NP7 p.p.) was established on the presence of *Discoaster* cf. *mohleri* and the absence of *H. kleinpellii*, while the late Thanetian Zone CNP11 (corresponding to Zone NP9) was recognized by the presence of *Fasciculithus lillianae*. The early Ypresian Zone CNE3 (corresponding to zones NP10 p.p.–NP11) was identified by the presence of *Girgisia gammation* (*Toweius*? *gammation*) and *Sphenolithus radians*. Biostratigraphic results point to an early Eocene age for the shaly-arenaceous and conglomeratic flysch facies (samples GR08, GR47, GR49); Ypresian zones CNE4 and CNE5 (corresponding to zones NP12 and NP13) were recognized, respectively, by the occurrence of *Tribrachiatus orthostylus* and the common presence of specimens belonging to Noelaerhabdaceae (see Table 6).

5. Structural analysis

5.a. Data collection and methods

The structural analysis aimed to discriminate structures related to the different stages of the tectonic evolution of the area. The relative timing of deformation was constrained by cross-cutting relationships observed in all rock units, both at the map and outcrop scale. Mesoscopic structural observations were collected at several sites within the study area, focusing on the major tectonic contacts. Fault-slip data were analysed in order to derive the palaeostress field associated with the stages of regional deformation. Palaeostress analysis was performed using the *Fault* software developed by Caputo & Caputo (1988) that calculates the orientation of the stress tensors σ_1, σ_2, and σ_3 (where σ_1 is the maximum compressional stress and $\sigma_1 > \sigma_2 > \sigma_3$) through the dihedron angle inversion method of Angelier & Mechler (1977). Basic limitations and assumptions of the palaeostress analysis were taken into account. Table 7 presents the parameters of the reduced stress tensors as well as the estimated shortening directions derived from the structural analysis of fold axes. In the next sections, the tectonic implications of these parameters will be interpreted and the results will be integrated into the regional geodynamic evolution of the study area.

https://doi.org/10.1017/S0016756817000942 Published online by Cambridge University Press

Table 7. Mesoscopic structural field data from sites of measurement of the study area

Site N.	Rock unit	Tectonic event	N. of data	σ_1	σ_2	σ_3	Estimated σ_1	Latitude (N)	Longitude (E)
10N	PLG	D1a	6	95/63	345/10	250/25		38° 44′ 57.1″	22° 17′ 54.2″
750N	LBF	D1a	7	269/75	158/06	66/14		38° 26′ 28.3′	22° 48′ 51.7″
891I	OPH	D1b	20				20/5	38° 41′ 8.12″	22° 37′ 44.39″
891I	OPH	D1b	16				340/5	38° 41′ 8.12″	22° 37′ 44.39″
885I	PLG	D2	9	63/02	333/06	169/84		38° 40′ 20.8″	22° 40′ 39.4″
Folds	LBF	D2	45				110/5		
926I	LBF	D3	11	357/4	266/7	118/83		38° 27′ 11.7″	22° 53′ 15.9″
750I	LBF	D3	12	–	–	–	north	38° 26′ 28.3″	22° 48′ 51.7″
Folds	LBF	D3	57				345/5		
Folds	UBF	D3	6				70/10		
790I	PAF	D4	10	10/01	100/01	229/88		38° 25′ 53.4″	22° 47′ 25.4″
849I	PAF	D4	15	26/03	117/16	270/83		38° 28′ 21.7″	22° 44′ 11.9″
852I	PAF	D4	14	128/01	38/02	242/88		38° 29′ 31.9″	22° 41′ 46.5″
909I	PAF	D4	7	134/11	226/10	359/75		38° 26′ 32.9″	22° 49′ 01.3″
762I	UBF	D4	8	223/01	314/27	132/63		38° 26′ 32.5″	22° 48′ 29.6″
941I	UBF	D4	6	200/76	8/14	99/03		38° 20′ 56.6″	22° 54′ 18.5″
876I	LBF	D4	13	340/01	70/05	244/85		38° 44′ 36.7″	22° 16′ 46.2″
750I	LBF	D4	7	101/11	9/10	239/75		38° 26′ 28.3″	22° 48′ 51.7″
27I	PAR	D4	7	150/17	50/31	265/53		38° 35′ 04.1″	22° 33′ 37.5″
51I	OPH	D4	7	154/04	64/04	292/84		38° 23′ 47.4″	22° 57′ 19.4″
835I	OPH	D4	7	94/11	340/65	189/22		38° 34′ 54.1″	22° 57′ 17.1″
Folds	PAF	D4	40				25/5		
Folds	UBF	D4	7				315/5		
Folds	LBF	D4	22				340/5		
Folds	PLF	D4bt	55				200/5		
900I	PLG	D4bt	8	27/15	120/10	242/72		38° 26′ 24.8″	22° 49′ 30.2″
965I	PAR	D4bt	6	209/21	110/22	338/59		38° 18′ 27.2″	22° 54′ 29.3″
965S	PAR	D4bt	5	299/36	161/45	46/23		38° 18′ 27.2″	22° 54′ 29.3″
33N	PAF	D5	6	341/70	213/12	120/15		38° 36′ 18.4″	22° 29′ 40.1″
854S	PLF	D5	6	1/45	146/39	252/19		38° 29′ 11.8″	22° 42′ 08.2″
762N	UBF	D5	9	27/09	296/05	179/80		38° 26′ 32.5″	22° 48′ 29.6″
764N	PAR	D5	9	218/70	338/10	71/17		38° 27′ 19.9″	22° 46′ 30.5″
876N	LBF	D5	8	168/81	328/09	58/03		38° 44′ 36.7″	22° 16′ 46.2″
965N	PAR	D5	7	248/84	156/00	66/06		38° 18′ 27.2″	22° 54′ 29.3″
2N	PLG	D5	15	137/82	329/08	239/02		38° 43′ 53.6″	22° 20′ 27.1″
852D	PAR	D5T	18	212/08	352/80	122/07		38° 29′ 31.9″	22° 41′ 46.5″
932D	MES	D5T	4	160/16	47/53	260/32		38° 28′ 51.9″	22° 52′ 11.2″
963D	BEO	D5T	11	57/13	305/58	154/28		38° 18′ 54.4″	22° 54′ 36.1″

The σ_1, σ_2, and σ_3 axes have been computed applying the dihedron angle method to fault populations (Angelier & Mechler, 1977) through the 'FAULT' software of Caputo & Caputo (1988). Fold axes, grouped according to both tectonic event and rock unit, allowed a rough estimate of the maximum horizontal palaeostress axis. Abbreviations: OPH – Ophiolitic Unit: mélange; PLG – Pelagonian Unit limestone; PLF – Pelagonian Flysch; LBF – Lower Boeotian Flysch; UBF – Upper Boeotian Flysch; PAR – Parnassus Unit limestone; PAF: Parnassus Flysch; BEO – Boeotian Unit limestone; MES – Mesoautochthonous Complex limestone.

The results of the field-based structural work are synthesized in a new geological–structural map and cross-section of the Levadhia region (Figs 10, 11) and a tectonic sketch map and two cross-sections across the whole studied area (Figs 6, 8). Some of the collected orientation data are summarized in equal-area plots.

5.b. Tectonic setting and major tectonic structures

The studied area is characterized by a complex structural evolution, deriving from the superposition of several tectonic phases, related to obduction, continental collision, subducting slab retreat and gravitational collapse of over-thickened crust (e.g. Bernoulli & Laubscher, 1972; Robertson & Dixon, 1984; Jacobshagen, 1986; Mercier *et al.* 1989; Le Pichon *et al.* 1995; Ricou *et al.* 1998; Brun & Faccenna, 2008).

Tectono-metamorphic events accompanied this long-lasting evolution (Fig. 4). Middle Jurassic HT–LP metamorphism is recorded at the base of the obducting nappe (Roddick, Cameron & Smith, 1979; Spray & Roddick, 1980; Dimo-Lahitte, Monié & Vergély, 2001) then followed by three major tectono-metamorphic events in the eastern Pelagonian Zone: (i) Early Cretaceous upper-greenschist to blueschist facies metamorphism and anatexis events (Barton, 1976; Yarwood & Dixon, 1977; Schermer, Lux & Burchfiel, 1990; Lips, White & Wijbrans, 1998; Schenker *et al.* 2014); (ii) Late Cretaceous blueschist facies metamorphism (Lips, White & Wijbrans, 1998; Lips, Wijbrans & White, 1999); (iii) Paleocene–Eocene blueschist to greenschist facies metamorphism (Schermer, Lux & Burchfiel, 1990; Lips, White & Wijbrans, 1998; Lips, Wijbrans & White, 1999). The latter tectono-metamorphic event is commonly related to the final westward emplacement of the Internal Hellenides upon the External Hellenides and the development of the Tertiary fold and thrust belt and high-pressure belt in the Olympos–Ossa, Pelion and Cyclades areas. Finally, since Eocene–Oligocene times the prolonged post-orogenic extensional tectonics drove exhumation of the previously stacked crustal and oceanic nappes in metamorphic domes (Lister, Banga & Feenstra, 1984; Jolivet *et al.* 1994; Jolivet & Brun, 2010; Burg, 2012).

https://doi.org/10.1017/S0016756817000942 Published online by Cambridge University Press

The generally NNW-striking structural fabric of the Hellenic Belt is deflected to an ESE-trend confined to the inner (eastern) border of the Parnassus Unit. In the studied area, the Jurassic thrusting of the ophiolite nappe onto the Pelagonian Platform, partly remobilized by Late Cretaceous and Tertiary tectonics, is preserved only in the Kallidromon Belt, north of the Parnassus Unit (Fig. 6 and profile A–A′ in Fig. 8).

North of the Parnassus Unit, mainly top-to-the-S thrusts are developed forming imbricate piles made of ophiolites, the Pelagonian Unit, Mesoautochthonous sequences, and Pelagonian and Boeotian flysches. South of the Kopais Plain the Parnassus Unit and carbonate basement of the Boeotian Unit are locally overthrust to the NW above the Eocene Pelagonian Flysch (Fig. 6 and cross-section B–B′–B″ in Fig. 8). The tectonic framework is particularly complicated in the Levadhia area where a new geological map and cross-section were produced (Figs 10, 11). The zone is characterized by a series of mainly S-verging thrust sheets variously superposing the Boeotian Flysch, the Mesoautochthonous Complex and the Tertiary Pelagonian and Parnassus flysches and, further southwards, by the triangular zone between S- and N-verging thrusts near the northeastern border of the Parnassus Platform (Fig. 11). Strike-slip and normal faults dislocate the previously described structures. Main dextral strike-slip faults are represented by the NNE-trending Distomon (Fig. 13b, c, d) and Aliki faults (DSTF and ALKF in Fig. 6), whereas a main sinistral strike-slip fault is represented by the NNW-trending Agia Triada Fault (ATRF in Fig. 6).

5.c. Mesoscopic structural analysis

Structural and palaeostress studies concentrated on all units cropping out in the study area and on key outcrops of the Pelagonian Unit and Boeotian Flysch in the Mount Iti area. Mesoscopic and macroscopic superposed folding phases, some of which linked to thrusting, affected the Boeotian Flysch and Tertiary flysches, while the carbonate-dominated units only registered large-scale folding and brittle structures. The structural analysis combined with the stratigraphic records enabled us to distinguish a succession of six major deformational events, hereafter referred to as D1, D2, D3, D4, $D4_{bt}$ and D5, directly related to the evolution of the study area. Brittle deformation related to Triassic rifting processes and older deformations are beyond the scope of this paper.

5.c.1. D1 phase deformations

The oldest deformations recognized in the area are related to the Middle–Late Jurassic obduction of the Maliac–Vardar Ocean lithosphere onto the eastern Adria continental margin (i.e. the Pelagonian Zone). Mesoscopic deformation related to this phase was recognized in the Pelagonian and Boeotian units. Deformations are differentiated in time and space according to relative position with respect to the advancing ophiolite nappe shifting from a normal stress regime (D1a sub-stage) to a compressive stress regime (D1b sub-stage). This subdivision is clearly evident in the Pelagonian Unit while the Boeotian Unit, in this phase, registered only deformations of the D1a sub-stage.

The D1a sub-stage is characterized by widespread syn-sedimentary deformations relative to different and subsequent episodes that affected the Upper Jurassic clastic deposits sedimented on top of the Pelagonian Platform and the LBF deposited onto the Boeotian carbonate sequence. Gravity-induced deformations such as slumping events, the formation of local wedge-shaped strata and repeated angular unconformities, as well as syn-sedimentary faults, are common in these deposits. Faults (Fig. 14, sites 10N and 750N) are characterized by cumulated episodes of faulting during sedimentation with variable throw ranging from some centimetres to half a metre (Fig. 15a). Syn-sedimentary faulting is particularly evident in the Upper Jurassic clastic sediments of the Pelagonian Unit up to the upper Tithonian–Hauterivian portions of the LBF (i.e. the LBFa and LBFb lithostratigraphic units). Stress inversion of the scarce fault-slip data collected in the LBF in the Levadhia area and in the ophiolite-bearing thin-bedded turbidites on top of the Pelagonian carbonates in the Mount Iti area results in an ENE–WSW direction of extension (Table 7; Fig. 14, sites 10N and 750N).

Since Barremian time, faulting in the LBF gave way to gravity-triggered deformations (slumps, disrupted layers, angular unconformities, erosional surfaces). The lack of any observable water-escape structures suggests that these deformations were induced by large-scale gravitational instability in the sedimentary basin rather than small-scale liquefaction of sediments due to increased pore-water pressure.

The most striking deformation related to the D1b sub-stage is the overthrusting of the ophiolite nappe with an underlying amphibolite sole and tectono-sedimentary mélange onto the Pelagonian Platform. In the studied area, the amphibolite sole always occurs as dismembered blocks embedded in the mélange matrix. Contacts of the Ophiolitic Unit onto the Pelagonian Unit were observed on the southern flank of the Kallidromon Mountains (Fig. 6). The footwall is characterized by highly sheared mélange showing pervasive scaly cleavage. A planar fabric is mainly represented by clay minerals enveloping lithic domains consisting of basalt, chert, serpentinite and sandstone. Well-developed kinematic indicators (S-C fabrics, asymmetric folds, asymmetric boudins) record a consistent top-to-the-SW sense of shear (Fig. 14, site 891I; Fig. 15b).

D1a syn-sedimentary faults were probably related to the lithospheric bending triggered in the Pelagonian Unit, first, and Boeotian Unit, later, by the obducting ophiolite nappe (Nirta *et al.* 2015). Finally,

https://doi.org/10.1017/S0016756817000942 Published online by Cambridge University Press

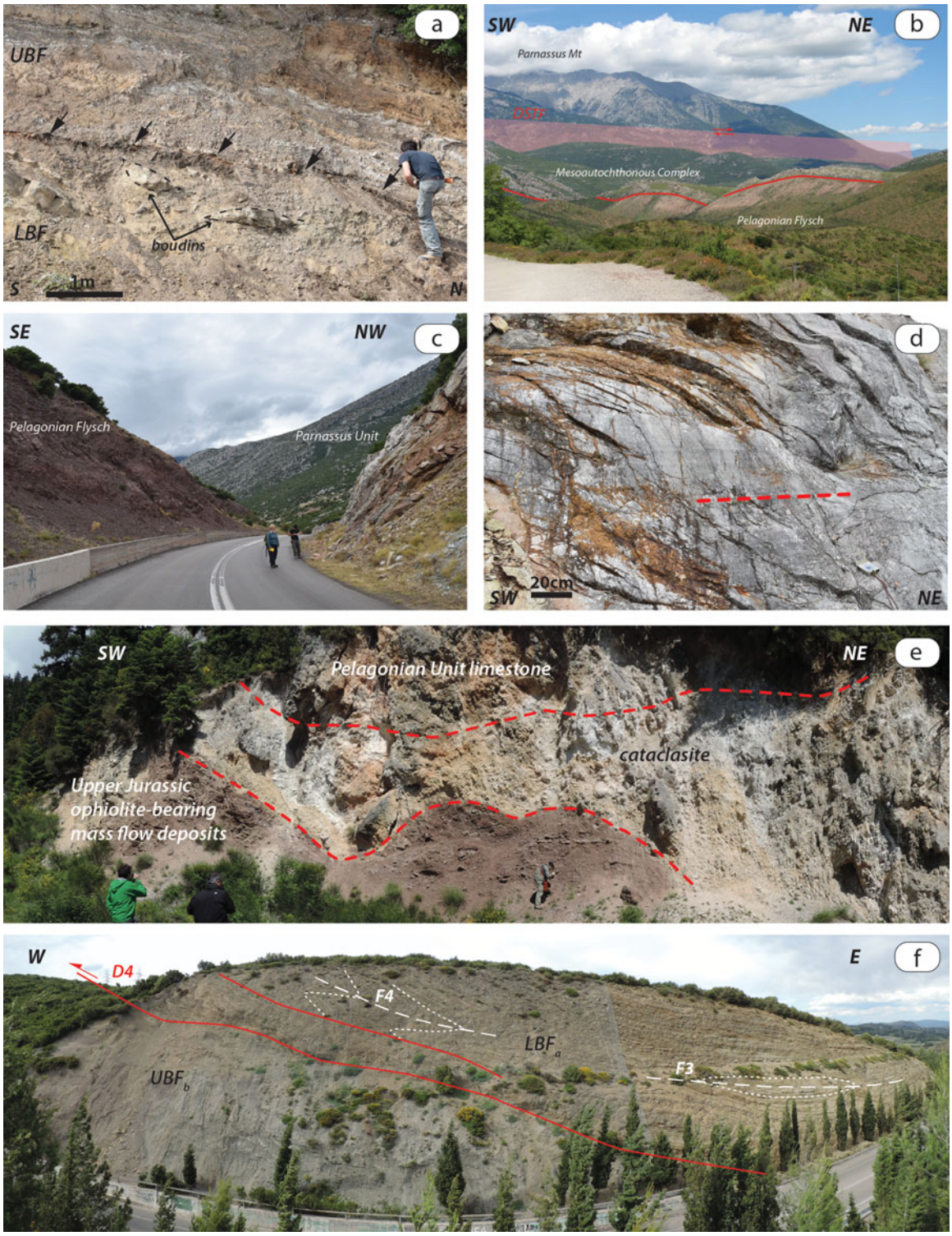


Figure 13. (Colour online) (a) UBF unconformably sedimented above the deformed LBF (Mount Iti area – 38° 47′ 5.4″ N; 22° 22′ 53.3″ E). (b) Panoramic view showing the overthrusting of the Mesoautochthonous Complex above the Pelagonian Flysch. In the background is evidenced the trace of the Distomon Fault (DSTF). (c) View towards the south within the core of the DSTF (38° 29′ 33.4″ N; 22° 41′ 47.9″ E). (d) Dextral strike-slip striae along the DSTF fault plane (38° 29′ 33.4″ N; 22° 41′ 47.9″ E). (e) Fault gouge between limestone of the Pelagonian Unit and Upper Jurassic ophiolite-bearing turbidites at the contact with the underlying Parnassus Flysch (Mount Iti area – 38° 43′ 53.6″ N; 22° 20′ 27.1″ E). (f) D4 tectonic contact between the LBFa (hangingwall) and UBFb (footwall) along the Levadhia–Arachova road-cut (38° 26′ 26.4″ N; 22° 48′ 44.5″ E).

D1b deformations marked the tectonic emplacement of the ophiolites and mélange onto the Pelagonian Platform (Fig. 15c) and the increasing gravity-triggered deformations in the Barremian–Aptian LBF (LBFc; Nirta *et al.* 2015).

5.c.2. D2 phase deformations

The earliest folding event (F2) developed in the LBF is characterized by pervasive close to sub-isoclinal mesoscopic non-cylindrical folds with approximately

https://doi.org/10.1017/S0016756817000942 Published online by Cambridge University Press

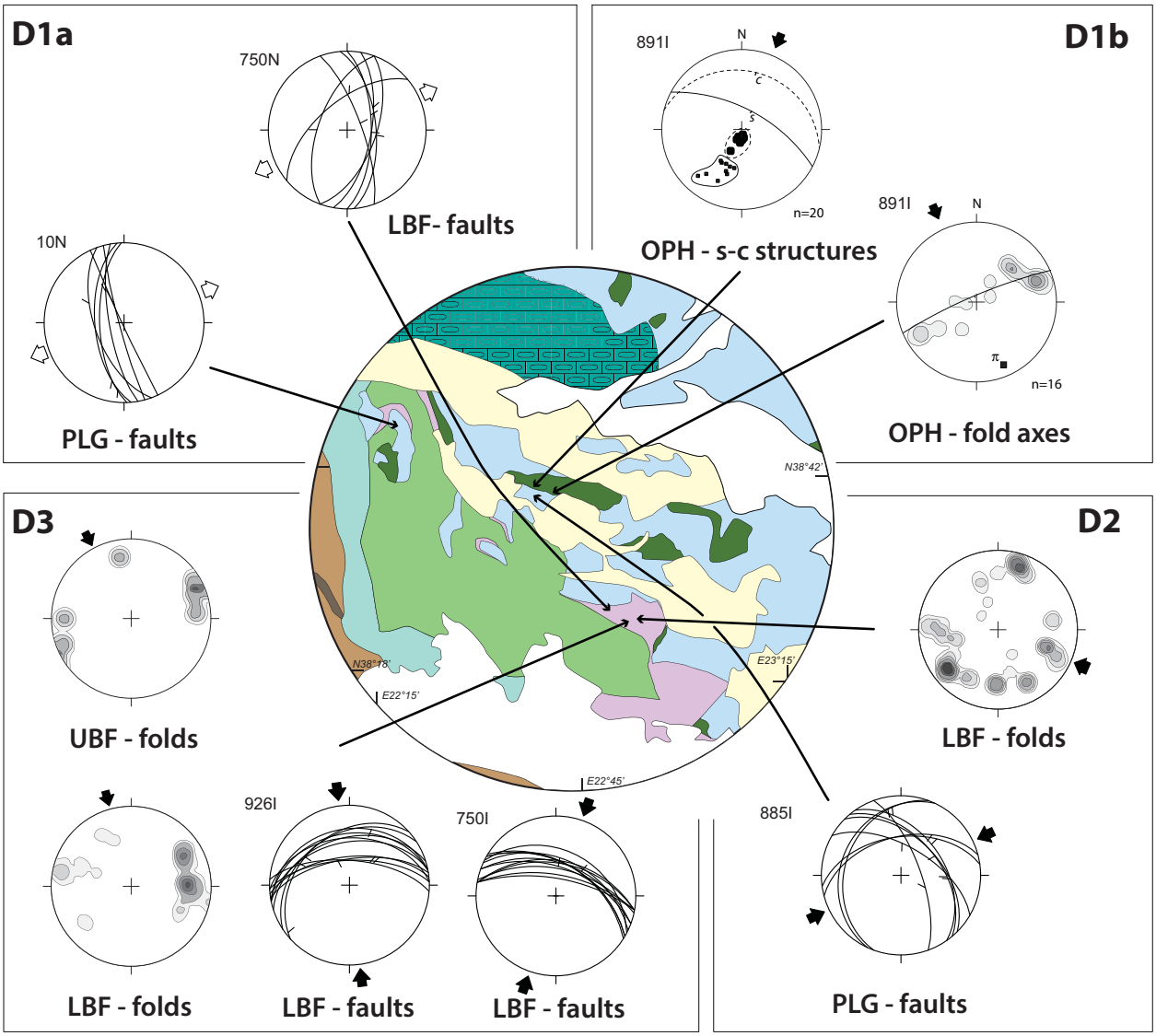


Figure 14. (Colour online) Distribution of mesostructural fault-slip data, fold axes and S-C structures relative to D1, D2 and D3 deformation phases. White arrows indicate direction of extension (σ_3) and black arrows indicate direction of compression (σ_1) calculated through inversion of fault-slip data. Black arrows of diagrams relative to folds and S-C structures are also indicative of the sense of tectonic movement. π-diagram on D1b fold axes in the OPH possibly indicates axis of successive deformation phases. All diagrams are equal-area lower hemisphere projections; density contours at 1% intervals. UBF – Upper Boeotian Flysch; LBF – Lower Boeotian Flysch; PLG – Pelagonian Unit; OPH – Ophiolitic Unit, mélange.

similar geometry (class 2 of Ramsay, 1967). Sandstone and limestone strata in the F2 fold limbs are often affected by boudinage with both symmetric and asymmetric geometries. Veins associated with the D2 deformational phase are oriented at a high angle to the bedding and filled with sparitic calcite. Despite the high strain ratio, which characterizes the F2 folds and the associated small-scale thrusts, these structures are rarely associated with cleavage. Fold axes and axial planes are strongly reoriented by successive folding and faulting, depicting a very dispersed pattern in the stereonet projections (D2 folds in Fig. 14). A tentative subtraction of the successive folding event (F3) seems to point to an original N–S-trending axes, whereas analysis of bedding-cleavage relationships, fold asymmetry and direction of younging point to a western vergence (Fig. 16).

D2 is possibly associated with renewed westward translation of the Ophiolitic Unit onto the Pelagonian Unit. This thrusting event in the Kallidromon zone cross-cuts the scaly cleavage acquired during the D1 phase of deformation and is associated with small-scale mesoscopic folds deforming the S1 foliation. Fault-slip data (Table 7, site 885I in Fig. 14) result in a NE–SW shortening direction, which is consistent with the major WNW–ESE-trending and N-dipping thrusts leading the ophiolites onto the Pelagonian Unit.

5.c.3. D3 phase deformations

D3 consists of a folding event (F3) well developed and exposed in the LBF and UBF. It is characterized by gentle to close folds with generally parallel geometry (class 1B of Ramsay, 1967) in the LBF and

https://doi.org/10.1017/S0016756817000942 Published online by Cambridge University Press

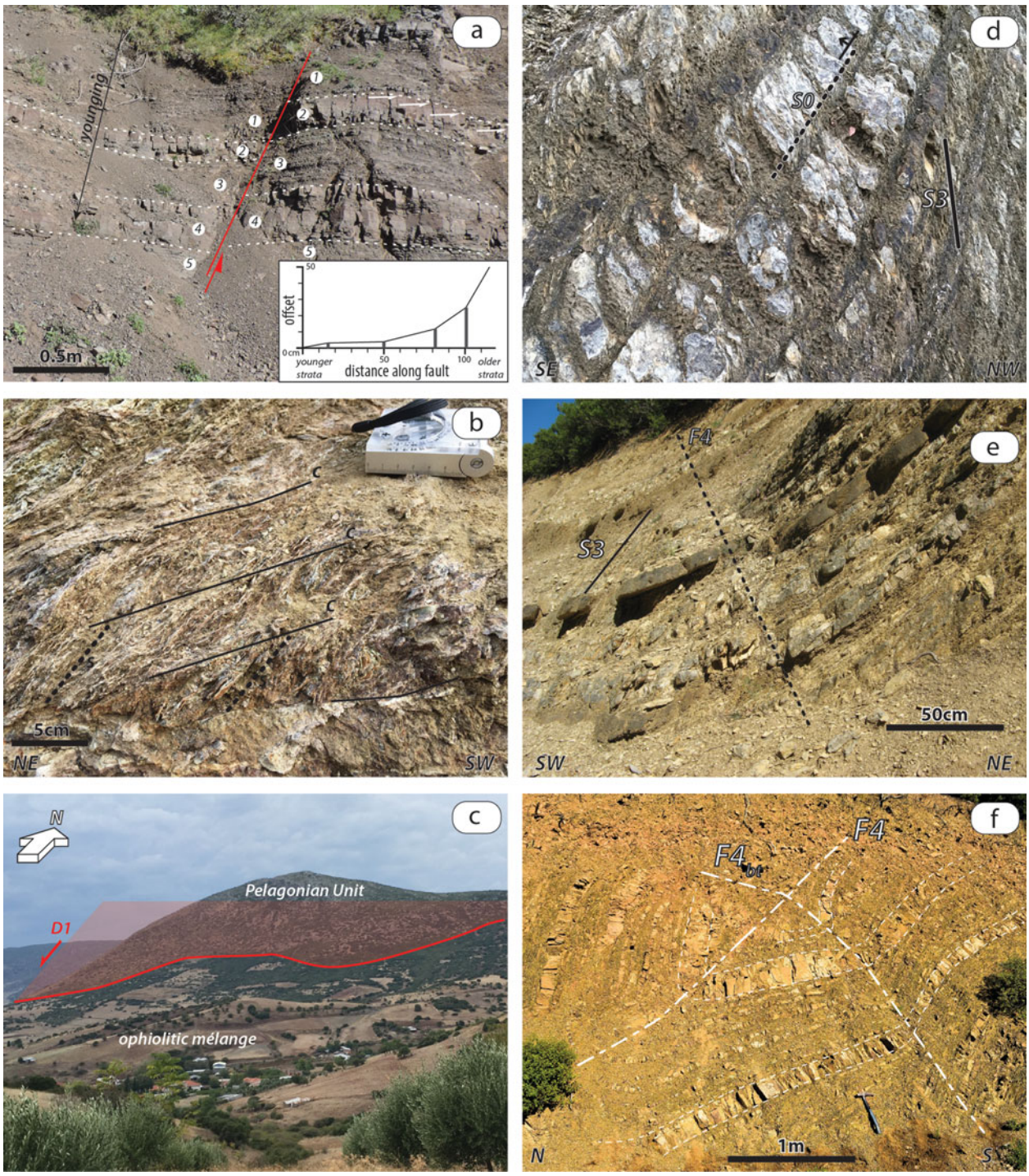


Figure 15. (Colour online) (a) Overturned syn-sedimentary fault showing cumulated episodes of faulting during sedimentation (ophiolite-bearing thin-bedded turbidites on top of the Pelagonian limestone; Iti area – 38° 44′ 56″ N; 22° 17′ 53″ E); the inset diagram shows cumulated offset on the fault. (b) S-C structures in the mélange sandwiched between the Pelagonian Unit and ophiolite nappe in the Kallidromon area (38° 41′ 08″ N; 22° 37′ 44″ E). (c) Overthrusting (D1 phase of deformation) of the Ophiolitic Unit above and the Pelagonian Unit. The tectonic contact was successively tilted by a large-scale anticline related to the D4 deformation phase to simulate a normal fault (Exarchos area, see Figs 8 and 11; 38° 35′ 53″ N; 22° 55′ 35″ E. (d) S3 disjunctive cleavage superimposed on the limb of F2 fold in the LBF_b (Levadhia–Arachova road-cut – 38° 27′ 37″ N; 22° 45′ 46″ E). (e) S3 cleavage folded by an open F4 fold in LBF_b (Levadhia–Arachova road-cut – 38° 27′ 37″ N; 22° 45′ 36″ E). (f) Interferences of $F4_{bt}$ open folds onto F4 tight fold near the back-thrust of the Parnassus units above the Parnassus Flysch (Levadhia area – 38° 25′ 57″ N; 22° 47′ 252″ E).

close to tight folds with mostly similar geometry in the shaly-silty strata packages of the UBF. Axial plane foliation S3 is marked by disjunctive cleavage that is well developed only in the shaly layers of the turbiditic sequences (Fig. 15d, e). Isolated F3-fold hinge zones are common in the shale-dominated lithologies of the UBF.

F3 fold axes are scattered, as a result of the post-D3 deformations (Fig. 17). However, an original E–W trend of the F3 axes and the main N-dipping direction

https://doi.org/10.1017/S0016756817000942 Published online by Cambridge University Press

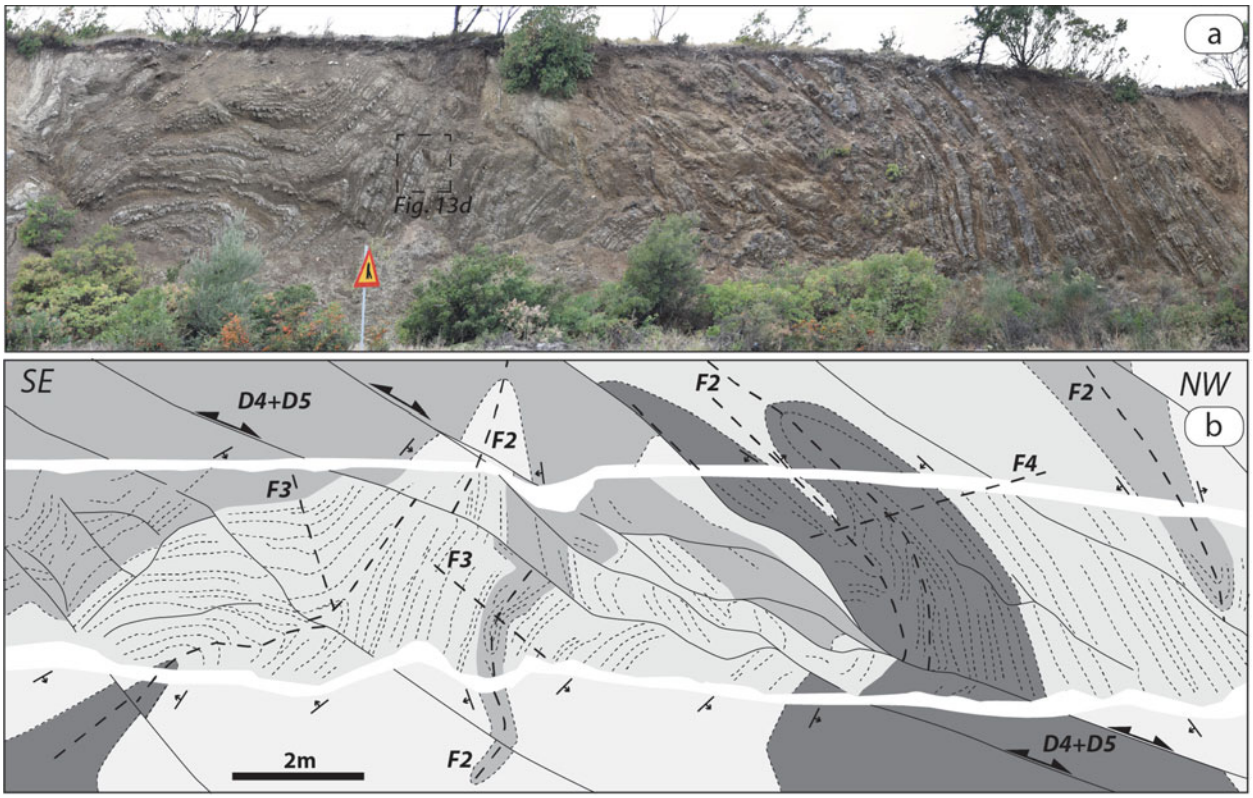


Figure 16. (Colour online) F2 + F3 + F4 interference patterns in the LBF. Fold assemblage is dissected by D4 (reverse) and D5 (normal) faults (38° 27′ 37″ N; 22° 45′ 46″ E). Black arrows show younging direction.

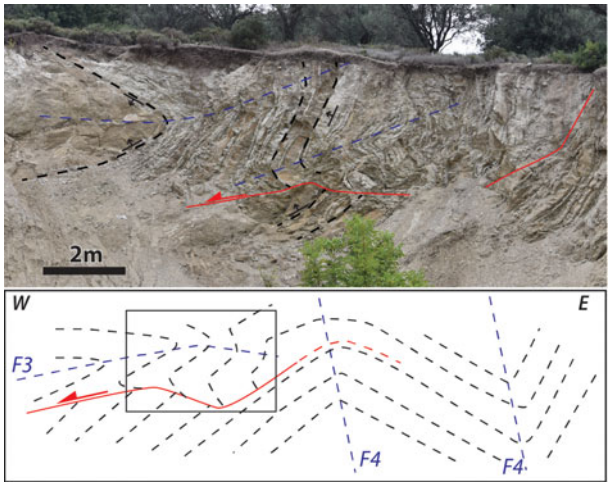


Figure 17. (Colour online) F3 + F4 interference pattern in the LBF. The overturned limb of the main F3 fold and the associated thrust plane are re-folded by F4, and rotated to simulate a low-angle normal fault (38° 27′ 29″ N; 22° 53′ 26″ E).

of the axial planes indicate a southward facing direction (F3 folds in the LBF and UBF of Fig. 14). Mostly N-dipping mesoscopic thrusts associated with folds were observed in the overturned limbs of tight folds (Fig. 17). Superimposed F2 + F3 interference results mostly in a type-3 pattern (Ramsay, 1967).

Widespread E- to NE-dipping thrusts cross-cut D1 and D2 planar structures in the Ophiolitic Unit and Pelagonian Unit. However, it was not possible to clearly distinguish in the field D3 structures from brittle events associated with younger compressive phases (D4–$D4_{bt}$).

5.c.4. *D4 phase deformations*

Mesoscopic and macroscopic structures related to this deformation phase are the most frequent and well developed in all the tectonic units.

F4 mesoscopic folds are mostly developed in the Pelagonian and Parnassus flysches and in both the LBF and UBF. Deformations in the Boeotian Flysch (LBF + UBF) are represented by gentle to tight isopach F4-folds associated with a disjunctive axial plane foliation S4 (Figs 15e, 16). In the Tertiary Pelagonian and Parnassus flysches, F4 folds are represented by close to tight structures with mostly similar geometry and with a weak continuous axial plane cleavage particularly evident only in the hinge zones. Axial plane attitude is generally upright to steeply inclined in the Boeotian Flysch and gently inclined to recumbent in the Tertiary flysches (Fig. 15f). Brittle shears commonly tear F4 hinge zones both in the Boeotian Flysch and in the Tertiary flysches.

Fold axes are gathered around a ENE–WSW trend in both the Tertiary flysches and Boeotian Flysch, plunging preferentially towards eastern sectors (F4 folds in the LBF, PAF and UBF of Fig. 18). Dispersion of F4 axes in the Tertiary flysches and the UBF appears to be caused by successive tectonic deformations, whereas most of the dispersion observed in the LBF seems to be also controlled, and locally forced, by

https://doi.org/10.1017/S0016756817000942 Published online by Cambridge University Press

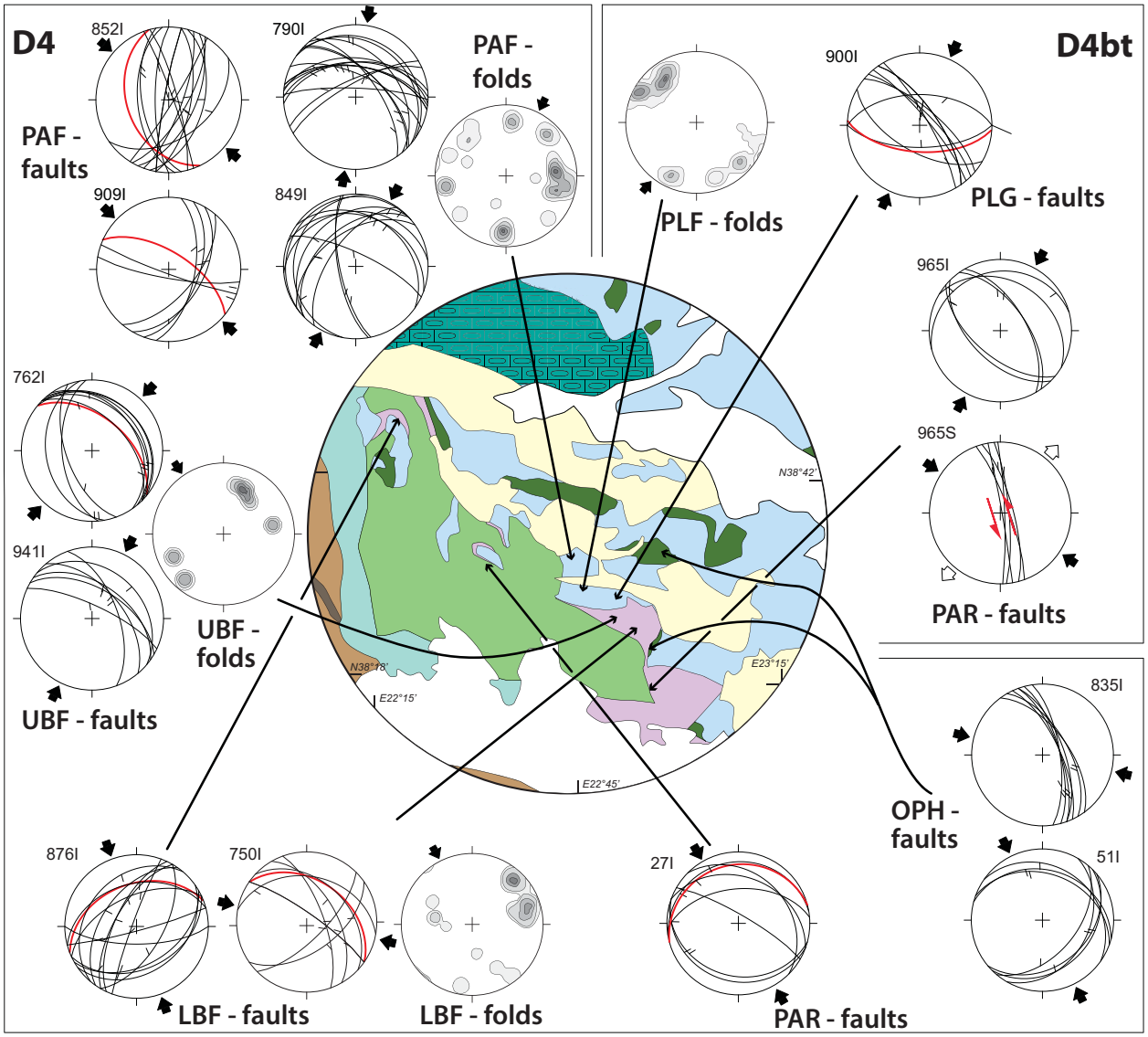


Figure 18. (Colour online) Distribution of mesostructural fault-slip data and fold axes relative to D4 and $D4_{bt}$ deformation phases. White arrows indicate direction of extension (σ_3) and black arrows indicate direction of compression (σ_1) calculated through inversion of fault-slip data. Black arrows of diagrams relative to folds are also indicative of the sense of vergence. All diagrams are equal-area lower hemisphere projections; density contours at 1 % intervals. UBF – Upper Boeotian Flysch; LBF – Lower Boeotian Flysch; PLG – Pelagonian Unit, limestones; PLF – Pelagonian Flysch; PAR – Parnassus Unit, limestones; PAF – Parnassus Flysch; OPH – Ophiolitic Unit, mélange.

the pre-existing structural fabric. Pole to axial plane processing on a π-diagram of F4 structures of the Pelagonian and Parnassus flysches points to an average axis trending N100. F4 axial planes steeply dip and gently dip towards northern sectors in the Boeotian Flysch and Tertiary flysches, respectively. The folds' asymmetry and its relationships with bedding polarity, along with slip indicators of fold-related brittle shears clearly point to a SSW vergence direction.

Asymmetric open megascopic F4 folds approximately E–W-trending and verging towards the south are well developed in the Mesoautochthonous carbonate sequences. These megastructures are bounded by thrust surfaces commonly isolating overturned fold limbs (Figs 11, 12, 13b). Mesoscopic fold interference patterns F2 + F4 and F3 + F4 observed in the LBF and UBF are mostly of type 3 (Ramsay, 1967) (Figs 16, 17). Along the Levadhia–Amphissa road – 5 km east of Levadhia – D4 brittle reverse faults and open folds overprint F3 close folds, tilting and locally reactivating the D1 syn-sedimentary normal fault systems of the LBF (Nirta *et al.* 2015) near a D4-thrust juxtaposing the LBFa onto the UBF (Fig. 13f).

Differences in the fold geometry among the Boeotian Flysch and Tertiary flysches are clearly linked to differentiation in structural levels, shallower in the Boeotian Flysch and deeper in the Tertiary flysches. In fact, the F4 folding event is associated with the westward overthrusting of the more internal tectonic units (Pelagonian, Boeotian and Ophiolitic units) above the Pelagonian Flysch, and the Parnassus Flysch in Tertiary times.

The overthrusting of the Pelagonian Unit and Ophiolitic Unit above the Boeotian and Parnassus units

https://doi.org/10.1017/S0016756817000942 Published online by Cambridge University Press

represents the major tectonic contact associated with this compressive phase. The superposition of the ophiolites, Pelagonian carbonates and slices of Boeotian Flysch above the Parnassus Flysch on Mount Iti and in the central Parnassus area (Amfiklia–Polydrosos area, Fig. 6) represent klippen related to this tectonic phase (Fig. 3, cross-section A–A′ in Fig. 8, Fig. 13e).

In the Kallidromon area and north of Exarchos village on the northern border of the Kopais plain, the Jurassic tectonic contact of the ophiolite nappe above the Pelagonian carbonates (D1 tectonic phase) is folded and cut by S-facing D4 structures (Figs 6, 8).

The Mesoautochthonous carbonate sequence is mostly detached from its substratum represented by the Pelagonian and Ophiolitic units, and overthrusts the Tertiary Pelagonian Flysch (Figs 12, 13b). During this tectonic phase, the progressive deformation enucleated N-dipping out-of-sequence thrusts in the Pelagonian Flysch and Boeotian Flysch mostly controlled by the structural buttress represented by the Parnassus Platform. The Triassic–Cretaceous Parnassus carbonates and Tertiary flysch are also deformed by N-dipping thrust structures.

Thrust structures are generally N-dipping, with angles varying from 10° to 50°; steeply dipping back-thrusts are less common. Major thrust structures are commonly accommodated by N–S-trending strike-slip faults, generally left-lateral.

The palaeostress analysis carried out on reverse and strike-slip faults related to the D4 phase indicates a NE–SW-trending shortening direction (Table 7; Fig. 18).

5.c.5. $D4_{bt}$ phase deformations

The $D4_{bt}$ deformations are well developed only at shallow structural levels in the Parnassus Flysch and in the Boeotian Unit carbonate sequence. They consist of thrust-related N-facing open to gentle $F4_{bt}$ folds, with SE–NW-trending axes and axial planes steeply dipping towards the southern sectors. These are associated with N-vergent thrusts (back-thrusts) leading both the Parnassus and Boeotian limestone units onto the Parnassus and Pelagonian flysches, respectively. Interferences of $F4_{bt}$ folds onto F4 folds have been found at various sites near the back-thrusts of the Parnassus and Boeotian units (Fig. 15f). Palaeostress analysis of thrusts and associated reverse faults indicates a NNE–SSW shortening direction (Table 7; Fig. 18).

5.c.6. D5 phase deformations

The D5 deformational event consists of both well-developed regional extensional faults and transtensive ($D5_T$) faults that cross-cut all the previous structures. Inversion of fault-slip data points to NE–SW and NW–SE extension directions, accommodated by NNE-trending dextral strike-slip faults (Table 7; Fig. 19). They in part represent reactivated ancient normal structures possibly developed during the early rifting stage preceding obduction, successively affected by both compressional and extensional stress regimes (Table 7, sites 852D, 854SN, 932D and 963D in Fig. 19). The Distomon (Fig. 13c, d) and Aliki faults (DSTF and ALKF in Fig. 6) represent the main transverse structures affecting the studied area.

5.c.7. Timing of deformation

The timing of deformation in the studied area is constrained by the age of syn-orogenic sedimentary units and by the Aptian regional unconformity underlying the Mesoautochthonous Complex and the UBF.

In the Pelagonian Unit the D1a sub-stage is dated as latest Jurassic as it is coeval with sedimentation of the ophiolite-bearing deposits topping the carbonate and pelagic succession (Figs 15a, 20). Syn-sedimentary extension-related deformations in the LBF were clearly observed only in the LBFa and in the lower part of the LBFb subunits allowing us to tentatively limit the age of the D1a sub-stage to the Tithonian–Valanginian time span.

The D1b sub-stage deformations often follow but are partly coeval with the D1a deformations recorded in the more external portion of the Pelagonian Unit. The D1b deformations affected the Pelagonian Unit after sedimentation of radiolarite and ophiolite-bearing deposits and do not affect the LBF, allowing the attribution of a Kimmeridgian–?Valanginian age to the deformations. Valanginian is also the youngest age of the deformed platform carbonate units partly preserved above the ophiolite nappe (namely the Munella Platform above Mirdita ophiolites in Albania Fig. 1; Schlagintweit *et al.* 2006) and successively sealed by the mildly deformed Mesoautochthonous Complex. This suggests that obduction-related deformations lasted at least until Valanginian time.

The UBF and First Mesoautochthonous Cycle sealed the D2 deformations acquired by the LBF and Pelagonian Unit, respectively. In the Koumaritsi area a little-deformed succession of the UBF (oldest age: Albian; Nirta *et al.* 2015) unconformably covers the LBFc subunit (youngest age: lower Aptian; Nirta *et al.* 2015) that shows evidence of faulting and F2-related boudinage (Fig. 13a). The oldest age of the First Mesoautochthonous Cycle lying onto deformed ophiolites and the Pelagonian Unit is late Aptian in the more internal sector (Vermion–Vourinos area, Fig. 1; Photiades *et al.* 2007) and Albian in the studied area. Considering the above data, it is possible to attribute an early to middle Aptian age to the D2 deformations.

The D3 deformations were clearly detected only in the LBF and UBF whereas it was not possible to ascertain their existence in the Mesoautochthonous Complex. On the other hand, they do not affect the Pelagonian and Parnassus flysches. As a consequence, the age and significance of this deformation phase remains so far ill-defined. Tentatively, it is possible to attribute a Santonian (youngest age of the UBF) to Paleocene age

https://doi.org/10.1017/S0016756817000942 Published online by Cambridge University Press

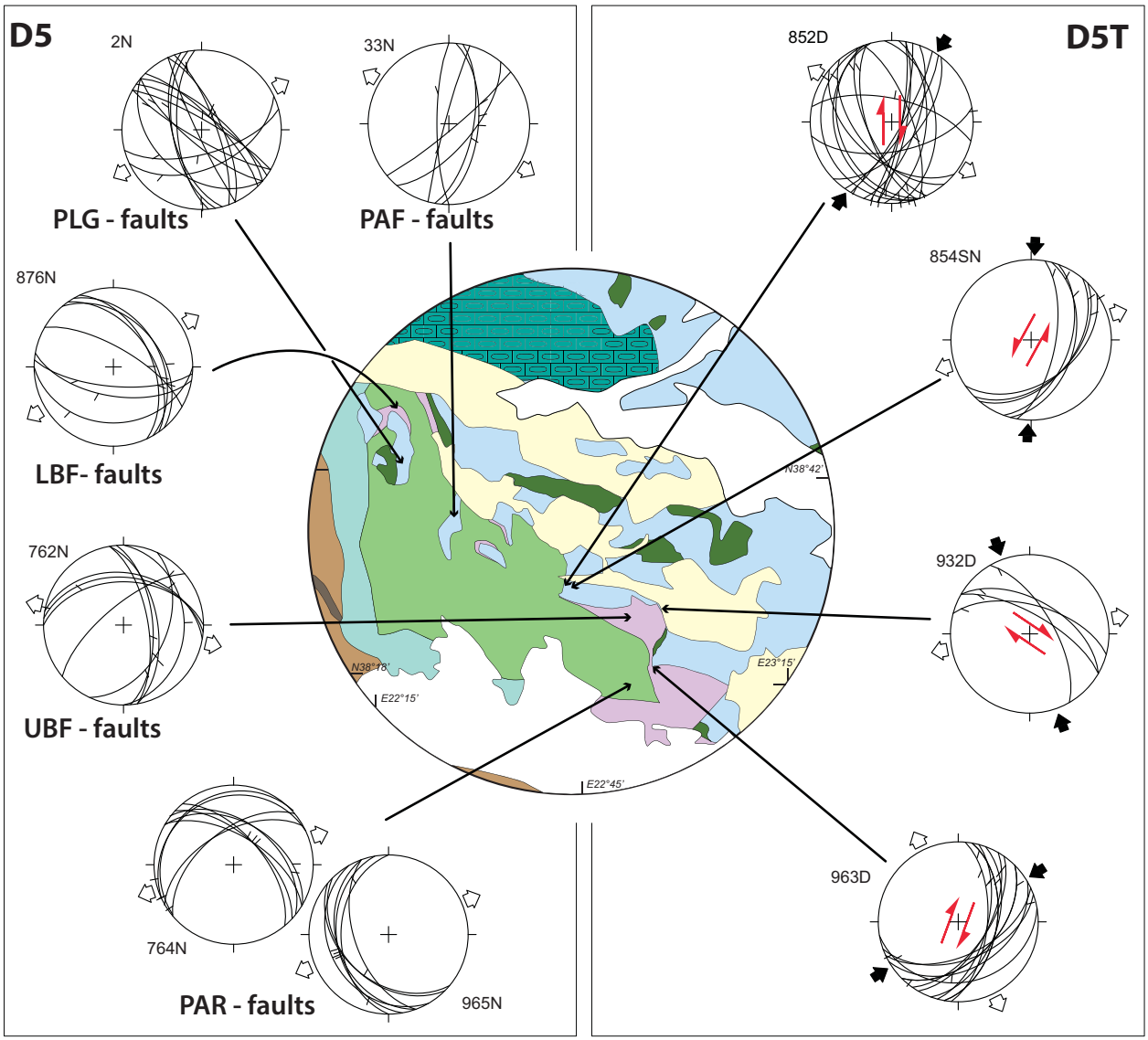


Figure 19. (Colour online) Schematic diagram illustrating areal distribution of mesostructural fault slip data and fold axes relative to D5 and $D5_T$ deformation phases. White arrows indicate direction of extension (σ_3) and black arrows indicate direction of compression (σ_1) calculated through inversion of fault slip data. All diagrams are equal-area lower hemisphere projections. UBF – Upper Boeotian Flysch; LBF – Lower Boeotian Flysch; PLG – Pelagonian Unit, limestones; PAR – Parnassus Unit, limestones; PAF – Parnassus Flysch.

(oldest age of the Parnassus and Pelagonian flysches) to the D3 phase.

The D4 and localized $D4_{bt}$ deformations took place after the Pelagonian and Parnassus Flysch sedimentation (early Eocene) and were later sealed by the oldest post-orogenic sediments known in the area (Serravallian lacustrine deposits of the Thiva Basin; Mettos, Ioakim & Rondoyanni, 2000).

6. Proposed geodynamic model

The presented biostratigraphic, stratigraphic and structural data along with consolidated first-order geological constraints concerning the whole orogen converge in the reconstruction of the following tectonic evolution for the area:

6.a. From rifting to the passive margin stage

The rifting stage, accompanied by transitional to alkaline volcanism, occurred during early–Middle Triassic time and was widely documented in the Pelagonian succession (Baud *et al.* 1991; Capedri *et al.* 1997; A. De Bono, unpub. Ph.D. thesis, Univ. Lausanne, 1998). Furthermore, events of alkaline to transitional rift-related volcanism are also recorded in the Pindos stratigraphy (Pe-Piper, 1982; Pe-Piper & Piper, 1991).

In the Othrys Massif and in the Argolis Peninsula (Fig. 1) the transition from the Pelagonian Platform to the more distal eastern marginal series (West Maliac Margin Units) and up to the oceanic crust is well documented. The onset of oceanization in the Maliac–Vardar basin is testified to by the oldest radiolarites (Anisian) deposited on top of MOR basalts (Bortolotti *et al.* 2006; Bortolotti *et al.* 2013; Ferrière *et al.*

https://doi.org/10.1017/S0016756817000942 Published online by Cambridge University Press

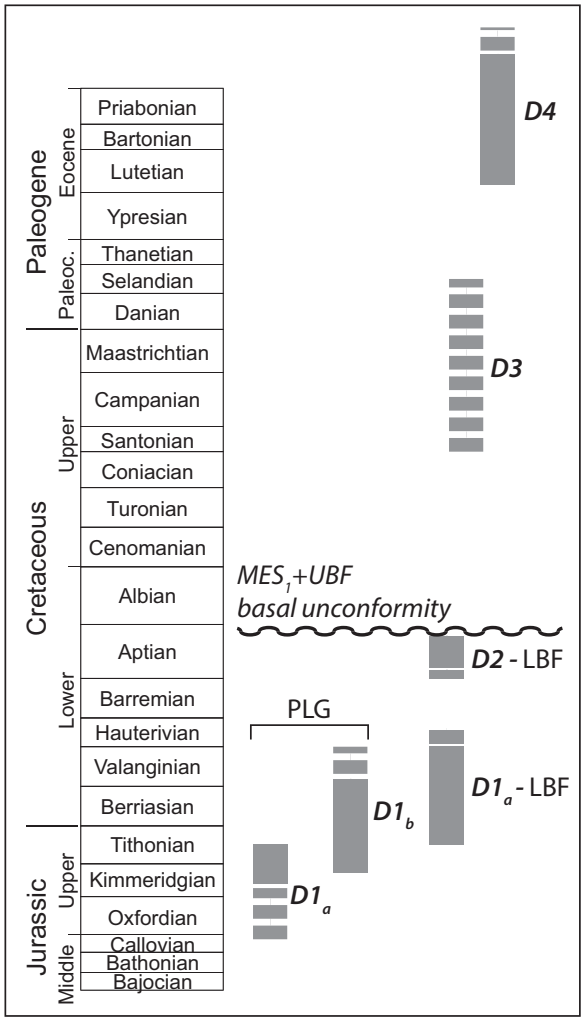


Figure 20. Inferred ages of the Late Jurassic to Eocene deformation phases (D1 to D4) in Central Greece.

2015). By contrast, since Early Jurassic time the Pindos and Ionian geotectonic zones are interpreted as pelagic intracontinental basins separated by an intervening carbonate platform represented by the Gavrovo Unit (Fig. 1); the scattered outcrops testifying to the existence of a rifting stage in the Pindos Basin are then not corroborated by evidence of oceanization.

During the passive margin stage, east of the Pindos Basin, only the Pelagonian Zone could be clearly identified as an isopic zone while the Boeotian and Parnassus zones are not yet differentiated and shared with the Pelagonian Zone a similar stratigraphy dominated by neritic carbonates of from Late Triassic to early Middle Jurassic age (Fig. 4).

In the proposed model, the Late Triassic geotectonic setting of the transition from the Adria continental margin to the Maliac–Vardar Ocean can be summarized as in Figure 21a.

6.b. Obduction – D1 tectonic phase

Intraoceanic subduction in the Maliac–Vardar Ocean is testified to by the occurrence of ophiolitic sequences developed in a supra-subduction environment (Beccaluva *et al*. 2005; Saccani *et al*. 2008*b*; Bortolotti *et al*. 2013) and by a subduction-related continental magmatic arc and back-arc basin towards the European margin (i.e. the Paikon arc and Guevgueli back-arc basin; Mercier, 1966; Ferrière & Stais, 1995; Brown & Robertson, 2003, 2004; Saccani *et al.* 2008*a*; Bortolotti *et al.* 2013) developed since early Middle Jurassic time (Fig. 22a). These magmatic events imply the existence of an E-dipping subducting plane since Early Jurassic time (Bortolotti *et al.* 2005).

During Middle Jurassic time, as a consequence of the continuing convergence between Adria and Europe, tectonically decoupled oceanic lithosphere started thrusting westwards (Bébien *et al.* 1980; Spray & Roddick, 1980). This event led to metamorphism at the sole of the overriding slab and mélange formation after off-scraping of the facing oceanic sediments and erosion of the advancing slab. At the Middle–Late Jurassic transition, the overriding slab approached the eastern margin of the Adria continental margin (i.e. the Pelagonian Zone). In late Middle Jurassic time, the advancing ophiolite nappe caused a rapid drowning of the distal continental margin (i.e. West Maliac Margin Units) that shifted from carbonate deposition to deep-sea siliceous deposition and then to ophiolite-bearing mass flow deposits. At the same time, to the west the continental margin experienced emersion episodes in the western Pelagonian Zone and in the Parnassus Zone (b1 bauxite horizon) (Figs 4, 21b). Emersion is correlated with the lithospheric forebulge induced by the load of the ophiolite nappe to the east (Nirta *et al.* 2015). The bending was accommodated by drowning of a large portion of the former Pelagonian Platform and development of the Boeotian Basin (Fig. 21b). Differentiation of the Parnassus and Pelagonian zones with interposition of the Boeotian Basin was a diachronous event. In fact, while some platform portions rapidly drowned to form the future Boeotian Basin (Aliki and Makariotissa sections; Danelian & Robertson, 1998), some other portions necessarily represent a continuous shallow-water environment to allow the migration of the allochthonous b1 bauxites from the ophiolites to the east throughout the western Pelagonian Platform and up to the future Parnassus Zone. An obduction-related extensional regime is registered by the syn-sedimentary faulting in the mass flow deposits on top of the Jurassic carbonates of the Pelagonian Unit and in the LBF throughout latest Jurassic time (D1a sub-stage; Fig. 21b). Final overthrusting of the ophiolites and associated mélange progressively shifted into a compressional tectonic regime in the Pelagonian Platform (D1b sub-stage; Fig. 21b). The time–space distribution of the ophiolite detritus supplied by the obducting units in the facing continental margin and top-to-the-SW kinematic indicators within the tectonic foliation S1 clearly point to an E-towards-W translation of the obducted units. This sedimentation versus obduction trend is clearly recognizable throughout Late Jurassic time and culminated with the beginning of sedimentation of the LBF

https://doi.org/10.1017/S0016756817000942 Published online by Cambridge University Press

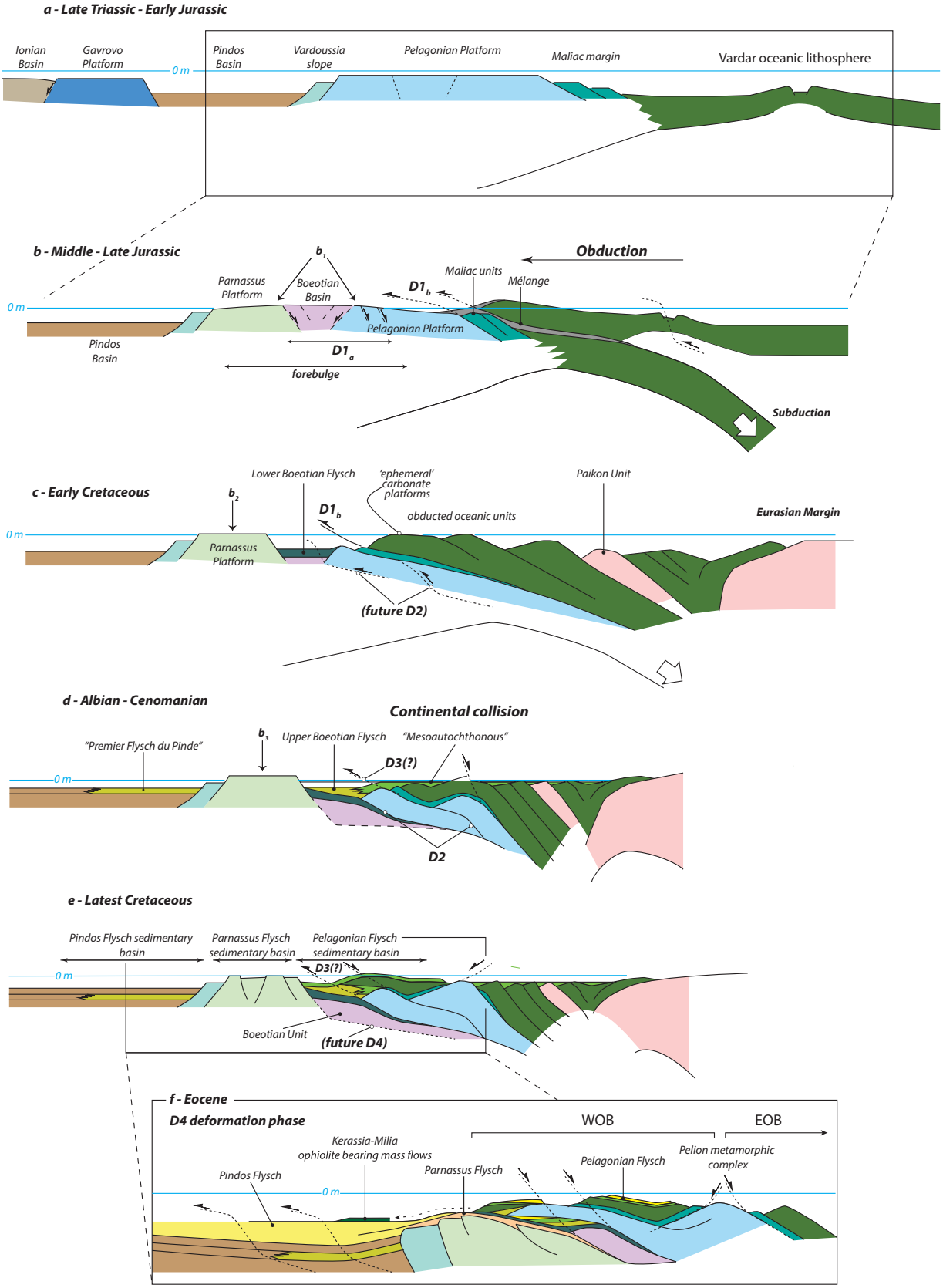


Figure 21. (Colour online) Proposed geodynamic model and tectonic evolution for the obduction and continental collision in the Hellenic belt. See text for discussion.

https://doi.org/10.1017/S0016756817000942 Published online by Cambridge University Press

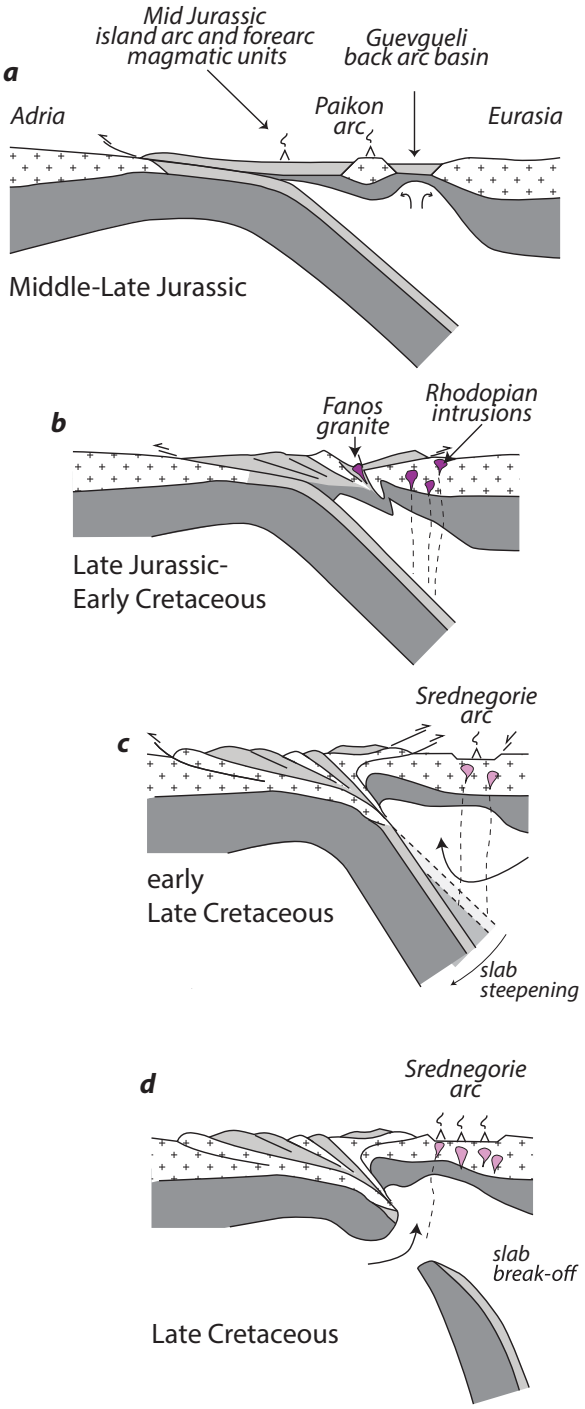


Figure 22. (Colour online) Schematic reconstruction of the evolution of subduction-related magmatism accompanying the closure of the Maliac–Vardar Ocean from Middle Jurassic time until Late Cretaceous post-collisional collapse. The Middle–Late Jurassic step is redrawn after figure 10 in Bortolotti *et al.* (2013). Not to scale.

in the Boeotian Basin. At this time, a new emersion episode was recognized in the Parnassus Platform (b2 horizon), which could possibly reflect a tectonically forced regression, induced during the climaxing phase of obduction (Fig. 21c). Obduction could be traced up to Valanginian time, as suggested by the age of the youngest ophiolite-derived clastic deposits on the top of the Pelagonian Platform and the youngest syn-obduction carbonate platform set on the top of the ophiolite nappe (i.e. the Munella Platform; Schlagintweit *et al.* 2006).

The youngest evidence of oceanic crust in the Maliac–Vardar Ocean is of latest Jurassic age (Bortolotti *et al.* 2013 and quoted references). Similarly, back-arc magmatism between the Paikon arc and the Eurasian margin (Guevgueli back-arc basin), induced by the E-directed subducting slab of the Maliac–Vardar Ocean (Saccani *et al.* 2008*a*) since Middle Jurassic time, continued until Late Jurassic time (Danelian, Robertson & Dimitriadis, 1996; Kukoč *et al*. 2012) and was also associated with the coeval emplacement of calc-alkaline granitoids both in the back-arc oceanic crust and in the nearby Eurasian continental margin (e.g. Fanos granite; Anders *et al.* 2005; Šarić *et al.* 2009). Moreover, arc-related calc-alkaline granitoids, now found as orthogneisses in the Rhodope Massif, are reported to intrude the Eurasian margin further east until Late Jurassic – Early Cretaceous times (Turpaud & Reischmann, 2010) ('Rhodopian intrusions' in Fig. 22b). Therefore, we assume that E-dipping subduction of the Maliac–Vardar Ocean continued throughout Early Cretaceous time. However, a high convergence rate between Adria and Europe during this period (Rosenbaum, Lister & Duboz, 2002; Bertrand, Guillou-Frottier & Loiselet, 2014) could have induced upper plate compression that prevented upward migration of magmas necessary to trigger widespread volcanic activity and, at the same time, could have facilitated sequestration of melts at deep to moderate crustal depths.

6.c. Continental collision: D2 tectonic phase

Ophiolite-derived mass flow gliding events progressively increased in the upper portion of the LBF of Barremian–Aptian age (LBFc). The sedimentation in the Boeotian trough was stopped by an intense tectonic event that produced the most pervasive deformations in the LBF. The beginning of sedimentation of the UBF of Albian age sealed D2 tectonic deformations in the underlying LBF (Nirta *et al.* 2015) allowing the attribution of an Aptian–Albian age to this tectonic event. In the same time span compressional deformation likely controlled the Parnassus Platform emersion soon after the deposition of allochthonous bauxitic laterites (b3 horizon) derived from degradation of penecontemporaneous weathering crusts developed on the more internal units (i.e. Pelagonian and Ophiolitic obducted units) (Fig. 21d). The stratigraphic gap corresponding to the third bauxite horizon (b3) is the longest one since it extended from part of the Aptian to at least the lower Turonian (> 20 Ma; Combes *et al.* 1981; Carras & Tselepidis, 2001). The stable and relatively high sea level record from Valanginian until Late Cretaceous times (Haq, 2014) allows ascribing the b3 emersion episode to the far-field effects of compressional tectonics.

https://doi.org/10.1017/S0016756817000942 Published online by Cambridge University Press

This prominent Aptian–Albian tectonic phase was also recorded by upper-greenschist to blueschist metamorphic events in the inner Pelagonian Zone (Barton, 1976; Yarwood & Dixon, 1977; Schermer, Lux & Burchfiel, 1990; Lips, White & Wijbrans, 1998) (Fig. 4), and by nappe stacking and high-pressure conditions in the Rhodope Massif (130–115 Ma; Burg, 2012). Furthermore, the ophiolitic units of the EOB, mostly represented by island arc and back-arc basin ophiolites (Ferrière & Stais 1995; Saccani *et al.* 2008*a*; Bonev *et al*. 2015), emplaced eastwards above the Eurasian margin units previously affected by Late Jurassic high-pressure metamorphism (Bonev *et al.* 2015 and quoted references). This emplacement was postdated by unconformable sedimentation of Lower Cretaceous carbonates in the Circum-Rhodope Belt (i.e. westernmost part of the Rhodope Massif; Mercier 1968; Stais & Ferrière, 1994; Ivanova, Bonev & Chatalov, 2015). This testifies that at the Late Jurassic – Early Cretaceous transition the magmatic arc and back-arc oceanic basin located to the west of the Eurasian margin (i.e. the Guevgueli back-arc ophiolites and the Paikon arc ophiolites) had already ceased their magmatic activity and were emplaced above deformed and metamorphosed units of the Eurasian margin (Bonev *et al.* 2015; Saccani *et al.* 2015; Ferrière, Baumgartner & Chanier, 2016) (Figs 21c, 22b).

Finally, anatectic melts of late Aptian age (Schenker *et al*. 2014) were recognized in the eastern Pelagonian rim.

All these events, along with the lack of evidence of ophiolites younger than Late Jurassic in the Albanian–Hellenic sector of the orogen, allow interpreting the D2 deformation phase as a manifestation of the final continental collision of the Pelagonian Margin (Adria Plate) with the Rhodope Massif (European Plate). In this interpretation the LBF sedimented in a temporal window placed between the ongoing obduction and continental collision (Fig. 21c).

Structural analysis of D2 structures points to a westward tectonic transport. The observable tectonic relationships between the LBF and the inner tectonic units allow explaining the D2 deformation as being the result of the activation of a sole thrust at the base of the Pelagonian Platform and rejuvenated westward tectonic translation of the overlying ophiolitic thrust sheets.

However, the occurrence of Late Cretaceous ophiolites in the Kozara Mountains (northern Bosnia and Herzegovina; Karamata *et al.* 2000; Ustaszewski *et al.* 2009, 2010) testifies that the collision in the northern sectors of the belt occurred in latest Cretaceous – Paleocene times (Schmid *et al.* 2008).

Two main hypotheses exist concerning the timing of collision in the Hellenic–Dinaric chain and final closure of the Maliac–Vardar Ocean: latest Cretaceous–Tertiary throughout the whole orogen (Robertson & Dixon, 1984; Robertson *et al.* 1991, 2013; Pamic, 2002; Schmid *et al.* 2008) or latest Jurassic – Early Cretaceous (Papanikolaou, 1997, 2009, 2013; Meinhold *et al.* 2009; Bortolotti *et al.* 2013; Schenker *et al.* 2014), at least in the Albanian–Hellenic sector. To date, both hypotheses could be considered valid; however, the evidence so far collected in Albania and Greece and the differences between the southern and northern sectors of the belt (see discussion in Saccani *et al.* 2015) lead us to prefer a diachronous closure model explaining earlier collision in the south and later in the northern sectors.

This diachronous closure could alternatively be explained as the consequence of variable widths of different oceanic sectors, possibly separated by lithospheric lineaments (e.g. the Scutari–Pec fault zone, Fig. 1; Dercourt, 1967; Kissel, Speranza & Milicevic, 1995), or due to oblique subduction (Smith & Spray, 1984).

6.d. The Late Cretaceous post-collisional tectonics

After the climax of the collisional event in the Boeotia region, the sedimentation resumed with the flysch deposition in the Boeotian Basin (i.e. UBF) and the neritic carbonates of the Mesoautochthonous Complex above the ophiolitic thrust sheets and Pelagonian Unit (Fig. 21d). Both the UBF and the first cycle of Mesoautochthonous sequences are underlined by unconformable contacts marked by lateritic crusts, coarse-grained mass flow deposits and erosional surfaces. The high proportion of ophiolite debris in the UBF along with common calcareous mass flows and lateritic debris (Nirta *et al.* 2015) implies still active tectonics along the eastern edge of the Boeotian Basin that triggered drowning of ephemeral platforms, emersion episodes and catastrophic collapses along the shelf break. The sedimentary environment of the UBF could be that of a foreland basin, while the Mesoautochthonous Complex contemporaneously sedimented in the subsiding hinterland sectors after the tectonic climax related to collision (D2 phase).

The correlation of the UBF with the coeval siliciclastic turbidite deposits of the Pindos Zone (Premier Flysch du Pinde; Aubouin, 1957; Fleury, 1975; Maillot, 1979; Wagreich *et al.* 1996; Neumann, 2001) is also proposed. A similar composition and palaeocurrent data of the UBF and 'Premier Flysch du Pinde' (Neumann, 2001) point to a common provenance from the internal (eastern) zones that produced turbidite currents then deposited in the basinal areas of the Boeotian Zone and those bordering the eastern Pindos Basin.

There is evidence of an older deformation phase preceding the ubiquitous Tertiary events that gave rise to the older deformations observed in the UBF and crosscuts D2 structures of the LBF (D3 deformation phase).

This deformation phase is poorly constrained because of the paucity of explicative outcrops in the UBF and resistance in developing mesoscale deformations in the Mesoautochthonous Complex. However, we tentatively attribute to this deformation a Late Cretaceous age as no D3 deformations were recognized in the Tertiary flysches.

https://doi.org/10.1017/S0016756817000942 Published online by Cambridge University Press

D3 deformations, showing westward vergence, could be linked with a renewed westward translation of the Internal Hellenid units related to the ongoing Africa–Eurasia convergence. Progressive westward thrusting was coupled with syn-orogenic exhumation of portions of the eastern Pelagonian Zone as testified to by available geochronological data (T. Most, unpub. Ph.D. thesis, Eberhardt-Karls-Universität Tubingen, 2003; Schenker, Fellin & Burg, 2015). Exhumation of metamorphic terrains of the Pelagonian Zone was linked with an uplifted dome, possibly through a regional antiformal structure (Kilias *et al.* 2010; Schenker *et al.* 2014), that was successively eroded and supplied both continental-derived metamorphic and ophiolitic debris to the adjacent Mesoautochthonous basins (T. Most, unpub. Ph.D. thesis, Eberhardt-Karls-Universität Tubingen, 2003; Photiades *et al.* 2007; Schenker *et al*. 2014) (Fig. 21d).

Sedimentation of the Mesoautochthonous Complex was synchronous with the development of an arc-related calc-alkaline magmatism in the upper plate, the Eastern Srednogorie and Panagyurishte area (Bulgaria). The northward continuation of these magmatic districts as far as Romania concurs to form the Apuseni–Banat–Timok–Srednogorie magmatic–metallogenic belt (ABTS; Jankovic, 1997; von Quadt *et al.* 2005; Zimmerman *et al.* 2008; Richards, 2015).

A wide debate exists on the mechanism guiding the magma generation in the ABTS and its development with respect to the onset of continental collision, with different models reflecting divergences in the palaeogeographic reconstructions. Summarizing, the proposed models include those favouring pre-collisional subduction-related magmatism, eventually accompanied by slab rollback (Lips, 2002; von Quadt *et al.* 2005; Chambefort & Moritz 2006; Zimmerman *et al.* 2008; Gallhofer *et al.* 2015) or syn-collisional slab tearing/slab break-off (Neubauer, 2002) and post-collisional orogenic collapse (Berza, Constantinescu & Vlad, 1998; Bojar, Neubauer & Fritz, 1998; Willingshofer, Neubauer & Cloetingh, 1999; Iancu *et al.* 2005). In particular, some authors (Lips, 2002; Gallhofer *et al.* 2015) considered the continuous subduction of oceanic crust and slab steepening/rollback as the only mechanism that guided the evolution of the whole ABTS during Late Cretaceous time. They assumed that a new oceanic subduction started in the Maliac–Vardar Ocean in Albian time, after the Early Cretaceous tectonic phase (D2). In this hypothesis, melt production started as soon as the subducting slab reached the partial melting zone and continued throughout Late Cretaceous time fuelled by a continuous subduction until continental collision in latest Cretaceous time (Gallhofer *et al.* 2015). On the other hand, recent research along the Alpine–Himalayan belt has revealed that many magmatic deposits previously assumed to be subduction related are in fact syn- or post-collisional (Shafiei, Haschke & Shahabpour, 2009; Moritz *et al.* 2010; Imer, Richards & Creaser, 2013) and sometimes occur long (30–40 Ma) after the end of oceanic lithosphere subduction (Hou *et al.* 2009, 2011).

In our interpretation, the evolution of the ABTS possibly follows the diachronism in the collision as testified to by the different ages of the older magmatic events (and beginning of extension) varying from Cenomanian–Turonian in the south (Eastern Srednogorie and Panagyurishte area, Bulgaria) up to Santonian–Campanian (Banat and Apuseni regions, Romania) in the north (see data compilation in Gallhofer *et al.* 2015). We interpret the Mesoautochthonous Complex and the Eastern Srednogorie and Panagyurishte magmatic arcs (roughly corresponding to the Hellenic and Albanian sectors of the belt) as connected to regional extension in the upper plate following an initial slab steepening started soon after the continental collision (i.e. Albian), followed by warming of the stalled slab and its successive break-off (Wortel & Spakman, 2000; Neubauer, 2002) and widespread orogenic collapse from late Cenomanian–Turonian times (Fig. 22c,d). Numerical modelling shows that the delay in time between the onset of collision and final slab break-off can be 20 Ma (Duretz, Gerya & May, 2011; van Hunen & Allen, 2011) in the case of old, and therefore cold and strong, subducting slabs. At the time of collision onset (*c*. 115 Ma) the subducted Maliac–Vardar oceanic lithosphere was represented by old and strong Triassic to Middle Jurassic crust, thus the final break-off could be postulated at *c*. 95 Ma (i.e. late Cenomanian–Turonian), which corresponds with the age of the comagmatic sediments in the Eastern Srednogorie area (Nachev & Dimitrova, 1995). The formation of the arc magmatism was facilitated by reduced plate convergence starting from early Late Cretaceous time (Rosenbaum, Lister & Duboz, 2002; Bertrand, Guillou-Frottier & Loiselet, 2014). Furthermore, we assume that after the Aptian–Albian continental collision, a slow subduction continued with the involvement of the Pelagonian thinned crust (Stampfli, Marcoux & Baud, 1991; Robertson *et al.* 1991). Collision and subduction of the portions of thinned continental crust concur in reducing the lateral force acting on the slab causing a rapid slab steepening enhanced by its vertical gravitational force (Fig. 22c). This mechanism may have favoured orogenic collapse in the upper plate and easier ascent of fertile magmas to the upper crust (Berza, Constantinescu & Vlad, 1998).

6.e. Tertiary crustal shortening and thickening: D4 and $D4_{bt}$ deformation phases

During late Paleocene time, ubiquitous shaly pelagic sediments (pre-flysch lithofacies) unconformably covered the tectonic stack levelling the sea floor morphology (Fig. 21e). The following turbiditic sedimentation onset in early Eocene time was almost synchronous in the different geotectonic zones. On the other hand, terminal ages are diachronous showing a younging trend towards the western sectors. In the studied area, the Pelagonian Flysch lasted until early Eocene

https://doi.org/10.1017/S0016756817000942 Published online by Cambridge University Press

time, the Parnassus Flysch until early–middle Eocene time and the Pindos Flysch until late Eocene time. This trend reflects the W-verging tectonic transfer related to late-stage thrusting that remobilized the previously formed tectonic stack above the Parnassus Platform (D4 deformation phase). The age of overthrusting of the internal tectonic units above the Parnassus Platform is constrained by the terminal age of the Parnassus Flysch (early–middle Eocene). Moreover, during Lutetian time, ophiolite slide blocks and debris flow deposits glided in the Pindos Flysch in the Etolia region just in front of the Vardoussia slope (C. Beck, unpub. Ph.D. thesis, Univ. Science and Technology, Lille, 1975; Beck, 1980; Figs 2, 21f). We locate the provenance area of these ophiolite-bearing mass flows in the Iti ocean-derived klippe located on top of the Parnassus Unit, thus dating the age of overthrusting of the Internal Hellenid units above the Parnassus Platform to middle Eocene (Lutetian) time.

Extensive nappe stacking and continental crust thickening characterized the Tertiary compressive phase. Protracted convergence between Adria and Eurasia during the D4 tectonic phase led to the final accretion of the Pelagonian Unit and its decoupling from the subducting Adriatic slab (Jolivet & Brun, 2010) and consequent shifting of the compressive front to the more external southwestern portions of the belt. As a result, the Pindos and Gavrovo zones were progressively involved in the fold and thrust belt and metamorphosed to form the Cycladic Blueschist Complex since middle Eocene time (Jolivet & Brun, 2010 and references therein) (Fig. 21f).

The last compressional event recognized in the study area ($D4_{bt}$) is localized on the northeastern rim of the Parnassus Platform that acted as a tectonic buttress locally conditioning the tectonic migration. Along the northern border of the Helicon mountain range, the Parnassus Cretaceous limestones thrust northwards folding and cross-cutting the previous D4 structures. Furthermore, the Boeotian Zone limestone sequence was squeezed between the Pelagonian and Parnassus units guiding it to thrust northwards above the previously stacked units including the Eocene Pelagonian Flysch (Figs 6, 8).

6.f. Aegean extensional regime: D5 deformation phase

The previously stacked units were then dissected by both high- and low-angle faults under an extensional stress field with a horizontal ENE-oriented minor principal (σ3) stress axis (Fig. 19). Extension inverted some D4 thrusts as low-angle fault zones (see Figs 16, 21f) or as regional detachments (Papanikolaou, Gouliotis & Triantaphyllou, 2009). Clear evidence within the studied area is represented by the tectonic contacts at the base of the internal units overthrust above the northern flank of the Parnassus Platform (Kranis & Papanikolaou, 2001; Fig. 6).

The extensional regime, whose main regional effect is the opening of the Aegean Sea and exhumation of the Cycladic Blueschist Complex, started in northern Greece in late Eocene time (Gautier *et al.* 1999; Lips, White & Wijbrans, 2000; Jolivet *et al.* 2003; Jolivet & Brun, 2010) and progressively moved southwards while accretion continued at the subduction zone. Aegean extension is commonly considered a consequence of the slab retreat of Adria with respect to Eurasia (Le Pichon & Angelier, 1979; Meulenkamp *et al.* 1988; Jolivet *et al.* 2013).

In the studied area, transition from a compressional to extensional regime was accompanied by clockwise block rotation accommodated by NNE-trending dextral transversal faults developed at the regional scale (e.g. Distomon (DSTF) and Aliki (ALKF) fault zones; see Fig. 6). Block rotations emphasized the northward back-thrust of the Boeotian Unit with the activation of the ATRF zone (Fig. 6) with left-lateral movement. Clockwise block rotations were possibly accentuated since *c.* 5 Ma by the interaction of the right-lateral North Anatolian Fault system (Armijo *et al.* 1996, 1999) that also enhanced extension in the North Aegean Sea, Euboea–Sperchios Graben and Corinth Basin (Goldsworthy, Jackson & Haines, 2002).

7. Final remarks

The Hellenic orogen developed (and is still evolving) as a result of the African–European convergence since Middle Jurassic time. Superimposed obduction and collision-related compressive tectonic phases followed by extension resulted in a complex arrangement of the ophiolitic outcrops along the belt, leading some authors to identify a multiplicity of 'ophiolitic belts' eventually interpreted as remnants of just as many oceanic branches or basins. The biostratigraphic, stratigraphic and structural data newly collected in the Boeotia region, along with consolidated first-order geological constraints concerning the whole orogen, were here used to reconstruct the tectonic evolution of this area, and to propose a 'single ocean' tectonic model spanning from Middle Jurassic up to Tertiary times. In the studied transect it is possible to consider two extra main geological constraints: the existence of a pelagic basin since Middle Jurassic time west of the Pelagonian Platform (i.e. the Boeotian Zone), and a persistent carbonate platform throughout the Mesozoic located further west, the Parnassus Zone.

In the Hellenic orogen obduction followed an earlier event of intraoceanic thrusting of Middle Jurassic age (174–160 Ma; Roddick, Cameron & Smith, 1979; Spray & Roddick, 1980; Dimo-Lahitte, Monié & Vergély, 2001) and culminated with ophiolite emplacement onto the Adria continental margin during Early Cretaceous time. The assemblage of geochemical signatures of the ophiolites of the WOB and EOB is substantially identical, and also similar are the isotopic ages of the metamorphic soles at their base. A differential origin of the WOB and EOB in two (or more) oceanic basins that emplaced contemporaneously onto continental margin(s) would thus contrast with the

https://doi.org/10.1017/S0016756817000942 Published online by Cambridge University Press

existence of a persisting carbonate platform throughout Cretaceous time in between (i.e. Parnassus), and with structural data relative to the Jurassic and Cretaceous tectonic phases pointing to a constant westward tectonic transfer.

In the Hellenic–Albanian sector of the belt the youngest ophiolites are of latest Jurassic age. This datum along with the documentation of a severe Early Cretaceous tectonic phase accompanied by erosion, metamorphism, ophiolite emplacement and nappe stacking both on the easternmost Adria margin units (i.e. the eastern Pelagonian Unit) and westernmost Eurasian margin units (Circum-Rhodope and Rhodope units; Burg, 2012; Bonev *et al.* 2015; Ivanova, Bonev & Chatalov, 2015) contrasts with a persisting oceanic basin throughout Cretaceous time.

These general considerations along with the reconstruction of the tectono-stratigraphic evolution of the studied units allow proposing the Aptian–Albian boundary as the age of collision between Adria and Eurasia, about 25 Ma after the end of obduction (Valanginian).

Acknowledgements. This research was supported by the Italian Ministry of Education, University and Research – PRIN 2010–2011 project: 'Birth and death of oceanic basins: geodynamic processes from rifting to continental collision in the Mediterranean and circum-Mediterranean orogens', grant no. 2011AZR98L_005. Many thanks go to Michele Marroni and Emilio Saccani for helpful observations, enlightening discussions and fruitful suggestions. We also wish to thank Špela Goričan for her useful suggestions. We are indebted to Jacky Ferrière and to an anonymous reviewer for their constructive reviews and useful comments that greatly improved the manuscript.

References

Agnini, C., Fornaciari, E., Raffi, I., Catanzariti, R., Pälike, H., Backman, J. & Rio, D. 2014. Biozonation and biochronology of Paleogene calcareous nannofossils from low and middle latitudes. *Newsletter on Stratigraphy* **47**, 131–81.

Ananiadis, G., Vakalas, I., Zelilidis, A. & Stoykova, K. 2004. Palaeographic evolution of Pindos basin during Paleogene using calcareous nannofossils. *Bulletin of the Geological Society of Greece* **36**, 836–45.

Anders, B., Reischmann, T., Poller, U. & Kostopoulos, D. 2005. Age and origin of granitic rocks of the eastern Vardar Zone, Greece: new constraints on the evolution of the Internal Hellenides. *Journal of the Geological Society, London* **162**, 857–80.

Angelier, J. & Mechler, P. 1977. Sur une méthode graphique de recherche des contraintes principales également utilisable en tectonique et en sismologie: la méthode des dièdres droits. *Bulletin de la Société géologique de France* **19**, 1309–18.

Armijo, R., Meyer, B., Hubert, A. & Barka, A. 1999. Westward propagation of the North Anatolian fault into the northern Aegean: timing and kinematics. *Geology* **27**, 267–70.

Armijo, R., Meyer, B., King, G. C. P., Rigo, A. & Papanastassiou, D. 1996. Quaternary evolution of the Corinth Rift and its implications for the Late Cenozoic evolution of the Aegean. *Geophysical Journal International* **126**, 11–53.

Aronis, G. 1955. Geographical distribution, geological placing and aspects on the genesis of the Greek bauxite. *Bulletin of the Geological Society of Greece* **2**, 55–79 (in Greek).

Aubouin, J. 1957. À propos de la Série du Pinde-Olonos. Essai de corrélations stratigraphiques dans le Pinde Méridional. *Annales Géologiques des Pays Helléniques* **8**, 246–263.

Aubouin, J. 1959. Contribution à l'étude géologique de la Grèce septentrionale: les confins de l'Epire et de la Thessalie. *Annales Géologiques des Pays Helléniques* **10**, 1–483.

Aubouin, J. 1965. *Geosynclines*. Amsterdam: Elsevier, 335 pp.

Barton, C. M. 1976. The tectonic vector and emplacement age of an allochthonous basement slice in the Olympos area, NE Greece. *Bulletin de la Société géologique de France* **7**, 253–8.

Baud, A., Jenny, C., Papanikolaou, D., Sideris, C. & Stampfli, G. 1991. New observations on Permian stratigraphy in Greece and geodynamic interpretation. *Bulletin of the Geological Society of Greece* **25**, 187–206.

Baumgartner, P. O. 1984. A Middle Jurassic–Early Cretaceous low-latitude radiolarian zonation based on Unitary Associations and age of Tethyan radiolarites. *Eclogae Geologicae Helvetiae* **77**, 729–837.

Baumgartner, P. O. 1985. *Jurassic Sedimentary Evolution and Nappe Emplacement in the Argolis Peninsula (Peloponnesus, Greece)*. Denkschriften der Schweizerischen Naturforschenden Gesellbauschaft Bd. 99. Basel: Birkhäuser Verlag AG, 111 pp.

Baumgartner, P. O. 1995. Towards a Mesozoic radiolarian database – updates 1984–1990. In *Middle Jurassic to Lower Cretaceous Radiolaria of Tethys: Occurrences, Systematics, Biochronology* (eds P. O. Baumgartner, L. O'Dogherty, Š. Goričan, E. Urquhart, A. Pillevuit & P. De Wever), pp. 689–700. Mémoires de Géologie, Lausanne no. 23.

Baumgartner, P. O., Bartolini, A. C., Carter, E. S., Conti, M., Cortese, G., Danelian, T., De Wever, P., Dumitrica, P., Dumitrica-Jud, R., Goričan, Š., Guex, J., Hull, D. M., Kito, N., Marcucci, M., Matsuoka, A., Murchey, B., O'Dogherty, L., Savary, J., Vishnevskaya, V., Widz, D. & Yao, A. 1995a. Middle Jurassic to Early Cretaceous radiolarian biochronology of Tethys based on Unitary Associations. In *Middle Jurassic to Lower Cretaceous Radiolaria of Tethys: Occurrences, Systematics, Biochronology* (eds P. O. Baumgartner, L. O'Dogherty, Š. Goričan, E. Urquhart, A. Pillevuit & P. De Wever), pp. 1013–48. Mémoires de Géologie, Lausanne no. 23.

Baumgartner, P. O. & Bernoulli, D. 1976. Stratigraphy and radiolarian fauna in a Late Jurassic–Early Cretaceous section near Achladi (Evvoia, Eastern Greece). *Eclogae Geologicae Helvetiae* **69**, 601–26.

Baumgartner, P. O. & Bernoulli, D. 2015. Diachronous Middle–Late Jurassic ophiolite obduction and exposure along the eastern Pelagonian Margin (Hellenides, Greece). In *Proceedings of the XIV INTERRAD Conference, Antalya, Turkey, 22–26 March 2015*, pp. 113–14.

Baumgartner, P. O., Danelian, T., Dumitrica, P., Goričan, Š., Jud, R., Dogherty, L. O., Carter, B., Conti, M., De Wever, P., Kito, N., Marcucci, M., Matsuoka, A., Murchey, B. & Urquart, E. 1993. Middle Jurassic–Early Cretaceous radiolarian

https://doi.org/10.1017/S0016756817000942 Published online by Cambridge University Press

biochronology of Tethys: implications for the age of radiolarites in the Hellenides. *Bulletin of the Geological Society of Greece* **28**, 13–23.

Baumgartner, P. O., O'Dogherty, L., Goričan, Š., Dumitrica-Jud, R., Dumitrica, P., Pillevuit, A., Urquhart, E., Matsuoka, A., Danelian, T., Bartolini, A. C., Carter, E. S., De Wever, P., Kito, N., Marcucci, M. & Steiger, T. A. 1995b. Radiolarian catalogue and systematics of Middle Jurassic to Early Cretaceous Tethyan genera and species. In *Middle Jurassic to Lower Cretaceous Radiolaria of Tethys: Occurrences, Systematics, Biochronology* (eds P. O. Baumgartner, L. O'Dogherty, Š. Goričan, E. Urquhart, A. Pillevuit & P. De Wever), pp. 37−685. Mémoires de Géologie, Lausanne no. 23.

Bébien, J., Ohnenstetter, D., Ohnenstetter, M. & Vergély, P. 1980. Diversity of the Greek ophiolites: birth of the oceanic basins in transcurrent systems. *Ofioliti* **2**, 129–97.

Bébien, J., Platvoet, B. & Mercier, J. 1994. Geodynamic significance of the Paikon Massif in the Hellenides: contribution of the volcanic rock studies. *Bulletin of the Geological Society of Greece* **30**, 63–7.

Beccaluva, L., Coltorti, M., Prempti, I., Saccani, E., Siena, F. & Zeda, O. 1994. Mid-ocean ridge and supra-subduction affinities in ophiolitic belts from Albania. *Ofioliti* **19**, 77–96.

Beccaluva, L., Coltorti, M., Saccani, E. & Siena, F. 2005. Magma generation and crustal accretion as evidenced by supra-subduction ophiolites of the Albanide-Hellenide Subpelagonian zone. *Island Arc* **14**, 551–63.

Beck, C. M. 1980. Essai d'interprétation structurale et paleogéographique des roches vertes du Pinde d'Etolie (Grèce continentale méridionale). *Annales de la Société Géologique du Nord* **99**, 355–65.

Bernoulli, D. & Laubscher, H. 1972. The palinspastic problem of the Hellenides. *Eclogae Geologicae Helvetiae* **65**, 107–18.

Bertrand, G., Guillou-Frottier, L., & Loiselet, C. 2014. Distribution of porphyry copper deposits along the western Tethyan and Andean subduction zones: insights from a paleotectonic approach. *Ore Geology Reviews* **60**, 174–90.

Berza, T., Constantinescu, E. & Vlad, Ş.-N. 1998. Upper Cretaceous magmatic series and associated mineralisation in the Carpathian – Balkan Orogen. *Resource Geology* **48**, 291–306.

Blanchet, R., Durand Delga, M., Moullade, M. & Sigal, J. 1970. Contribution à l'étude du Crétacé des Dinarides internes: la région de Maglaj, Bosnie (Yougoslavie). *Bulletin de la Société géologique de France* **12**, 1003–9.

Bojar, A. V., Neubauer, F. & Fritz, H. 1998. Cretaceous to Cenozoic thermal evolution of the southwestern South Carpathians: evidence from fission-track thermochronology. *Tectonophysics* **297**, 229–49.

Bonev, N., Marchev, P., Moritz, R. & Collings, D. 2015. Jurassic subduction zone tectonics of the Rhodope Massif in the Thrace region (NE Greece) as revealed by new U–Pb and $^{40}Ar/^{39}Ar$ geochronology of the Evros ophiolite and high-grade basement rocks. *Gondwana Research* **27**, 760–75.

Bornemann, A., Aschwer, U. & Mutterlose, J. 2003. The impact of calcareous nannofossils on the pelagic carbonate accumulation across the Jurassic–Cretaceous boundary. *Palaeogeography, Palaeoclimatology, Palaeoecology* **199**, 187–228.

Bortolotti, V., Carras, N., Chiari, M., Fazzuoli, M., Marcucci, M., Nirta, G., Principi, G. & Saccani, E. 2009. The ophiolite-bearing mélange in the early Tertiary Pindos flysch of Etolia (Central Greece). *Ofioliti* **34**, 83–94.

Bortolotti, V., Carras, N., Chiari, M., Fazzuoli, M., Marcucci, M., Photiades, A. & Principi, G. 2003. The Argolis Peninsula in the paleogeographic and geodynamic frame of the Hellenides. *Ofioliti* **28**, 79–94.

Bortolotti, V., Carras, N., Chiari, M., Fazzuoli, M., Photiades, A. & Principi, G. 2004a. Sedimentary evolution of the Upper Jurassic Zyghosti platform, Kozani, Northern Greece. In *Proceedings of the International Symposium on Earth System Sciences 2004, Istanbul–Turkey*, pp. 705–12.

Bortolotti, V., Chiari, M., Kodra, A., Marcucci, M., Marroni, M., Mustafa, F., Pandolfi, L., Prela, M., Principi, G. & Saccani, E. 2006. Triassic MORB magmatism in the Southern Mirdita zone (Albania). *Ofioliti* **31**, 1–9.

Bortolotti, V., Chiari, M., Marcucci, M., Marroni, M., Pandolfi, L., Principi, G. & Saccani, E. 2004b. Comparison among the Albanian and Greek ophiolites, in search of constraints for the evolution of the Mesozoic Tethys Ocean. *Ofioliti* **29**, 19–35.

Bortolotti, V., Chiari, M., Marcucci, M., Photiades, P., Principi, G. & Saccani, E. 2008. New geochemical and age data on the ophiolites from the Othris area (Greece): implication for the Triassic evolution of the Vardar Ocean. *Ofioliti* **33**, 135–51.

Bortolotti, V., Chiari, M., Marroni, M., Pandolfi, L., Principi, G. & Saccani, E. 2013. The geodynamic evolution of the ophiolites from Albania and Greece, Dinaric-Hellenic belt: one, two or more oceanic basins? *International Journal of Earth Science* **102**, 783–811.

Bortolotti, V., Kodra, A., Marroni, M., Mustafa, F., Pandolfi, L., Principi, G. & Saccani, E. 1996. Geology and petrology of ophiolitic sequences in the Mirdita region (northern Albania). *Ofioliti* **21**, 3–20.

Bortolotti, V., Marroni, M., Pandolfi, L. & Principi, G. 2005. Mesozoic to Tertiary tectonic history of the Mirdita ophiolites, northern Albania. *The Island Arc* **14**, 471–93.

Bortolotti, V. & Principi, G. 2005. Tethyan ophiolites and Pangea break-up. *The Island Arc* **14**, 442–70.

Bown, P. R. 1998. *Calcareous Nannofossils Biostratigraphy*. British Micropalaeontological Society Publication Series. Cambridge: Chapman & Hall, 328 pp.

Brown, S. A. M. & Robertson, A. H. F. 2003. Sedimentary geology as a key to understanding the tectonic evolution of the Mesozoic–Early Tertiary Paikon Massif, Vardar suture zone, N Greece. *Sedimentary Geology* **160**,179–212.

Brown, S. A. M. & Robertson, A. H. F. 2004. Evidence for Neotethys rooted within the Vardar suture zone from the Voras Massif, northernmost Greece. *Tectonophysics* **381**, 143–73.

Brunn, J. H. 1956. Contribution à l'étude du Pinde septentrional et d'une partie de la Macédoine occidentale. *Annales Géologiques des Pays Helléniques* **7**, 1–358.

Brunn, J. H. 1960. Les zones helléniques internes et leur extension. Réflexions sur l'orogénèse alpine. *Bulletin de la Société géologique de France* **7**, 470–86.

Brun, J.-P. & Faccenna, C. 2008. Exhumation of high-pressure rocks driven by slab rollback. *Earth and Planetary Science Letters* **272**, 1–7.

https://doi.org/10.1017/S0016756817000942 Published online by Cambridge University Press

Burg, J.-P. 2012. Rhodope: from Mesozoic convergence to Cenozoic extension. Review of petro-structural data in the geochronological frame. In *The Geology of Greece* (eds E. Skourtsos & G. S. Lister). *Journal of the Virtual Explorer* **42**, paper 1. doi: 10.3809/jvirtex.2011.00270.

Capedri, S., Toscani, L., Grandi, R., Venturelli, G., Papanikolaou, D. & Skarpelis, N. S. 1997. Triassic volcanic rocks of some type-localities from the Hellenides. *Chemie der Erde* **57**, 257–76.

Caputo, M. & Caputo, R. 1988. Structural analysis: new analytical approach and applications. *Annales Tectonicae* **2**, 84–9.

Carosi, R., Cortesogno, L., Gaggero, L. & Marroni, M. 1996. Geological and petrological features of the metamorphic sole from the Mirdita ophiolites, northern Albania. *Ofioliti* **21**, 21–40.

Carras, N. 1995. *The Parnassus carbonate platform during the Late Jurassic–Early Cretaceous (stratigraphy and palaeogeographical evolution)*. Ph.D. thesis, University of Athens, D. Mavrommati Publ., Athens, 232 pp. (in Greek, with extended Italian summary). Published thesis.

Carras, N. & Tselepidis, V. 2001. Stratigraphy of the Alpine formations of the Parnassus zone and of some allochthonous sequences in the Distomon area (Boeotia, Greece). In *The Parnassus Zone, Central Greece* (eds N. Solakius & M. Kati), pp. 17–36. Meddelanden Fran Lunds Universitets, Geografiska Institutioner, Avhandlingar 139.

Celet, P. 1962. Contribution à l'étude géologique du Parnasse-Kiona et d'une partie des régions méridionales de la Grèce continentale. *Annales Géologiques des Pays Helléniques* **13**, 1–446.

Celet, P. 1979. Les bordures de la zone du Parnasse (Grèce). Evolution paléogéographique au Mésozoïque et caractères structuraux. In *Proceedings of the VI Colloquium on the Geology of the Aegean Region, Athens* 2, pp. 725–40.

Celet, P. & Clément, B. 1971. Sur la présence d'une nouvelle unité paléogéographique et structurale en Grèce continentale du sud: L'unité du flysch béotien. *Compte Rendu sommaire des séances de la Société géologique de France* **17**, 43–7.

Celet, P., Clément, B. & Ferrière, J. 1976. La zone béotienne en Grèce: implications paléogéographiques et structurales. *Eclogae Geologicae Helvetiae* **69**, 577–99.

Celet, P., Clément, B. & Ferrière, J. 1988. Evolution géodynamique de la plate-forme Pélagonienne au Mésozoïque. *Bulletin of the Geological Society of Greece* **20**, 215–22.

Celet, P., & Ferrière, J. 1978. Les Hellénides internes: le Pélagonien. *Eclogae Geologicae Helvetiae* **71**, 467–95.

Celet, P., Ferrière, J. & Wigniolle, E. 1977. Le problème de l'origine des blocs exogènes du mélange à éléments ophiolitiques au sud du Sperchios et dans le massif de l'Othrys (Grèce). *Bulletin de la Société géologique de France* **7**, 935–42.

Chambefort, I. & Moritz, R. 2006. Late Cretaceous structural control and Alpine overprint of the high-sulfidation Cu–Au epithermal Chelopech deposit, Srednogorie Belt, Bulgaria. *Mineralium Deposita* **42**, 259–80.

Chiari, M., Baumgartner, P. O., Bernoulli, D., Bortolotti, V., Marcucci, M., Photiades, A. & Principi, G. 2013. Late Triassic, early and middle Jurassic Radiolaria from ferromanganese-chert 'nodules' (Angelokastron, Argolis, Greece): evidence for prolonged radiolarite sedimentation in the Maliac-Vardar Ocean. *Facies* **59**, 391–424.

Chiari, M., Bortolotti, V., Marcucci, M., Photiades, A. & Principi, G. 2003. The Middle Jurassic siliceous sedimentary cover at the top of the Vourinos ophiolite (Greece). *Ofioliti* **28**, 95–103.

Chiari, M., Bortolotti, V., Marcucci, M., Photiades, A., Principi, G. & Saccani, E. 2012. Radiolarian biostratigraphy and geochemistry of the Koziakas Massif ophiolites (Greece). *Bulletin de la Société géologique de France* **183**, 287–306.

Clément, B. 1971. Découverte d'un flysch éocrétacé en Béotie (Grèce continentale). *Comptes Rendus de l'Academie des Sciences, Paris* **272**, 791–2.

Clément, B. 1972. Sur une nouvelle interprétation tectonique du Sud Ouest des monts Géranées (Grèce continentale). *Annales de la Société Géologique du Nord* **42**, 171–5.

Clément, B. 1976. Essai d'interprétation structurale d'un secteur des zones internes helléniques: l'Attique-Béotie. *Bulletin de la Société géologique de France* **7** (18), 303–16.

Clift, P. D. & Dixon, J. E. 1998. Jurassic ridge collapse, subduction initiation and ophiolite obduction in the southern Greek Tethys. *Eclogae Geologicae Helvetiae* **91**, 128–38.

Çollaku, A, Cadet, J. P., Bonneau, M. & Jolivet, L. 1992. L'édifice structural de l'Albanie septentrionale: des éléments de réponse sur les modalités de la mise en place des ophiolites. *Bulletin de la Société géologique de France* **163**, 455–68.

Combes, P.-J. 1977. Observations et remarques sédimentologiques, paléogéographiques et géochimiques sur les bauxites du 3e horizon dans la zone du Parnasse (Grèce). *Comptes Rendus de l'Academie des Sciences, Paris* **284**, 871–4.

Combes, P.-J. 1979. Observations sédimentologiques, paléogéographiques, minéralogiques et géochimiques sur les bauxites du deuxième horizon dans la zone du Parnasse (Grèce). *Bulletin de la Société géologique de France* **7** (21), 485–94.

Combes, P.-J. 1984. Regards sur la géologie des bauxites; aspects récents sur la genèse de quelques gisements à substratum carbonaté. *Bulletin des Centres de Recherche Exploration-Production Elf-Aquitaine* **8**, 251–74.

Combes, P.-J., Fourcade, E., Masse, J.-P. & Philip, J. 1981. Observations stratigraphiques et paleontologiques sur le Cretace de la zone du Parnasse (Grece). *Académie Yougoslave des Sciences et des Arts (Travaux du Comité international pour l'étude des bauxites, de l'alumine et de l'aluminium)* **11** (16), 347–65.

Danelian, T. 1994. Palaeo-oceanographic significance of mid-Jurassic radiolarites from the Maliac (Sub-Pelagonian) margin of Othris (Greece). *Bulletin of the Geological Society of Greece* **32**, 167–75.

Danelian, T. & Robertson, A. H. F. 1998. Palaeogeographic implications of the age of radiolarian-rich sediments in Beotia (Greece). *Bulletin of the Geological Society of Greece* **32**, 21–9.

Danelian, T. & Robertson, A. H. F. 2001. Neotethyan evolution of Eastern Greece (Pagondas Mélange, Evia island) inferred from radiolarian biostratigraphy and the geochemistry of associated extrusive rocks. *Geological Magazine* **138**, 345–63.

Danelian, T., Robertson, A. H. F. & Dimitriadis, S. 1996. Age and significance of radiolarian sediments within basic extrusives of the marginal basin Guevgueli

https://doi.org/10.1017/S0016756817000942 Published online by Cambridge University Press

Ophiolite (northern Greece). *Geological Magazine* **133**, 127–36.

De Bono, A., Martini, R., Zaninetti, L., Hirsch, F., Stampfli, G. M. & Vavassis, I. 2001. Permo-Triassic stratigraphy of the Pelagonian zone in Central Evia Island (Greece). *Eclogae Geologicae Helvetiae* **94**, 289–311.

Degnan, P. J. & Robertson, A. H. F. 1998. Mesozoic–early Tertiary passive margin evolution of the Pindos ocean (NW Peloponnese, Greece). *Sedimentary Geology* **117**, 33–70.

Degnan, P. J. & Robertson, A. H. F. 2006. Synthesis of the tectonic-sedimentary evolution of the Mesozoic–Early Cenozoic Pindos ocean: evidence from the NW Peloponnese, Greece. In *Tectonic Development of the Eastern Mediterranean Region* (eds A. H. F. Robertson & D. Mountrakis), pp. 467–91. Geological Society of London, Special Publication no. 260.

Dercourt, J. 1967. Sur l'accident de Scutari-Pec, la signification paléogéographique de quelques series condensées en Albanie septentrionale. *Annales de la Société Géologique du Nord* **9**, 1–109.

Dercourt, J. 1972. The Canadian Cordillera, the Hellenides, and the sea-floor spreading theory. *Canadian Journal of Earth Sciences* **9**, 709–43.

De Wever, P. 1995. Radiolarians overlying ophiolites of the Almopias domain (Macedonia, Greece). In *Middle Cretaceous to Lower Cretaceous Radiolaria of Tethys: Occurrences, Systematics, Biochronology* (eds P. O. Baumgartner, L. O'Dogherty, Š. Goričan, E. Urquhart, A. Pillevuit & P. De Wever), pp. 877–9. Mémoires de Géologie, Lausanne no. 23.

Dilek, Y., Shallo, M. & Furnes, H. 2005. Rift-drift, seafloor spreading and subduction tectonics of Albanian ophiolites. *International Geology Review* **46**, 147–76.

Dimo-Lahitte, A., Monié, P. & Vergély, P. 2001. Metamorphic soles from the Albanian ophiolites: petrology, $^{40}Ar/^{39}Ar$ geochronology, and geodynamic evolution. *Tectonics* **20**, 78–96.

Dumitrica, P., Immenhauser, A. & Dumitrica-Jud, R. 1997. Mesozoic radiolarian biostratigraphy from Masirah ophiolite, Sultanate of Oman, Part 1. Middle Triassic, Uppermost Jurassic and Lower Cretaceous spumellarians and multisegmented nassellarians. *Bulletin of the National Museum of Natural Sciences Taiwan* **9**, 1–106.

Duretz, T., Gerya, T. V. & May, D. 2011. Numerical modelling of spontaneous slab breakoff and subsequent topographic response. *Tectonophysics* **502**, 244–56.

Fazzuoli, M. & Carras, N. 2007. Development and demise of a carbonate platform by compressional and extensional tectonics: the Zyghosti platform (Late Jurassic) and the Cretaceous transgression, Kozani, Northern Greece. In *25th IAS Meeting of Sedimentology, 2007, Patras-Greece, Field Trip P7, Field Trips Guide Book*, pp. 173–90.

Fazzuoli, M., Menna, F., Nirta, G., Carras, N. & Principi, G. 2008. The Cretaceous transgression in the Dinaric-Hellenic orogen. *Rendiconti della Società Geologica Italiana* **1**, 77–9.

Ferrière, J. 1975. Sur la signification des séries du massif de l'Othris (Grèce continentale orientale): la zone isopique maliaque. *Annales de la Société Géologique du Nord* **96**, 121–34.

Ferrière, J. 1982. Paléogéographies et tectoniques superposées dans les Hellénides internes au niveau de l'Othrys et du Pelion (Grèce). *Société Géologique du Nord* **8**, 970 pp.

Ferrière, J. 1985. Constitution and development of the Hellenic ophiolites from the Othrys-Pelion area, Greece. [Nature et développement des ophiolites helléniques du secteur Othrys-Pelion]. *Ofioliti* **10**, 255–77.

Ferrière, J., Baumgartner, P. O. & Chanier, F. 2016. The Maliac Ocean: the origin of the Tethyan Hellenic ophiolites. *International Journal of Earth Sciences* **105**, 1941–63.

Ferrière, J, Chanier, F., Baumgartner, P. O., Dumitrica, P., Caridroit, M., Bout-Roumazeilles, V., Graveleau, F., Danelian, T. & Ventalon, S. 2015. The evolution of the Triassic–Jurassic Maliac oceanic lithosphere: insights from the supra-ophiolitic series of Othris (continental Greece). *Bulletin de la Société géologique de France* **186**, 399–411.

Ferrière, J., Chanier, F. & Ditbanjong, P. 2012. The Hellenic ophiolites: eastward or westward obduction of the Maliac Ocean, a discussion. *International Journal of Earth Sciences* **101**, 1559–80.

Ferrière, J. & Stais, A. 1995. New interpretation of the Vardarian Tethysian area based on the Peonian series [Nouvelle interprétation de la suture téthysienne vardarienne d'après l'analyse des séries de Péonias (Vardar oriental, Hellénides internes)]. *Bulletin de la Société géologique de France* **166**, 327–39.

Fleury, J. J. 1975. Le 'Premier Flysch du Pinde' témoin de l'ensemble des événements orogéniques mésozoïques anté-crétacé supérieur ayant affecté les Hellénides internes. *Comptes Rendus de l'Académie des Sciences, Paris* **281**, 1459–61.

Fleury, J. J. 1980. Evolution d'une platforme et d'un bassin dans leur cadre alpin: les zones de Gavrovo-Tripolitza et du Pinde-Olonos. *Annales de la Société Géologique du Nord* **4**, 1–651.

Gallhofer, D., Quadt, A. V., Peytcheva, I., Schmid, S. M. & Heinrich, C. A. 2015. Tectonic, magmatic, and metallogenic evolution of the Late Cretaceous arc in the Carpathian-Balkan orogen. *Tectonics* **34**, 1813–36.

Gautier, P., Brun, J. P., Moriceau, R., Sokoutis, D., Martinod, J. & Jolivet, L. 1999. Timing, kinematics and cause of Aegean extension: a scenario based on a comparison with simple analogue experiments. *Tectonophysics* **315**, 31–72.

Ghikas, C., Dilek, Y. & Rassios, A. E. 2010. Structure and tectonics of subophiolitic mélanges in the western Hellenides (Greece): implications for ophiolite emplacement tectonics. *International Geological Review* **52**, 423–53.

Goldsworthy, M., Jackson, J. & Haines, J. 2002. The continuity of active fault systems in Greece. *Geophysical Journal International* **148**, 596–618.

Gregou, S. 1996. The pre-flysch and basal shaly flysch deposition in the Parnassus-Ghiona Zone, central Greece. *Lund Publications in Geology* **132**, 1–30.

Gregou, S. & Solakius, N. 1997. The pre-flysch and the basal shaly flysch deposition in Osios Loukas and Distomo areas, central Parnassus, central Greece, during the late Paleocene to the early Eocene. *Neues Jahrbuch fur Geologie und Palaontologie – Abhandlungen* **204**, 35–82.

Gregou, S., Solakius, N. & Pomoni-Papaioannou, F. 1994. The carbonate-flysch transition in the Arachova sequence of the Parnassus-Ghiona Zone, Central Greece. *Geological Magazine* **131**, 819–36.

Haq, B. U. 2014. Cretaceous eustasy revisited. *Global and Planetary Change* **113**, 44–58.

Hou, Z., Yang, Z., Qu, X., Meng, X., Li, Z., Beaudoin, G., Rui, Z., Gao, Y. & Zaw, K. 2009. The Miocene

https://doi.org/10.1017/S0016756817000942 Published online by Cambridge University Press

Gangdese porphyry copper belt generated during post-collisional extension in the Tibetan Orogen. *Ore Geology Reviews* **36**, 25–51.

Hou, Z., Zhang, H., Pan, Z. & Yang, Z. 2011. Porphyry Cu (–Mo–Au) deposits related to melting of thickened mafic lower crust: examples from the eastern Tethyan metallogenic domain. *Ore Geology Reviews* **39**, 21–45.

Hynes, A. J., Nisbet, E. G., Smith, A. G., Welland, J. P. & Rex, D. C. 1972. Spreading and emplacement of some ophiolites in the Othris region (Eastern Central Greece). *Zeitschrift der Deutschen Gesellschaft für Geowissenschaften* **123**, 455–68.

Iancu, V., Berza, T., Seghedi, A., Gheuca, I. & Hann, H. P. 2005. Alpine polyphase tectono-metamorphic evolution of the South Carpathians: a new overview. *Tectonophysics* **410**, 337–65.

Imer, A., Richards, J. P. & Creaser, R. A. 2013. Age and tectonomagmatic setting of the Eocene Çöpler–Kabataş magmatic complex and porphyry-epithermal Au deposit, East Central Anatolia, Turkey. *Mineralium Deposita* **48**, 557–83.

Ivanova, D., Bonev, N. & Chatalov, A. 2015. Biostratigraphy and tectonic significance of lowermost Cretaceous carbonate rocks of the Circum-Rhodope Belt (Chalkidhiki Peninsula and Thrace region, NE Greece). *Cretaceous Research* **52**, 25–63.

Jacobshagen, V. 1986. *Geologie von Griechenland*. Beitraege zur Regionalen Geologie der Erde. Berlin-Stuttgart: Gerbrueder Borntraeger, 363 pp.

Jacobshagen, V., Durr, S., Kockel, F., Kopp, K. O., Kowalczyk, G., Berckhamer, H. & Buttner, D. 1978. Structure and geodynamic evolution of the Aegean region. In *Alps, Apennines, Hellenides* (eds H. Closs, D. Roeder & K. Schmidt), pp. 537–64. Inter-Union Commission on Geodynamics Scientific Report 38. Stuttgart: Schweizerbart.

Jaeger, P. 1980. Nouvelles données sur la géologie de la région de Mouzaki, province de Karditsa (Grèce continentale). Relations entre les séries pindique, béotienne et ultrapindique. *Bulletin de la Société géologique de France* **22**, 135–43.

Jankovic, S. 1997. The Carpatho-Balkanides and adjacent area: a sector of the Tethyan Eurasian metallogenic belt. *Mineralium Deposita* **32**, 426–33.

Jolivet, L., Brun, J.-P., Gautier, P., Lallemant, S. & Patriat, M. 1994. 3D-kinematics of extension in the Aegean region from the early Miocene to the present, insights from the ductile crust. *Bulletin de la Société géologique de France* **165**, 195–209.

Jolivet, L. & Brun, J.-P. 2010. Cenozoic geodynamic evolution of the Aegean. *International Journal of Earth Sciences* **99**, 109–38.

Jolivet, L., Faccenna, C., Goffé, B., Burov, E. & Agard, P. 2003. Subduction tectonics and exhumation of high-pressure metamorphic rocks in the Mediterranean orogens. *American Journal of Science* **303**, 353–409.

Jolivet, L., Faccenna, C., Huet, B., Labrousse, L., Le Pourhiet, L., Lacombe, O., Lecomte, E., Burov, E., Denèle, Y., Brun, J.-P., Philippon, M., Paul, A., Salaün, G., Karabulut, H., Piromallo, C., Monié, P., Gueydan, F., Okay, A. I., Oberhänsli, R., Pourteau, A., Augier, R., Gadenne, L. & Driussi, O. 2013. Aegean tectonics: strain localisation, slab tearing and trench retreat. *Tectonophysics* **597–598**, 1–33.

Jolivet, L., Labrousse, L., Agard, P., Lacombe, O., Bailly, V., Lecomte, E., Mouthereau, F. & Mehl, C. 2010. Rifting and shallow-dipping detachments, clues from the Corinth Rift and the Aegean. *Tectonophysics* **483**, 287–304.

Jones, G., De Wever, P. & Robertson, A. H. F. 1992. Significance of radiolarian age data to the Mesozoic tectonic and sedimentary evolution of the northern Pindos Mountains, Greece. *Geological Magazine* **129**, 385–400.

Jones, G. & Robertson, A. H. F. 1991. Tectonostratigraphy and evolution of the Mesozoic Pindos ophiolite and related units, northwestern Greece. *Journal of the Geological Society, London* **148**, 261–88.

Jones, G. & Robertson, A. H. F. 1994. Rift-drift-subduction and emplacement history of the Early Mesozoic Pindos Ocean: evidence from the Advella Mélange, northern Greece. *Bulletin of the Geological Society of Greece* **30**, 45–58.

Kalpakis, G. 1979. La sédimentation phosphatée dans la zone Parnasse-Kiona au sommet du Crétacé. *Annales Géologiques des Pays Helléniques* **29**, 758–95.

Kaplanis, A., Koukouvelas, I., Xypolias, P. & Kokkalas, S. 2013. Kinematics and ophiolite obduction in the Gerania and Helicon Mountains, central Greece. *Tectonophysics* **595–596**, 215–34.

Karamata, S., Olujić, J., Protić, L., Milovanović, D., Vujnović, L., Popević, A., Memović, E., Radovanović, Z. & Resimić-Sarić, K. 2000. The western belt of the Vardar Zone – the remnant of a marginal sea. In *International Symposium Geology and Metallogeny of the Dinarides and the Vardar Zone* (eds S. Karamata & S. Janković), pp. 131–5. Banja Luka, Sarajevo: Academy of Sciences & Arts Republic of Srpska Vol. 1.

Katsikatsos, G. 1979. La structure tectonique d'Attique et de l'ile d'Eubée. *Proceedings of the Institute of Geology and Mining Research* **1**, 211–20.

Kilias, A., Frisch, W., Avgerinas, A., Dunkl, I., Falalakis, G. & Gawlick, H.-J. 2010. Alpine architecture and kinematics of deformation of the northern Pelagonian nappe pile in the Hellenides. *Austrian Journal of Earth Sciences* **103**, 4–28.

Kilias, A. A., Tranos, M. D., Papadimitriou, E. E. & Karakostas, V. G. 2008. Die rezente Krustendeformation des hellenischen Orogens im zentralen Griechenland; die Kremasta- und Sperchios- Störungssysteme und ihre Verhältnisse zu den benachbarten großen Bruchstrukturen. *Zeitschrift der Deutschen Gesellschaft fur Geowissenschaften* **159**, 533–47.

Kissel, C., Speranza, F. & Milicevic, V. 1995. Paleomagnetism of external southern and central Dinarides and northern Albanides: implications for the Cenozoic activity of the Scutari-Pec Transverse zone. *Journal of Geophysical Research* **100**, 14 999–15 007.

Kranis, H. D. & Papanikolaou, D. I. 2001. Evidence for detachment faulting on the NE Parnassos mountain front (Central Greece). *Bulletin of the Geological Society of Greece* **34**, 281–7.

Kukoč, D., Goričan, Š., Kosir, A., Belak, M., Halamic, J. & Hrvatović, H. 2012. Middle Jurassic age of basalts and transition to Upper Jurassic carbonates in the Guevgueli Ophiolite Complex (Republic of Macedonia). In *Proceedings of the XIII INTERRAD Conference, Cadiz, Spain, 25–29 March 2012*, pp. 227–9.

Lefèvre, C., Cabanis, B., Ferrière, J., Thiebault, F. & Platevoet, R. 1993. Mise en evidence d'une dualité dans le volcanise triasique hellénique: apport de la géochimie des éléments traces. *Comptes Rendus de l'Académie de Sciences, Paris série II* **316**, 1311–8.

https://doi.org/10.1017/S0016756817000942 Published online by Cambridge University Press

Le Pichon, X. & Angelier, J. 1979. The Hellenic arc and trench system: a key to the neotectonic evolution of the eastern Mediterranean area. *Tectonophysics* **60**, 1–42.

Le Pichon, X., Chamot-Rooke, N., Lalleman, S., Noomen, R. & Veis, G. 1995. Geodetic determination of the kinematics of central Greece with respect to Europe: implications for eastern Mediterranean tectonics. *Journal of Geophysical Research* **100**, 12 675–90.

Lips, A. L. W. 2002. Correlating magmatic–hydrothermal ore deposit formation over time with geodynamic processes in SE Europe. In *The Timing and Location of Major Ore Deposits in an Evolving Orogen* (eds D. J. Blundell, F. Neubauer & A. von Quadt), pp. 69–79. Geological Society London, Special Publication no. 204.

Lips, A. L. W., White, S. H. & Wijbrans, J. R. 1998. ^{40}Ar–^{39}Ar laserprobe direct dating of discrete deformational events: a continuous record of early Alpine tectonics in the Pelagonian Zone, NW Aegean area, Greece. *Tectonophysics* **298**, 133–53.

Lips, A. L. W., White, S. H. & Wijbrans, J. R. 2000. Middle–Late Alpine thermotectonic evolution of the southern Rhodope Massif, Greece. *Geodinamica Acta* **13**, 281–92.

Lips, A. L. W., Wijbrans, J. R. & White, S. H. 1999. New insights from ^{40}Ar/ ^{39}Ar laserprobe dating of white mica fabrics from the Pelion Massif, Pelagonian Zone, Internal Hellenides, Greece: implications for the timing of metamorphic episodes and tectonic events in the Aegean region. In *The Mediterranean Basins: Tertiary Extension within the Alpine Orogen* (eds B. Durand, L. Jolivet, F. Horváth & M. Séranne), pp. 457–74. Geological Society of London, Special Publication no. 156.

Lister, G. S., Banga, G. & Feenstra, A. 1984. Metamorphic core complexes of Cordilleran type in the Cyclades, Aegean Sea, Greece. *Geology* **12**, 221–5.

Maillot, H. 1979. Etude sédimentologique du 'Premier Flysch' en Peloponnèse occidental (Grèce): La Formation d'Andritsena. *Bulletin of the Geological Society of Greece* **14**, 94–115.

Maratos, G., Rigopoulos, K. & Athanassiou, A. 1965. *Geological Map of Greece, Scale 1:50,000, Atalanti Sheet*. Athens: IGME.

Maratos, G., Rigopoulos, K. & Athanassiou, A. 1967. *Geological Map of Greece, Scale 1:50,000, Elateia Sheet*. Athens: IGME.

Marinos, G., Papastamatiou, J., Maratos, G., Melidonis, N., Andronopoulos, B., Tataris, A., Betoulis, D., Katsikatsos, G., Maragoudakis, N. & Lalechos, N. 1967. *Geological Map of Greece, Lamia Sheet*. Athens: IGME.

Martini, E. 1971. Standard Tertiary and Quaternary calcareous nannoplankton zonation. In *Proceedings of the 2nd International Conference on Planktonic Microforaminifera, Roma* (ed. A. Farinacci), pp. 739–85. Ed. Tecnosc. no. 2.

Meinhold, G., Kostopoulos, D., Reischmann, T., Frei, D. & Bou Dagher-Fadel, M. K. 2009. Geochemistry, provenance and stratigraphic age of metasedimentary rocks from the eastern Vardar suture zone, northern Greece. *Palaeogeography, Palaeoclimatology, Palaeoecology* **277**, 199–225.

Mercier, J. 1966. Mouvements orogéniques et magmatisme d'age Jurassique supérieur-Éocrétacé dans les Zones Internes des Hellénides (Macédoine, Grèce). *Revue de Géographie Physique et Géologie Dynamique* **8**, 265–78.

Mercier, J.-L. 1968. Étude géologique des zones Hellénides en Macèdoine centrale (Grece). *Annales Géologiques des Pays Helléniques* **20**, 1–792.

Mercier, J., Sorel, D., Vergély, P. & Simeakis, K. 1989. Extensional tectonic regimes in the Aegean basins during the Cenozoic. *Basin Research* **2**, 49–71.

Mercier, J.-L., Vergély, P. & Bébien, J. 1975. Les ophiolites helléniques « obductées » au Jurassique supérieur sont-elles les vestiges d'un Océan téthysien ou d'une mer marginale périeuropeénne? *Comptes Rendus Sommaires de la Société géologique de France* **1975** (4), 108–12.

Mettos, A., Ioakim, C. & Rondoyanni, T. 2000. Palaeoclimatic and palaeogeographic evolution of Attica-Beotia (Central Greece). *Special Publications of the Geological Society of Greece* **9**, 187–96.

Meulenkamp, J. E., Wortel, M. J. R., van Wamel, W. A., Spakman, W. & Hoogerduyn Strating, E. 1988. On the Hellenic subduction zone and the geodynamic evolution of Crete since the late Middle Miocene. *Tectonophysics* **146**, 203–15.

Moritz, R., Márton, I., Ortelli, M., Marchev, P., Voudouris, P., Bonev, N., Spikings, R. & Cosca, M. 2010. A review of age constraints of epithermal precious and base metal deposits of the Tertiary Eastern Rhodopes: coincidence with Late Eocene–Early Oligocene tectonic plate reorganization along the Tethys. In *Proceedings of the XIX Congress of the Carpathian Balkan Geological Association* (eds G. Christofides, N. Kantiradis, D. S. Kostopoulos & A. A. Chatziperos), pp. 351–8.

Morycowa, E. & Marcopoulou-Diacantoni, A. 2002. Albian corals from the Subpelagonian Zone of Central Greece (Agrostylia, Parnassos region). *Annales Societatis Geologorum Poloniae* **72**, 1–65.

Myhill, R. 2011. Constraints on the evolution of the Mesohellenic Ophiolite from subophiolitic metamorphic rocks. In *Mélanges–Processes of Formation and Societal Significance* (eds J. Wakabayashi & Y. Dilek), pp. 75–94. Geological Society of America, Special Paper no. 480.

Nachev, I. & Dimitrova, E. 1995. Upper Cretaceous stratigraphy of the Eastern Sredna Gora zone. *Geologica Balcanica* **25**, 3–26.

Nance, D. 1981. Tectonic history of a segment of the Pelagonian zone, northeastern Greece. *Canadian Journal of Earth Sciences* **18**, 1111–26.

Neubauer, F. 2002. Contrasting Late Cretaceous with Neogene ore provinces in the Alpine–Balkan–Carpathian–Dinaride collision belt. In *The Timing and Location of Major Ore Deposits in an Evolving Orogen* (eds D. J. Blundell, F. Neubauer & A. von Quadt), pp. 81–102. Geological Society London, Special Publication no. 204.

Neumann, P. 2001. Turbidite deposition in the early Late Cretaceous Pindos Basin (External Hellenides). *Bulletin of the Geological Society of Greece* **34**, 771–7.

Neumann, P. & Zacher, W. 2004. The Cretaceous sedimentary history of the Pindos basin (Greece). *International Journal of Earth Sciences* **93**, 119–31.

Nirta, G., Bortolotti, V., Chiari, M., Menna, F., Saccani, E., Principi, G. & Vannucchi, P. 2010. Ophiolites from the Grammos-Arrenes area, northern Greece: geological, paleontological and geochemical data. *Ofioliti* **35**, 103–15.

Nirta, G., Moratti, G., Piccardi, L., Montanari, D., Catanzariti, R., Carras, N. & Papini, M. 2015. The Boeotian flysch revisited: new constraints on

https://doi.org/10.1017/S0016756817000942 Published online by Cambridge University Press

ophiolite obduction in central Greece. *Ofioliti* **40**, 107–23.

Ozsvart, P., Dosztaly, L., Migiros, G., Tselepidis, V. & Kovacs, K. 2012. New radiolarian biostratigraphic age constraints on Middle Triassic basalts and radiolarites from the Inner Hellenides (Northern Pindos and Othris Mountains, Northern Greece) and their implications for the geodynamic evolution of the early Mesozoic Neotethys. *International Journal of Earth Sciences* **101**, 1487–501.

Pamic, J. 2002. The Sava-Vardar zone of the Dinarides and Hellenides versus the Vardar Ocean. *Eclogae Geologicae Helvetiae* **95**, 99–113.

Papanikolaou, D. 1997. The tectonostratigraphic terranes of the Hellenides. *Annales Géologiques des Pays Helléniques* **37**, 495–514.

Papanikolaou, D. 2009. Timing of tectonic emplacement of the ophiolites and terrane paleogeography in the Hellenides. *Lithos* **108**, 262–80.

Papanikolaou, D. 2013. Tectonostratigraphic models of the Alpine terranes and subduction history of the Hellenides. *Tectonophysics* **595–596**, 1–24.

Papanikolaou, D., Gouliotis, L. & Triantaphyllou, M. 2009. The Itea–Amfissa detachment: a pre-Corinth rift Miocene extensional structure in central Greece. In *Collision and Collapse at the Africa–Arabia–Eurasia Subduction Zone* (eds D. J. J. van Hinsbergen, M. A. Edwards & Rob Govers), pp. 293–310. Geological Society of London, Special Publication no. 311.

Papastamatiou, J. 1960. La géologie de la région montagneuse du Parnasse–Kiona–Oeta. *Bulletin de la Société géologique de France* **7**, 398–409.

Papastamatiou, J., Tataris, A., Katsikatsos, G. & Maragoudaxis, N. 1962a. *Geological Map of Greece, Scale 1:50 000, Sheet 'Galaxidhion'*. I.G.S.R.

Papastamatiou, J., Tataris, A., Kounis, G. D., Maragoudaxis, N., Monopolis, D., Albadakis, N. & Koukouzos, R. 1971. *Geological Map of Greece, Scale 1:50 000, Levadhia Sheet*. Athens: I.G.M.E.

Papastamatiou, J., Tataris, A., Vetoulis, D., Katsikatsos, G., Lalechos, N. & Eleutheriou, A. 1962b. *Geological Map of Greece, Scale 1:50 000, Sheet 'Amphiklia'*. I.G.S.R.

Pe-Piper, G. 1982. Geochemistry, tectonic setting and metamorphism of mid-Triassic volcanic rocks of Greece. *Tectonophysics* **85**, 253–72.

Pe-Piper, G. 1998. The nature of Triassic extension-related magmatism in Greece: evidence from Nd and Pb isotope geochemistry. *Geological Magazine* **135**, 331–48.

Pe-Piper, G. & Hatzipanagiotou, K. 1993. Ophiolitic rocks of the Kerassies-Milia Belt, continental Greece. *Ofioliti* **18**, 157–69.

Pe-Piper, G., Matarangas, D. & Jacobshagen, V. 1996. The Mesozoic metavolcanic rocks of Alonnisos and Kyra Panagia islands, Sporades, Greece. *Neues Jahrbuch für Mineralogie, Monatshefte* **37**, 251–63.

Pe-Piper, G. & Piper, D. J. W. 1991. Early Mesozoic oceanic subduction-related volcanic rocks, Pindos Basin, Greece. *Tectonophysics* **192**, 273–92.

Pe-Piper, G. & Piper, D. J. W. 2002. *The Igneous Rocks of Greece. The Anatomy of an Orogen*. Berlin: Gebruder Borntraeger, 573 pp.

Perch-Nielsen, K. 1985a. Mesozoic calcareous nannofossils. In *Plankton Stratigraphy* (eds H. M. Bolli, J. B. Saunders & K. Perch-Nielsen), pp. 329–426. Cambridge: Cambridge University Press.

Perch-Nielsen, K. 1985b. Cenozoic calcareous nannofossils. In *Plankton Stratigraphy* (eds H. M. Bolli, J. B. Saunders & K. Perch-Nielsen), pp. 427–553. Cambridge: Cambridge University Press.

Photiades, A., Carras, N., Bortolotti, V., Fazzuoli, M. & Principi, G. 2007. The Late Early Cretaceous transgression on the laterites in Vourinos and Vermion massifs (Western Macedonia, Greece). Proceedings of the 11th International Congress of the Geological Society of Greece, Athens, May 2007. *Bulletin of the Geological Society of Greece* **40**, 182–90.

Pomoni-Papaioannou, F. & Solakius, N. 1991. Phosphatic hardgrounds and stromatolites from the limestone/shale boundary section at Prossilion (Maastrichtian–Paleocene) in the Parnassus–Ghiona Zone, Central Greece. *Palaeogeography, Palaeoclimatology, Palaeoecology* **86**, 243–54.

Ramsay, J. 1967. *Folding and Fracturing of Rocks*. New York: McGraw-Hill.

Rassios, A. & Dilek, Y. 2009. Rotational deformation in the Jurassic Mesohellenic ophiolites, Greece, and its tectonic significance. *Lithos* **108**, 207–23.

Rassios, A. & Smith, A. G. 2000. Constraints on the formation and emplacement age of western Greek ophiolites (Vourinos, Pindos and Othris) inferred from deformation structure in peridotites. In *Ophiolite and Oceanic Crust: New Insights from Field Studies and Ocean Drilling Program* (eds Y. Dilek, E. M. Moores, D. Elthon & A. Nicolas), pp. 473–83. Geological Society of America, Special Paper no. 349.

Renz, C. 1955. *Die Vorneogene Stratigraphie der Normalsedimentaren Formationen Griechenlands*. Athens: Institute of Geological Subsurface Research, 637 pp.

Richards, J. P. 2015. Tectonic, magmatic, and metallogenic evolution of the Tethyan orogen: from subduction to collision. *Ore Geology Reviews* **70**, 323–45.

Richter, D. & Mariolakos, I. 1974a. Neue Erkenntnisse über die Palaeogeographie des Gebietes sudwestlich Levadhia von Beginn der Flysch-Sedimentation. *Praktika tis Akadimias Athinon* **48**, 407–25.

Richter, D. & Mariolakos, I. 1974b. Der Flysch und seine Unterlage im Gebiet westlich Galaxidion. *Bulletin of the Geological Society of Greece* **10**, 413–24.

Richter, D. & Mariolakos, I. 1975. Stratigraphische Untersuchungen an der Kreide/Tertiär-Wende im Gebiet von Delfi-Amfissa-Amfiklia (Parnass-Giona zone, Griechenland). *Annales Géologiques des Pays Helléniques* **26**, 417–34.

Richter, D., Mariolakos, I. & Risch, H. 1978. The main flysch stages of the Hellenides. In *Alps, Apennines, Hellenides* (eds H. Closs, D. Roeder & K. Schmidt), pp. 434–8. Inter-Union Commission on Geodynamics Scientific Report 38. Stuttgart: Schweizerbart.

Richter, D., Müller, C., Hottinger, L. & Risch, H. 1995. Die Flysch-Zonen Griechenlands X. Neue Daten zur Stratigraphie und Paläogeographie des Flysches und seiner Unterlage im Giona-Parnass-Elikon-Gebirge (Parnass-Zone, Griechenland). *Neues Jahrbuch für Geologie und Paläontologie, Abhandlungen* **197**, 295–329.

Richter, D., Müller, C. & Mihm, A. 1996. Die Flysch Zonen Griechenlands XII. Das Boeotikum und seine Flysche im Bereich des Iti-Parnass-Elikon-Gebirges, des nordwestlichen Kallidromon-Gebirges und des suedwestlichen Othrys-Gebirges (Mittelgriechenland). *Neues Jahrbuch für Geologie und Paläontologie, Abhandlungen* **201**, 367–409.

Richter, D., Müller, C. & Risch, H. 1996. Die Flysch-Zonen Griechenlands XI. Neue Daten zur Stratigraphie und Paläogeographie des Flysches und seiner Unterlage

https://doi.org/10.1017/S0016756817000942 Published online by Cambridge University Press

in der Pelagonischen Zone (Griechenland). *Neues Jahrbuch für Geologie und Paläontologie, Abhandlungen* **201**, 327–66.

Ricou, L.-E., Burg, J.-P., Godfriaux, I. & Ivanov, Z. 1998. The Rhodope and Vardar: the metamorphic and olistostromic paired belts related to the Cretaceous subduction under Europe. *Geodinamica Acta* **11**, 503–11.

Robertson, A. H. F. 2012. Late Palaeozoic–Cenozoic tectonic development of Greece and Albania in the context of alternative reconstructions of Tethys in the Eastern Mediterranean region. *International Geology Review* **54**, 373–454.

Robertson, A. H. F. & Degnan, P. J. 1993. Kerassia-Milia Complex: evidence of a Mesozoic–Early Tertiary oceanic basin between the Apulian continental margin and the Parnassus carbonate platform in western Greece. *Bulletin of the Geological Society of Greece* **28**, 233–46.

Robertson, A. H. F., Clift, P. D., Degnan, P. J. & Jones, G. 1991. Palaeogeographic and palaeotectonic evolution of the Eastern Mediterranean Neotethys. *Palaeogeography, Palaeoclimatology, Palaeoecology* **87**, 289–343.

Robertson, A. H. F. & Dixon, J. E. 1984. Introduction: aspects of the geological evolution of the Eastern Mediterranean. In *The Geological Evolution of the Eastern Mediterranean* (eds J. E. Dixon & A. H. F. Robertson), pp. 1–74. Geological Society of London, Special Publication no. 17.

Robertson, A. H. F., Dixon, J. E., Brown, S., Collins, A., Morris, A., Pickett, E., Sharp, I. & Ustaömer, T. 1996. Alternative tectonic models for the Late Palaeozoic–Early Tertiary development of Tethys in the Eastern Mediterranean region. In *Palaeomagnetism and Tectonics of the Mediterranean Region* (eds A. Morris & D. H. Tarling), pp. 239–63. Geological Society of London, Special Publication no. 105.

Robertson, A. H. F. & Shallo, M. 2000. Mesozoic–Tertiary tectonic evolution of Albania in its regional Eastern Mediterranean context. *Tectonophysics* **316**, 197–254.

Robertson, A. H. F., Trivić, B., Đerić, N. & Bucur, I. 2013. Tectonic development of the Vardar ocean and its margin: evidence from the Republic of Macedonia and Greek Macedonia. *Tectonophysics* **595–596**, 25–54.

Roddick, J. C., Cameron, W. A. & Smith, A. G. 1979. Permo-Triassic and Jurassic $^{40}Ar/^{39}Ar$ ages from Greek ophiolites and associated rocks. *Nature* **279**, 788–90.

Rosenbaum, G., Lister, G. S. & Duboz, C. 2002. Relative motions of Africa, Iberia and Europe during Alpine orogeny. *Tectonophysics* **359**, 117–29.

Saccani, E., Bortolotti, V., Marroni, M., Pandolfi, L., Photiades, A. & Principi, G. 2008a. The Jurassic association of backarc basin ophiolites and calc-alkaline volcanics in the Guevgueli Complex (northern Greece): implication for the evolution of the Vardar Zone. *Ofioliti* **33**, 209–27.

Saccani, E., Chiari, M., Bortolotti, V., Photiades, A. & Principi, G. 2015. Geochemistry of volcanic and subvolcanic rocks and biostratigraphy on radiolarian cherts from the Almopias ophiolites and Paikon unit (Western Vardar, Greece). *Ofioliti* **40**, 1–25.

Saccani, E., Photiades, A., Santato, A. & Zeda, O. 2008b. New evidence for supra-subduction zone ophiolites in the Vardar zone of northern Greece: implications for the tectono-magmatic evolution of the Vardar oceanic ocean. *Ofioliti* **33**, 65–85.

Šarić, K., Cvetkoviç, V., Romer, R. L., Christofides, G. & Koroneos, A. 2009. Granitoids associated with East Vardar ophiolites (Serbia, F.Y.R. of Macedonia and northern Greece): origin, evolution and geodynamic significance inferred from major and trace element data and Sr-Nd-Pb isotopes. *Lithos* **108**, 131–50.

Schenker, F. L., Burg, J.-P., Kostopoulos, D., Moulas, E., Larionov, A. & Von Quadt, A. 2014. From Mesoproterozoic magmatism to collisional Cretaceous anatexis: tectonomagmatic history of the Pelagonian Zone, Greece. *Tectonics* **33**, 1552–76.

Schenker, F. L., Fellin, M. G. & Burg, J.-P. 2015. Polyphase evolution of Pelagonia (northern Greece) revealed by geological and fission-track data. *Solid Earth* **6**, 285–302.

Schermer, E. R., Lux, D. R. & Burchfiel, B. C. 1990. Temperature-time history of subducted continental crust, Mount Olympos region, Greece. *Tectonics* **9**, 1165–95.

Scherreiks, R., Meléndeu, G., Boudagher-Fadel, M., Fermeli, G. & Bosence, D. 2014. Stratigraphy and tectonics of a time-transgressive ophiolite obduction onto the eastern margin of the Pelagonian platform from Late Bathonian until Valanginian time, exemplified in northern Evvoia, Greece. *International Journal of Earth Sciences* **103**, 2191–216.

Schmid, S. M., Bernoulli, D., Fügenschuh, B., Matenco, L., Schefer, S., Schuster, R., Tischler, M. & Ustaszewski, K. 2008. The Alpine-Carpathian-Dinaridic orogenic system: correlation and evolution of tectonic units. *Swiss Journal of Geosciences* **101**, 139–83.

Searle, M. & Cox, J. 1999. Tectonic setting, origin, and obduction of the Oman ophiolite. *Bulletin of the Geological Society of America* **111**, 104–22.

Shafiei, B., Haschke, M. & Shahabpour, J. 2009. Recycling of orogenic arc crust triggers porphyry Cu mineralization in Kerman Cenozoic arc rocks, southeastern Iran. *Mineralium Deposita* **44**, 265–83.

Shallo, M. 1994. Outline of the Albanian ophiolites. In *Albanian Ophiolites–State of the Art and Perspectives* (ed. L. Beccaluva), pp. 57–75. *Ofioliti*, Special Issue 19.

Shallo, M., Kodra, A. & Gjata, K. 1992. Geotectonics of the Albanian ophiolites. In *Ophiolites: Oceanic Crustal Analogues* (eds J. Malpas, E. M. Moores, A. Panayiotou & C. Xenophontos), pp. 165–70. Proceedings of the Symposium 'Troodos 1987'. Nicosia, Cyprus: Geological Survey Department.

Sissingh, W. 1977. Biostratigraphy of Cretaceous calcareous nannoplankton. *Geologie en Mijnbouw* **56**, 37–65.

Schlagintweit, F., Gawlick, H. J., Missoni, S., Hosha, L., Lein, R. & Frisch, W. 2008. The eroded Late Jurassic Kurbnesh carbonate platform in the Mirdita Ophiolite Zone of Albania and its bearing on the Jurassic orogeny of the Neotethys realm. *Swiss Journal of Geosciences* **101**, 125–38.

Schlagintweit, F., Gawlick, H. J., Missoni, S., Lein, R. & Hosha, L. 2006. Late Jurassic to Early Cretaceous dasycladales and benthonic foraminifera from the Munella carbonate platform s.l. of the Mirdita Zone (Albania). In *Proceedings of the XVIIIth Congress of the Carpathian-Balkan Geological Association* (eds. M. Sudar, M. Ercegovac & A. Grubic), pp. 527–30. National Committee of the Carpathian–Balkan Geological Association; Belgrade: Serbian Geological Society.

Skourlis, K. & Doutsos, T. 2003. The Pindos Fold-and-thrust belt (Greece): inversion kinematics of a passive

https://doi.org/10.1017/S0016756817000942 Published online by Cambridge University Press

continental margin. *International Journal of Earth Sciences* **92**, 891–903.

Smith, A. G. 1993. Tectonic significance of the Hellenic-Dinaric ophiolites. In *Magmatic Processes and Plate Tectonics* (eds H. M. Prichard, T. Alabaster, N. B. W. Harris & C. R. Neary), pp. 213–43. Geological Society of London, Special Publication no. 76.

Smith, A. G. & Spray, J. G. 1984. A half-ridge transform model for the Hellenic-Dinaric ophiolites. In *The Geological Evolution of the Eastern Mediterranean* (eds J. E. Dixon & A. H. F. Robertson), pp. 629–44. Geological Society of London, Special Publication no. 17.

Smuc, A. & Goričan, Š. 2005. Jurassic sedimentary evolution of a carbonate platform into a deep-water basin, Mt. Mangart (Slovenian–Italian Border). *Rivista Italiana di Paleontologia e Stratigrafia* **111**, 45–70.

Solakius, N., Pomoni-Papaioannou, F. & Marangoudakis, N. 1989. Planktic foraminiferal biostratigraphy and sedimentology of the Cretaceous–Tertiary boundary in the Sernikaki section (the Parnassus–Ghiona Zone, central Greece). *Revista Española de Micropaleontologia* **21**, 373–89.

Spray, J. G., Bébien, J., Rex, D. C. & Roddick, J. C. 1984. Age constraints on the igneous and metamorphic evolution of the Hellenic-Dinaric ophiolites. In *The Geological Evolution of the Eastern Mediterranean* (eds J. E. Dixon & A. H. F. Robertson), pp. 619–27. Geological Society of London, Special Publication no. 17.

Spray, J. G. & Roddick, J. C. 1980. Petrology and $^{40}Ar/^{39}Ar$ geochronology of the some Hellenic sub-ophiolite metamorphic rocks. *Contributions to Mineralogy and Petrology* **72**, 43–55.

Stais, A. & Ferrière, J. 1994. Peonias (Axios-Vardar oriental; Hellenides): données nouvelles sur les séries ante-Cretacé et interpretations géodynamiques. *Bulletin of the Geological Society of Greece* **30**, 121–32.

Stampfli, G. M. & Borel, G. 2004. The TRANSMED transects in space and time: constraints on the paleotectonic evolution of the Mediterranean domain. In *The TRANSMED Atlas, The Mediterranean Region from Crust to Mantle* (eds W. Cavazza, F. M. Roure, W. Spakman, G. M. Stampfli & P. A. Ziegler), pp. 53–90. Berlin-Heidelberg: Springer-Verlag.

Stampfli, G., Marcoux, J. & Baud, A. 1991. Tethyan margins in space and time. *Palaeogeography, Palaeoclimatology, Palaeoecology* **87**, 373–409.

Steuber, T. 1993. Late Cretaceous paleogeography and hippuritid biostratigraphy of Beotia (Greece). *Bulletin of the Geological Society of Greece* **28**, 39–53.

Steuber, T. 1999. Cretaceous rudists of Boeotia, Central Greece. *Special Papers in Palaeontology* **61**, 1–229.

Steuber, T., Gotzes, R., Raeder, M. & Walter, J. 1993. Palaeogeography of the western Pelagonian continental margin in Boeotia (Greece) during the Cretaceous – biostratigraphy and isotopic compositions ($\delta^{13}C$, $\delta^{18}O$) of calcareous deposits. *Palaeogeography, Palaeoclimatology, Palaeoecology* **102**, 253–71.

Steuber, T., Raeder, M. & Walter, J. 1994. Parnassus–Pelagonian transitional facies recorded in the Cretaceous Paleokastron section (W. Beotia, central Greece). *Bulletin of the Geological Society of Greece* **30**, 177–85.

Taylor, B., Weiss, J. R., Goodliffe, A. M., Sachpazi, M., Laigle, M. & Hirn, A. 2011. The structures, stratigraphy and evolution of the Gulf of Corinth rift, Greece. *Geophysical Journal International* **185**, 1189–219.

Terry, J. & Mercier, M. 1971. Sur l'existence d'une série détritique berriasienne intercalée entre la nappe des ophiolites et le flysch éocène de la nappe du Pinde (Pinde septentrional, Grèce). *Comptes Rendus Sommaires de la Société géologique de France* **2**, 71–3.

Thiébault, F. 1982. Évolution géodynamique des Hellénides externes en Péloponnèse méridionale (Grèce). *Société Géologique du Nord* **6**, 1–574.

Thiébault, F., Fleury, J. J., Clément, B. & Dégardin, J. M. 1994. Paleogeographic and paleotectonic implications of clay mineral distribution in late Jurassic – early Cretaceous sediments of the Pindos–Olonos and Beotian Basins, Greece. *Palaeogeography, Palaeoclimatology, Palaeoecology* **108**, 23–40.

Turpaud, P. & Reischmann, T. 2010. Characterisation of igneous terranes by zircon dating: implications for UHP occurrences and suture identification in the Central Rhodope, northern Greece. *International Journal of Earth Science* **99**, 567–91.

Ustaszewski, K., Kounov, A., Schmid, S. M., Schaltegger, U., Krenn, E., Frank, W. & Fügenschuh, B. 2010. Evolution of the Adria-Europe plate boundary in the northern Dinarides: from continent-continent collision to back-arc extension. *Tectonics* **29**, TC6017, doi: 10.1029/2010TC002668.

Ustaszewski, K., Schmid, S. M., Lugovic, B., Schuster, R., Schaltegger, U., Bernoulli, D., Hottinger, L., Kounov, A., Fügenschuh, B. & Schefer, S. 2009. Late Cretaceous intra-oceanic magmatism in the internal Dinarides (northern Bosnia and Herzegovina): implications for the collision of the Adriatic and European plates. *Lithos* **108**, 106–25.

Valeton, I., Biermann, M., Reche, R. & Rosenberg, F. 1987. Genesis of nickel laterites and bauxites in Greece during the Jurassic and Cretaceous, and their relation to ultrabasic parent rocks. *Ore Geology Review* **2**, 359–404.

van Hunen, J. & Allen, M. B. 2011. Continental collision and slab break-off: a comparison of 3-D numerical models with observations. *Earth and Planetary Science Letters* **302**, 27–37.

von Quadt, A., Moritz, R., Peytcheva, I. & Heinrich, C. A. 2005. Geochronology and geodynamics of Late Cretaceous magmatism and Cu–Au mineralization in the Panagyurishte region of the Apuseni–Banat–Timok–Srednogorie belt, Bulgaria. *Ore Geology Reviews* **27**, 95–126.

Wagreich, M., Pavlopoulos, A., Faupl, P. & Migiros, G. 1996. Age and significance of Upper Cretaceous siliciclastic turbidites in the central Pindos Mountains, Greece. *Geological Magazine* **133**, 325–31.

Wigniolle, E. 1977. Données nouvelles sur la géologie du massif de l'Iti (Grèce continentale). *Annales de la Société Géologique du Nord* **47**, 239–51.

Willingshofer, E., Neubauer, F. & Cloetingh, S. 1999. The significance of Gosau-type basins for the Late Cretaceous history of the Alpine-Carpathian Belt. *Physics and Chemistry of the Earth, Part A: Solid Earth and Geodesy* **24**, 687–95.

Wortel, M. J. R. & Spakman, W. 2000. Subduction and slab detachment in the Mediterranean–Carpathian region. *Science* **290**, 1910–7.

Yarwood, G. A. & Dixon, J. E. 1977. Lower Cretaceous thrusting in the Pelagonian rocks of the High Pieria, Greece. *Proceedings of the VI Colloquium on the Geology of the Aegean Region, Athens* **1**, 269–80.

Zimmerman, J. 1972. Emplacement of the Vourinos ophiolite complex, northern Greece. In *Studies in Earth and Space Sciences* (eds R. Shagam, R. B. Hargraves, W.

https://doi.org/10.1017/S0016756817000942 Published online by Cambridge University Press

J. Morgan, F. B. Van Houten, C. A. Burk, H. D. Holland & L. C. Hollister), pp. 225–39. Geological Society of America, Memoir no. 132.

Zimmerman, J. & Ross, J. V. 1976. Structural evolution of the Vardar root zone, northern Greece. *Geological Society of America Bulletin* **87**, 1547–50.

Zimmerman, A., Stein, H., Hannah, J., Koželj, D., Bogdanov, K. & Berza, T. 2008. Tectonic configuration of the Apuseni–Banat–Timok–Srednogorie belt, Balkans-South Carpathians, constrained by high precision Re–Os molybdenite ages. *Mineralium Deposita* **43**, 1–21.

https://doi.org/10.1017/S0016756817000942 Published online by Cambridge University Press